CHARACTERIZATION AND EXPRESSION OF HISTONE DEACETYLASE 1 (AtHD1) IN *Arabidopsis thaliana*

A Thesis

by

MAN KIM FONG

Submitted to the Office of Graduate Studies of
Texas A&M University
in partial fulfillment of the requirements for the degree of

MASTER OF SCIENCE

May 2005

Major Subject: Molecular & Environmental Plant Sciences

CHARACTERIZATION AND EXPRESSION OF HISTONE DEACETYLASE 1 (AtHD1) IN *Arabidopsis thaliana*

A Thesis

by

MAN KIM FONG

Submitted to the Office of Graduate Studies of
Texas A&M University
in partial fulfillment of the requirements for the degree of

MASTER OF SCIENCE

Approved as to style and content by:

Z. Jeffrey Chen (Chair of Committee)	Mary Bryk (Member)
Timothy C. Hall (Member)	
Marla Binzel (Chair of Molecular & Environmental Plant Sciences Faculty)	Mark A. Hussey (Head of Department)

May 2005

Major Subject: Molecular & Environmental Plant Sciences

ABSTRACT

Characterization and Expression of Histone Deacetylase 1

(AtHD1) in *Arabidopsis thaliana.*

(May 2005)

Man Kim Fong, B.S.; M.S., The Chinese University of Hong Kong, PRC

Chair of Advisory Committee: Dr. Z. Jeffrey Chen

The reversible process of histone acetylation and deacetylation is an important mechanism of epigenetic regulation in the control of gene expression and chromatin structure. In general, histone acetylation is related to gene activation, whereas histone deacetylation is associated with transcriptional gene silencing and maintenance of heterochromatin. A large number of histone deacetylases (HDACs), the enzymes that catalyze the reaction of histone deacetylation, have been identified in plants and other eukaryotes, and they were found to play crucial roles in plant growth and development.

In *Arabidopsis thaliana*, histone deacetylase 1 (AtHD1) is a homolog of S*accharomyces cerevisiae* Rpd3 that is a global transcriptional regulator. Downregulation of *AtHD1* in transgenic *Arabidopsis* results in histone hyperacetylation and induces a variety of phenotypic and developmental defects, suggesting that AtHD1 is also a global regulator of many physiological and developmental processes.

To characterize the expression pattern and distribution of AtHD1 in cells, the subcellular location of AtHD1 was determined by monitoring the expression of an AtHD1-GFP fusion protein in a transient expression assay and in transgenic *Arabidopsis*.

The results show that AtHD1 is localized in the nucleus and appears to be excluded from the nucleolus.

The histone deacetylase activity of AtHD1 was studied in an *in vitro* assay using radiolabeled histone peptides as a substrate. Recombinant AtHD1 produced by bacteria demonstrated a moderate but significant HDAC activity, whereas that produced by the baculovirus expression system did not have activity. This suggests that AtHD1 may require other cofactors or association with other proteins, rather than post-translational modifications, in order to have full HDAC activity.

To study the possible interactions of AtHD1 with other proteins, a recombinant AtHD1 protein with two units of c-myc epitope fused to its C-terminus was expressed in transgenic *Arabidopsis*. We attempted to isolate proteins interacting with AtHD1 by co-immunoprecipitation (Co-IP). However, in the first few trials of Co-IP, a lot of contaminating proteins were present in the eluent along with the recombinant AtHD1-cmyc protein. Improvements in the experimental conditions are required for further investigation.

DEDICATION

To my parents, Wa Fong and Kaisim So, for their love, support and encouragement that nourishes my heart and helps me overcome any adversity in life.

ACKNOWLEDGEMENTS

I would like to express my sincere gratitude to my advisor, Dr. Z. Jeffrey Chen, who gave me the chance to work in his laboratory. His guidance, support and encouragement has been very valuable and important in helping me to complete my study. I also want to express my utmost respect to him as a dedicated scientist.

I would like to extend my sincere gratitude to other members of my advisory committee, Dr. Mary Bryk, Dr. Timothy Hall, and Dr. Alan Pepper, for their valuable guidance and helpful advice on my research.

I thank Dr. Linda Guarino for allowing me to work in her laboratory for insect cell culture. I also thank Dr David Stelly for allowing and teaching me to use the fluorescence microscope in his lab.

I am grateful to the friendly and wonderful members of the Chen lab. I appreciate Dr. Tian Lu for her helpful advice on my experimental work and study. I am thankful to my colleagues and previous lab members, Dr. Hyeon-Se Lee, Dr. Osama Hassan, Dr. Wenxiang Gao, Dr Jianlin Wang, Dr Samuel Yang, and my fellow lab members, Meng Chen, Misook Ha, Grace Kim, Jinsuk Lee, Sheetal Rao and Edward Wei. I also thank Teresa Legate, Barbara Adams, Lindsey Cozad, Lauren Wells, Lauren Williamson and Jose Trejo for their assistance and help in lab maintenance.

TABLE OF CONTENTS

CHAPTER Page

LIST OF FIGURES

CHAPTER I

INTRODUCTION

Researchers have found that gene expression is regulated not only by cis- and trans-acting elements that are located within the DNA itself, but also by histone proteins that package DNA into chromatin, by enzymes that modify histones and DNA, and even by some small RNAs (Pennisi, 2001). Epigenetic regulation, which is defined as the heritable changes in gene expression that occur without a change in DNA sequence (Wolffe and Matzke, 1999), is involved in many biological phenomena and processes such as genomic imprinting (Joyce et al., 1997; Reik and Murrell, 2000), X-chromosome inactivation (Lyon, 1993), paramutation (Stam et al., 2002) and transposon regulation (Singer et al., 2001).

Epigenetic regulation of gene expression is mediated by a large number of proteins that can affect the chromatin structure and thus modulate the accessibility of other transcriptional regulators to the DNA. The identification, characterization and elucidation of the mechanisms of this large number of chromatin remodeling and modifying proteins have proven to be the most challenging part of epigenetic research.

CHROMATIN REMODELING MECHANISMS

In eukaryotic cells, nuclear DNA is organized and packaged into compact structures called chromatin through association with basic globular proteins called histones. The basic unit of chromatin is nucleosome that consists of 146 bp of DNA wrapped twice around a

---

This thesis follows the format of The Plant Cell.

histone octamer containing two molecules of H2A, H2B, H3 and H4 (Luger et al., 1997). The nucleosomes on the DNA are described as “beads on a string” that can be further condensed into a more compact helical structure called the 30-nm fiber by the association of histone H1 with linker DNA (Lusser, 2002). Further compaction of the chromatin above the level of the 30-nm fiber is generally termed higher-order chromatin structure.

Recent studies revealed that the chromatins are highly dynamic structures that can change during plant development or in response to environmental changes. For instance, the positions of nucleosomes surrounding the upstream regions of particular genes and the nuclease accessibility of such regions have been shown to change in response to environmental and developmental changes (Paul and Ferl, 1998; Li et al., 2001). Recent studies on chromatin modifications and identification of chromatin remodeling machineries have unveiled some regulatory mechanisms at the nucleosome level that regulate gene activity by changing the higher-order chromatin structures (Lusser, 2002). These mechanisms include chromosome remodeling by ATP-dependent chromatin remodeling complexes, DNA methylation and histone modifications.

ATP-dependent chromatin remodeling complexes

The ATP-dependent chromatin remodeling complexes are characterized by having an ATPase subunit that can use the energy from ATP hydrolysis to disrupt and reorder nucleosome position and conformation, and thus affecting the access of transcription factors to DNA packaged in the nucleosome (Havas et al., 2000; Gavin et al., 2001). They usually function as transcriptional coactivators but some may act as transcriptional repressors or are involved in other processes such as chromatin assembly (Kingston and Narlikar, 1999).

There are several groups of chromatin remodeling complexes including the SWI/SNF

(Switch/Sucrose Non-Fermenting), CHRAC (Chromatin Accessibility Complex) and NURF (Nucleosome Remodeling Factor), all of which contain an ATPase subunit of the SWI2/SNF2 superfamily (Corona et al., 1999; Phelan et al., 2000), which in turn, can be divided into different subfamilies according to their functions and phylogenetics (Eisen et al., 1995).

Three subfamilies of SWI2/SNF2 were identified and demonstrated to have chromatin remodeling activity. First, the SNF2/BRM (Brahma) subgroup was found to regulate transcription by controlling the accessibility of cis-regulatory elements to transcriptional regulators by altering the position or conformation of nucleosomes (Wagner, 2003). Mutations in the *Arabidopsis SYD* (*Splayed*) gene, which encodes a SNF2/BRM chromatin remodeling factor, caused severe developmental defects. This implies a role for SYD in the repression of floral transition, the expression of floral homeotic genes, and ovule development (Wagner and Meyerowitz, 2002). Second, the subgroup ISWI (Imitation Switch) first identified in *Drosophila* was found to alter the position of nucleosomes by a sliding mechanism (Narlika et al., 2002). ISWI may play a role in chromatin assembly, transcriptional regulation and the maintenance of higher order chromatin structure (Wagner, 2003). The third subgroup called CHD (Chromodomain-Helicase-DNA-binding protein) is characterized by having a chromodomain, a SNF2-like helicase/ATPase domain and a DNA-binding protein (Ogas et al., 1999). Mutations in *Arabidopsis PKL* (*Pickle*) gene, a member of the CHD subgroup, result in the ectopic expression of embryonic developmental genes, suggesting that PKL functions as a corepressor of these genes (Lusser, 2002).

Recent studies have revealed a functional relationship among chromatin remodeling complexes, histone and DNA modifying enzymes. For instance, members of the CHD

subfamily of chromatin remodeling factors were shown to act in complexes with histone deacetylases to repress genes in *Drosophila* and mammals (Wade et al., 1998; Zhang et al., 1998). Moreover, the *Arabidopsis* chromatin remodeling factors DDM1 (Decreased DNA Methylation 1) and MOM1 (Morpheus' Molecule 1) are required for the maintenance of global DNA methylation (Jeddeloh et al., 1999; Dennis et al., 2001) and silencing of a methylated transgene (Amedeo et al., 2000), respectively, suggesting a link between chromatin remodeling factors and DNA methylation.

DNA methylation

Symmetric DNA methylation (CpG and CpNpG) on cytosine residues is an evolutionarily conserved DNA modification found in vertebrates, plants and some fungi (Finnegan and Kovac, 2000; Bird, 2002). In addition, plants have asymmetric DNA methylation in non-CG sequences (Finnegan and Kovac, 2000). DNA methylation is believed to be a mechanism that defends the genome against transposable elements and retroviruses (Martienssen and Colot, 2001; Bird, 2002). In the eukaryotic genomes, regions containing abundant heterochromatin and silenced transgenes usually have high levels of DNA methylation (Eden and Cedar, 1994).

The *Arabidopsis thaliana* genome contains at least ten genes that encode DNA methyltransferases that can be divided into three main families based on their functions and/or sequence homology to mammalian DNA Methyltransferases (DNMT) (Tariq and Paszkowski, 2004). First, *Arabidopsis* MET1 (Methyltransferase 1) is a homolog of mammalian DNMT1 and is responsible for maintenance of CG methylation (Finnegan and Kovac, 2000). *MET1* missense mutations (*met1-1* and *met1-2*) showed delayed flowering and derepression of silenced genes (Kankel et al., 2003). Second, DRM1

(Domain-Rearranged Methyltransferase 1) and DRM2, which are similar to the mammalian DNMT3 family of methyltransferases, were identified as *de novo* methyltransferases in genome defense (Cao and Jacobsen, 2002a). DRM proteins were shown to be involved in the establishment but not the maintenance of silencing at the *FWA (Flowering Wageningen)* and *SUPERMAN* loci, and *drm1/drm2* double mutants were unable to perform *de novo* methylation at non-CG sites in *FWA* and *SUPERMAN* loci (Cao and Jacobsen, 2002b). Third, CMT3 (Chromomethylase 3) is a plant-specific methyltransferase that contains a chromodomain and was shown to be responsible for asymmetric DNA methylation in both *Arabidopsis* (Lindroth et al., 2001) and maize (Papa et al., 2001).

DDM1, a SWI/SNF-type ATPase chromatin remodeling factor described earlier, is required to maintain global methylation and has been shown to control transposon and transgene silencing (Jeddeloh et al., 1999), and to maintain methylation of Lysine 9 on histone H3 (Gendrel et al., 2002). Moreover, it was shown that methylated DNA can recruit methyl-DNA binding proteins which in turn recruit histone-modifying enzymes and chromatin-remodeling factors for heterochromatin formation (Lusser, 2002). Overall, these studies suggest a mechanistic link among chromatin remodeling, DNA and histone methylation.

Histone modifications

The post-translational modifications of core histone N-terminal tails have emerged as a versatile means to regulate gene expression and determine higher-order chromatin structures. The N-terminal tails of histones contain conserved amino acid residues that are subjected to a variety of covalent modifications including acetylation/deacetylation, methylation, phosphorylation, ubiquitination, sumoylation and ADP-ribosylation (Jenuwein

and Allis, 2001; Shiio and Eisenman, 2003). The identification of chromatin proteins and their native complexes has led to the postulation of the histone code hypothesis, which states that the covalent modifications on histone tails provide binding sites for chromatin-associated proteins, which in turn induce alterations in chromatin structure and thereby lead to downstream transcriptional regulation (Strahl and Allis, 2000; Jenuwein and Allis, 2001). The histone codes can act as epigenetic marks which are heritable and can be translated into biological functions (Jenuwein and Allis, 2001).

Histone acetylation/deacetylation

Core histones can be reversibly acetylated or deacetylated on specific lysine residues of the histone N-terminal tails. Histone acetylation is catalyzed by the enzymes histone acetyltransferases (HATs) that transfer an acetyl group from acetyl coenzyme A to the ε-amino group of specific lysine residues, while the reverse reaction is catalyzed by another group of enzymes called histone deacetylases (HDACs). The competing action of HAT and HDAC determines the histone acetylation levels that ultimately affect the higher-order chromatin structure and gene activities at a chromosomal region. In general, genomic regions with hyperacetylated histones are associated with increased gene activity, while those containing hypoacetylated histones are associated with reduced gene activity.

Histone acetylation is thought to make the chromatin more “open” to transcriptional regulators by neutralizing the positive charge of histone tails and thus decreasing their affinity for the negatively charged DNA (Kuo and Allis, 1998). Hence, histone hyperacetylation tends to disrupt higher-order chromatin structure and activates genes. In contrast, histone deacetylation restores the positive charge of core histones and increases their affinity to the DNA, resulting in chromatin compaction into higher-order structure and

gene inactivation (Horn and Peterson, 2002). It has also been proposed that the acetylation/deacetylation status of specific lysine residues, together with other modifications on the histone N-terminal tails, acts as epigenetic marks or binding surfaces for the recruitment of transcriptional regulators and/or chromatin remodeling factors (Jenuwein and Allis, 2001).

There are two major classes of HATs in eukaryotes, Type B and Type A, which are responsible for acetylation of histones before and after their incorporation into chromatin, respectively (Imhof and Wolffe, 1999; Carrozza et al., 2003). Type A HATs are more directly involved in transcriptional regulation because they acetylate histones in the chromatin. In plants, type A HATs, including homologs of the transcriptional coactivators Gcn5 (General Control of Amino Acid Synthesis protein 5) and p300/CBP (CREB-binding protein), were identified (Stockinger et al., 2001; Bordoli et al., 2001). Recombinant *Arabidopsis* GCN5 homolog and PCAT2 (p300/CBP class) have been shown to have histone acetyltransferase activity (Stockinger et al., 2001). Moreover, *Arabidopsis* GCN5 has been shown to interact *in vitro* with *Arabidopsis* orthologs of the yeast HAT-adaptor protein ADA2, resulting in the recruitment of the HAT complex to cold- and dehydration-inducible promoters through the action of the transcription factor CBF1 (C-repeat/DRE binding factor 1) (Stockinger et al., 2001).

While 12 HATs have been identified in plants, there is a larger number (18) of histone deacetylases in the plant genomes (Pandey et al., 2002). Their activities, functions and roles in plant physiological and developmental processes will be discussed in later sections.

Histone methylation

Early studies showed that lysines 4, 9, 27 and 36 of histone H3 and lysine 20 in histone H4 can be mono-, di- or tri-methylated (reviewed in Zhang and Reinberg, 2001). However, their significance in epigenetic regulation of gene expression and the enzymes involved have not been revealed until recently. The mammalian homolog of *Drosophila* SU(VAR)3-9 (Suppressor of Variegation 3-9), SUV39h, was the first histone methyltransferase identified and it was shown to methylate histone H3 at lysine 9 (Rea et al., 2000). The catalytic domain of histone methyltransferases (HMTs) is a conserved protein sequence motif called the SET domain (**S**uvar3-9 **e**nhancer of zeste **t**rithorax domain) first identified in the *Drosophila* position effect variegation suppressor Su-var3-9, the polycomb group protein enhancer of zeste and the trithorax-group protein trithorax (Rea et al., 2000). Homologs of SUV39h histone methyltransferase have also been identified in fission yeast, *Neurospora* and *Arabidopsis*. *Arabidopsis* KYP (Kryptonite) is the first H3-K9-specific histone methyltransferase identified in plants (Jackson et al., 2002; Malagnac et al., 2002). Although *Arabidopsis* contains at least 29 SET domain proteins (Baumbusch et al., 2001), KYP is implicated to be responsible for the majority of H3-K9 methylation because mutation in *KYP* leads to a dramatic reduction of H3-K9 methylation levels at chromocenters (Johnson et al., 2002; Jasencakova et al., 2003).

Methylation at lysine 9 of histone H3 is by far the best characterized histone methylation and it is one of the characteristics of heterochromatin (Rea et al., 2000). In *Arabidopsis,* H3-K9 methylation is abundant in centromeric and pericentromeric heterochromatin (Probst et al., 2003; Tariq et al., 2003) and it is associated with heterochromatic silencing at specific loci (Grendel et al., 2002). On the other hand, H3-K4

methylation is associated with transcriptionally active regions (Strahl et al., 1999; Noma et al., 2001; Nagy et al., 2002). Interestingly, methylation at H3-K4 and H3-K79 is required for gene silencing near the telomeric region in *S. cerevisiae* (Krogan et al., 2003).

Histone H3 methylation at K9 appears to be recognized by a chromodomain containing protein called Heterochromatin Protein 1 (HP1) (Bannister et al., 2001; Lachner et al., 2001). In mammals, *Drosophila* and *Neurospora*, HP1 failed to associate with heterochromatin in chromocenters or centromeric regions when the levels of H3-K9 methylation were reduced (Schotta et al., 2002; Freitag et al., 2004; Pal-Bhadra et al., 2004). A plant homolog of HP1, called LHP1 (Like Heterochromatin Protein 1), was identified in *Arabidopsis* and its mutation caused altered flowering time and upregulation of *CONSTANS* (Gaudin et al., 2001) and a series of homeotic genes (Kotake et al., 2003). LHP1 has been shown to interact directly with CMT3, implying a mechanistic link between DNA methylation at CpNpG and heterochromatin formation associated with H3-K9 methylation (Jackson et al., 2002). Recent findings also revealed that H3-K9 methylation was dramatically reduced in heterochromatin regions in *ddm1* and *met1* mutants, suggesting a link between H3-K9 methylation and heterochromatin formation via DNA methylation (Grendel et al., 2002).

In human and *Drosophila*, H3-K27 methylation is also associated with gene silencing mediated by the polycomb-group (PcG) proteins such as the SET domain protein enhancer of zeste (Cao et al., 2002; Czermin et al., 2002; Kuzmichev et al., 2002; Muller et al., 2002). In plants, a PcG protein VERNALIZATION 2 (VRN2) is required for maintenance of vernalization during which the floral repressor gene *FLOWERING LOCUS C* (*FLC*) acquires methylation at H3-K9 and H3-K27 (Grendall et al., 2001; Bastow et al.,

2004; Sung and Amasino, 2004).

In contrast to the highly dynamic nature of histone acetylation and phosphorylation, histone and DNA methylation appears to be irreversible processes and hence they are regarded as stable epigenetic marks (Jenuwein and Allis, 2001).

Histone phosphorylation

Like histone acetylation, phosphorylation on histone N-terminal tails is a reversible process. However, it occurs on serine residues. Histone H3-S10 phosphorylation is the best-characterized histone phosphorylation so far. Studies have shown that H3-S10 phosphorylation acts in concert with other histone modifications, rather than acting alone, to modulate transcription. For instance, H3-S10 phosphorylation impairs the subsequent methylation of H3-K9 by SUV39h1, while acetylation of H3-K14 and H3-K9 stimulates the phosphorylation of H3-S10 by the mitotic kinase Ipl1/aurora (Rea et al., 2000). Most studies of histone phosphorylation were conducted in *Drosophila* and mammals. Its role in plants has not been extensively studied yet.

Histone ubiquitination

The covalent attachment of a small ubiquitin protein (~76 amino acids) to certain target proteins is a mark for degradation by the proteosome (Conaway et al., 2002). However, ubiquitination of histones was associated with transcriptional activation (Strahl and Allis, 2000). For instance, increased levels of ubiquitinated histone H2A and H2B were found in actively transcribed regions in the chromatin of human (Varshavsky et al., 1982; Davie and Murphy, 1990).

Histone sumoylation

Small ubiquitin-related modifier (SUMO) is a family of ubiquitin-like proteins that has not been linked to protein degradation. In mammals, SUMO proteins are divided into three families: SUMO-1, SUMO-2 (SMT3a), and SUMO-3 (SMT3b), which show partly overlapping yet distinct functions (Saitoh and Hinchey, 2000; Tatham et al., 2001). It has been shown in mammals that histone H4 sumoylation mediates transcriptional repression through recruitment of histone deacetylases and heterochromatin protein 1 (HP1) (Shiio and Eisenman, 2003).

HISTONE DEACETYLASES

Histone deacetylases (HDACs) are enzymes that are responsible for the removal of an acetyl group covalently attached to the ε-amino group of lysine residues on the histone N-terminal tails. The first histone deacetylase identified was mammalian HDAC1 that shows high sequence homology to the yeast protein Rpd3 (Reduced potassium dependency protein 3) (Taunton et al., 1996). Since then, a large number of HDACs have been identified in many eukaryotes and 18 HDAC genes have been identified in *Arabidopsis* so far (Pandey et al., 2002). HDACs are divided into 4 classes based on their sequence homology, substrate specificity and requirement of cofactors. Class I and class II HDACs are homologous to the yeast Rpd3 and Hda1 proteins, respectively, while class III HDACs are related to the yeast Sir2 (Silent information regulator 2) protein (Wu et al., 2003). While the first 3 classes of HDACs can be found in yeast, animals and plants, the fourth class of HDAC called HD2-like HDACs are found in plants only.

Sequence analyses show that most class I HDACs contain a large conserved domain homologous to the N-terminal region of yeast RPD3 and a short C-terminal region with a

more variable sequence (Khochbin and Wolffe, 1997). In yeast and mammalian cells, the Rpd3-type HDACs have been shown to mediate transcriptional repression by interacting with specific DNA-binding proteins or associated corepressors and by recruitment to target promoters (Alland et al., 1997; Hassig et al., 1997; Kadosh and Struhl, 1997).

In yeast, Rpd3 and Sin3 are tightly associated and they coexist in a large multiprotein complex that has been shown to repress target genes involved in diverse processes such as meiosis, cell-type specificity, potassium transport, phosphate and phospholipid metabolism, and methionine biosynthesis (Vidal and Garber, 1991; McKenzie et al., 1993; Stillman et al., 1994; Jackson and Lopes, 1996). The Rpd3-Sin3 complex can be recruited to the promoters of target genes by Ume6, a repressor that specifically binds an upstream repression sequence present in a wide variety of yeast promoters (Strich et al., 1994; Kadosh and Struhl, 1997).

In mammals, class I HDACs include HDAC1, 2, 3, 8 and 11. HDAC1 and HDAC2 coexist in at least 3 distinct multiprotein complexes including the SIN3, NuRD/NRD/Mi2, and CoREST complexes (Hassig et al., 1997; Laherty et al., 1997; Zhang et al., 1998; Tong et al., 1998; Ayer; 1999; Humphrey et al., 2001; You et al., 2001). HDAC3 is found in another corepressor complex called N-CoR (nuclear receptor corepressor) that has been shown to inhibit JNK activation through an integral subunit, GPS2 (Zhang et al., 2002).

In plants, the first RPD3 homolog was identified in maize and it complemented the phenotype of a *rpd3* null mutant of yeast (Rossi et al., 1998). There are four class I HDACs identified in *Arabidopsis*, including AtHD1 (AtRPD3A, HDA19), AtHD6 (AtRPD3B), HDA7 and HDA9. There are two other *Rpd3*-like sequences identified (*HDA10* and *HDA17*) but they are believed to be pseudogenes derived from the 3'-end of *HDA9* (Pandey et al., 2002).

Class II HDACs, also called HDA1-like HDACs, share sequence homology with RPD3-type HDACs in their catalytic domain but have distinct structural and functional features (Wade, 2001). There are 6 class II HDACs in mammals and they have been shown to exist in large multiprotein complexes and are capable of interacting with other proteins. In yeast, Hda1 is the primary class I HDAC. In *Arabidopsis*, 6 putative class II HDAC genes were identified but their functions and characterization are poorly studied.

The class III HDACs, also called SIR2-like HDACs or Sirtuin, differ greatly from other classes of HDACs in sequence and function, and are distinct in the requirement of NAD as a coenzyme for HDAC activity (Imai et al., 2000; Smith et al., 2000; Marmorstein, 2001). Studies of SIR2-like HDACs in yeast, *Drosophila* and mammals showed that they are involved in the regulation of cellular metabolism and aging (reviewed by Guarente, 2000; Blander and Guanrente, 2004; Rogina and Helfand, 2004; Wood et al., 2004). Two *SIR2*-like genes have been identified in *Arabidopsis* but they have not been characterized yet (Pandey et al., 2002).

Finally, the HD2-like HDACs are plant specific and the first HD2 protein was identified in maize as a tightly chromatin-bound phosphoprotein localized in the nucleolus whose HDAC activity can be regulated by phosphorylation (Lusser et al., 1997; Kolle, 1999). Four HD2-like HDACs have been identified in *Arabidopsis* and in maize (Pandey et al., 2002). It has been shown that three HD2-like HDACs in *Arabidopsis*, including AtHD2A, AtHD2B and AtHD2C, can repress transcription when targeted to a reported gene *in vivo* as a fusion protein with a transcription factor (Wu et al., 2000a; Wu et al., 2003). Moreover, blocking *AtHD2A* by expression of an antisense version of the gene results in aborted seed development, suggesting that AtHD2A plays an important role in the reproductive

development of *Arabidopsis* (Wu et al., 2000a).

Histone deacetylase 1 in *Arabidopsis* (AtHD1)

AtHD1 is a single-copy gene located on the short arm of chromosome 4 (Tian and Chen, 2001). The AtHD1 protein shares 56 and 55% amino acid sequence identity to HD1 in mammals (Taunton et al., 1996) and Rpd3 in yeast (Vidal and Gaber, 1991), respectively. RNA blot analysis showed that *AtHD1* is expressed in seedlings, leaves, flower buds, siliques, stems and roots, suggesting that AtHD1 is a global regulator involved in many physiological and developmental processes in plants (Tian and Chen, 2001). Sequence analysis of the deduced amino acid sequence of AtHD1 protein identified two components, a N-terminal region (201 amino acids) homologous to yeast Rpd3 and a C terminal region (300 amino acids) that is highly hydrophobic and specific to multicellular eukaryotes, including plants and mammals (Tian and Chen, 2001). The histidines at positions 148/149 and 186/187 are conserved catalytic sites for deacetylation activity in yeast (Kadosh and Struhl, 1998).

The functional role of AtHD1 was studied by antisense inhibition of *AtHD1* expression in transgenic *Arabidopsis* which displayed various phenotypic and developmental defects including early senescence, serrated leaves, formation of aerial rosettes, delayed flowering and defects in floral organ identity (Tian and Chen, 2004). The downregulation of *AtHD1* also leads to the hyperacetylation of histone H4 but causes no change in the DNA methylation levels in the transgenic plants. Downregulation of *AtHD1* by T-DNA insertion in the exon 2 of *AtHD1* gene results in similar phenotypic defects and hyperacetylation as in the antisense inhibition study (Tian et al., 2003). Moreover, when the homozygous T-DNA insertion line is crossed with wild type plants, the phenotypic defects as

well as the histone acetylation levels are restored to normal in the F1 progeny, demonstrating the reversible nature of histone acetylation (Tian et al., 2003).

The characterization of AtHD1 protein including the demonstration of HDAC activity *in vitro*, the cellular distribution and localization, and its interaction with other proteins are unknown and will be addressed in this study.

CHAPTER II

SUBCELLULAR LOCALIZATION OF HISTONE DEACETYLASE 1 IN *Arabidopsis*

INTRODUCTION

Histone deacetylases (HDACs) regulate gene transcription and modify chromatin structure by deacetylating specific lysine residues at the N-termini of core histones. Since the substrates for HDACs are located in the nucleus, the activity of HDACs can be regulated by controlling their localization in the cells (Sengupta & Seto, 2004). Studies on human HDACs found that the activity of some HDACs is regulated by translocation between the nucleus and cytoplasm. For instance, the mammalian class II HDACs, HDAC4, 5, 7 and 9, associate with 14-3-3 proteins upon phosphorylation of conserved serine residues on their N-terminal regions, resulting in sequestration of the HDACs to the cytoplasm (Grozinger & Schreiber, 2000; McKinsey et al., 2000; Wang et al., 2000; Kao et al., 2001; Miska et al., 1999). In contrast, the class I HDACs, including HDAC1, 2 and 8, are predominantly localized in the nucleus and seem not to be regulated by subcellular localization (Sengupta & Seto, 2004). Exceptionally, class I HDAC3 is present in both the cytoplasm and the nucleus. It is translocated from the nucleus to the cytoplasm in response to interleukin-1β signaling, resulting in derepression of a specific subset of NF-κB regulated genes (Baek et al, 2002).

The studies of subcellular localization may also provide clues to the function of a HDAC. One of the best-characterized HDACs in plants is maize histone deacetylase 2 (HD2)

that was found to be localized in the nucleolus using immunofluorescence methods. Together with other findings that maize HD2 is tightly chromatin-bound and shares homology to other nucleolar proteins, it was suggested that HD2 may play a role in regulating the expression and organization of ribosomal DNA by deacetylating nucleolar core histones (Lusser et al., 1997). An *Arabidopsis* HD2-type HDAC called HDT1 was also shown to be localized in the nucleolus of onion cells in a transient expression assay and was required for H3-K9 deacetylation (Lawrence et al., 2004). The study also showed that HDT2 is involved in an epigenetic switch in which concerted changes in the DNA methylation and histone deacetylation/methylation of the rRNA gene promoter control the rRNA gene dosage in *Arabidopsis suecica* (Lawrence et al., 2004). In another study, the subcellular localizations of three *Arabidopsis* HD2 homologs, namely HD2A, HD2B and HD2C, were determined by examining the fluorescence signals of the GFP-HD2 fusion proteins in transgenic *Arabidopsis* (Zhou et al., 2004). The results indicated that the GFP-HD2 fusion proteins were localized and confined to a small region in the nuclei. However, since the nuclei were not stained in the study to reveal the detail structure of the nucleus, the nucleolar localization of these *Arabidopsis* HD2 proteins was not confirmed.

Interestingly, the study of the expression profile and cellular localization of three RPD3-type HDACs in maize, termed ZmRpd3/101, ZmRpd3/102 and ZmRpd3/108, showed that they are present in both cytoplasm and nuclei during different stages of kernel, shoot and anther development (Varotto et al., 2003). This suggests that the three maize class I HDACs may be regulated by nuclear cytoplasmic shuttling and involved extensively in the regulation of various physiological and developmental processes (Varotto et al., 2003).

Previous studies of the RPD3-type HDACs in *Arabidopsis* have been focused on their

functions in the regulation of gene expression and plant development. The subcellular localization, which is a key characteristic that determines the range of functions of an enzyme, has not been experimentally determined for any of the RPD3-type HDACs in *Arabidopsis*. In this part of my study, the *Arabidopsis* histone deacetylase 1 (AtHD1) was fused with an engineered GFP at its C-terminus. The *AtHD1-GFP* chimeric gene was expressed transiently in onion cells and permanently in transgenic *Arabidopsis* plants to determine the subcellular localization of the AtHD1 protein.

RESULTS

Transient expression of AtHD1-GFP fusion protein in onion cells

In the transient expression assay, plasmid DNA harboring the *AtHD1-GFP* chimeric gene under the control of the cauliflower mosaic virus (CaMV) 35S RNA promoter (Figure 2.1) was coated on tungsten particles and introduced into onion epidermal cells by particle bombardments using the helium-driven Biolistic PDS-1000/He system (Bio-Rad). After 24 hours of incubation at 25°C, the expression of the GFP fusion protein was examined under a fluorescence microscope. In the non-stained onion cells viewed under UV light with band-pass filter for GFP (Figures 2.2B and D), green fluorescence signals were detected, and their positions and sizes were consistent with the nucleus-like structures seen when the same onion cells were viewed under white light (Figures 2.2A and C). To confirm the identity of the nucleus-like structures that gave green fluorescence signals, the onion epidermal cells were stained with DAPI (4',6-diamidino-2-phenylindole), a water soluble fluorescent dye that binds DNA and fluoresces to give blue light under UV excitation. The nuclei of the stained onion cells were revealed under UV light with band-pass filter for blue color (Figures 2.2E and G). When the same tissue was illuminated with blue light and viewed

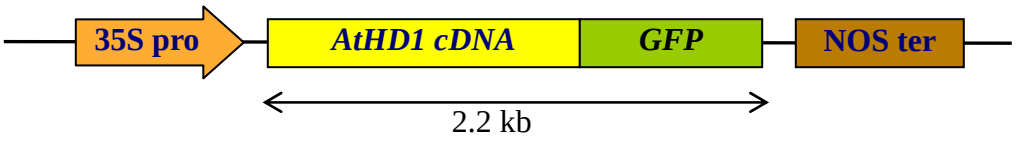

Figure 2.1. The construct of *AtHD1-GFP* chimeric gene.

The expression cassette of *AtHD1-GFP* chimeric gene is put under the control of the CaMV 35S promoter (35S pro) and the nopaline synthase terminator (NOS ter). The construct is harbored in a pUC18 plasmid that was coated onto tungsten particles and introduced into onion epidermal cells by particle bombardments. The sizes of the *AtHD1-GFP* chimeric gene and the recombinant protein are 2.2 kb and 83.1 kDa, respectively.

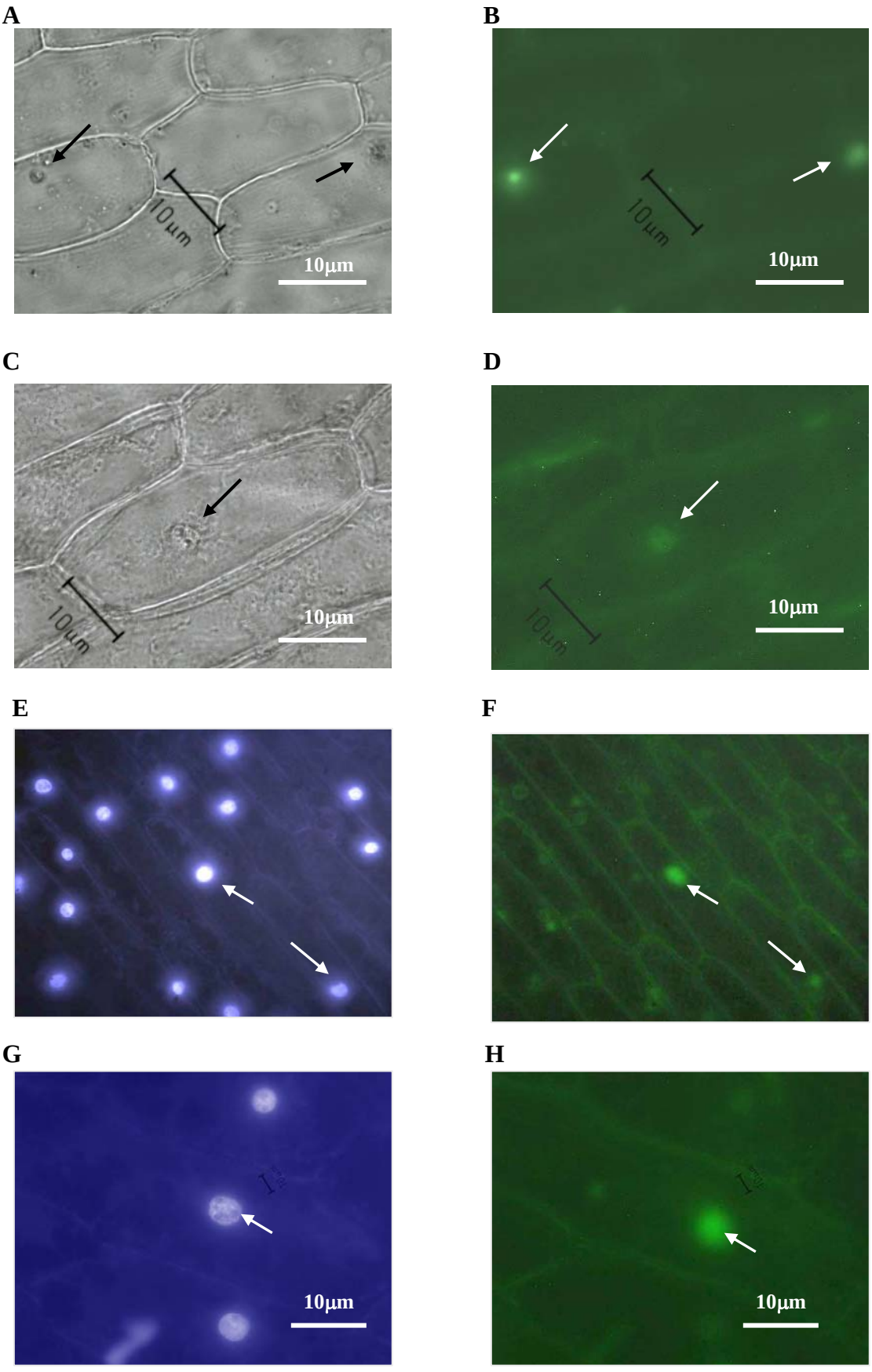
A
10μm
10μm
B
10μm
10μm
C
10μm
10μm
D
10μm
10μm
E
F
G
10μm
H
10μm

Figure 2.2. Localization of AtHD1-GFP fusion protein in onion cells.

(A) and (C) show the onion epidermal cells viewed under white light with phase contrast microscopy. The nuclei are marked by an arrow. **(B) and (D)** show the corresponding view under blue light with specific filter for GFP. The light green spots indicated by the white arrows in **(B) and (D)** correspond to the nuclei seen in **(A) and (C)**, respectively. **(E) and (G)** show the onion cells stained with DAPI and viewed under UV light. The bluish white spots are the nuclei marked with white arrows. **(F) and (H)** show the GFP signals (white arrows) detected in the same areas of **(E) and (G)**, respectively.

using a band-pass filter for detection of green fluorescence signal, the transformed onion cells (about 1 in 20) gave green fluorescence signal which is localized in the nuclei (Figures 2.2F and H). The results indicate that GFP fusion protein can be used to determine the subcellular localization of the target protein which appears to be confined to the nucleus.

Expression of AtHD1-GFP fusion protein in transgenic *Arabidopsis*

Transgenic *Arabidopsis* plants carrying the same *AtHD1-GFP* chimeric gene shown in Figure 2.1 were created by *Agrobacterium*-mediated transformation. These plants were termed **SHG** for the transgene (*35**S**::At**H**D1-**G**FP*) they contain. In the first round of selection for successful transformants, the transformation efficiency was found to be about 1%, which is a typical value for the floral dipping method. The seeds collected from the first generation of transformants (T_0) were germinated in selective medium to generate the T_1 transgenic plants, which were used for the assay of *AtHD1-GFP* gene expression.

Genomic DNA from eight transgenic lines was digested with *EcoR* I, separated by electrophoresis in a 1% agarose gel and transferred to a nylon membrane. The blot was hybridized with radiolabeled probe specific for the GFP coding sequence in the transgene. The results of Southern blot analysis (Figure 2.3B) show that the *35S::AtHD1-GFP* transgene was present in four of the eight transgenic lines.

Total RNA from the four transgenic plants containing the SHG transgene was used in northern blot analysis. The RNA was separated by electrophoresis in a 1.5% agarose gel with 2% formaldehyde and then transferred to a nylon membrane. The same probe used in Southern blot analysis was used in the hybridization. The *AtHD1-GFP* transcript was detected in three of the transgenic samples (Figure 2.4).

Meanwhile, the expression of the AtHD1-GFP fusion protein in the SHG transgenic

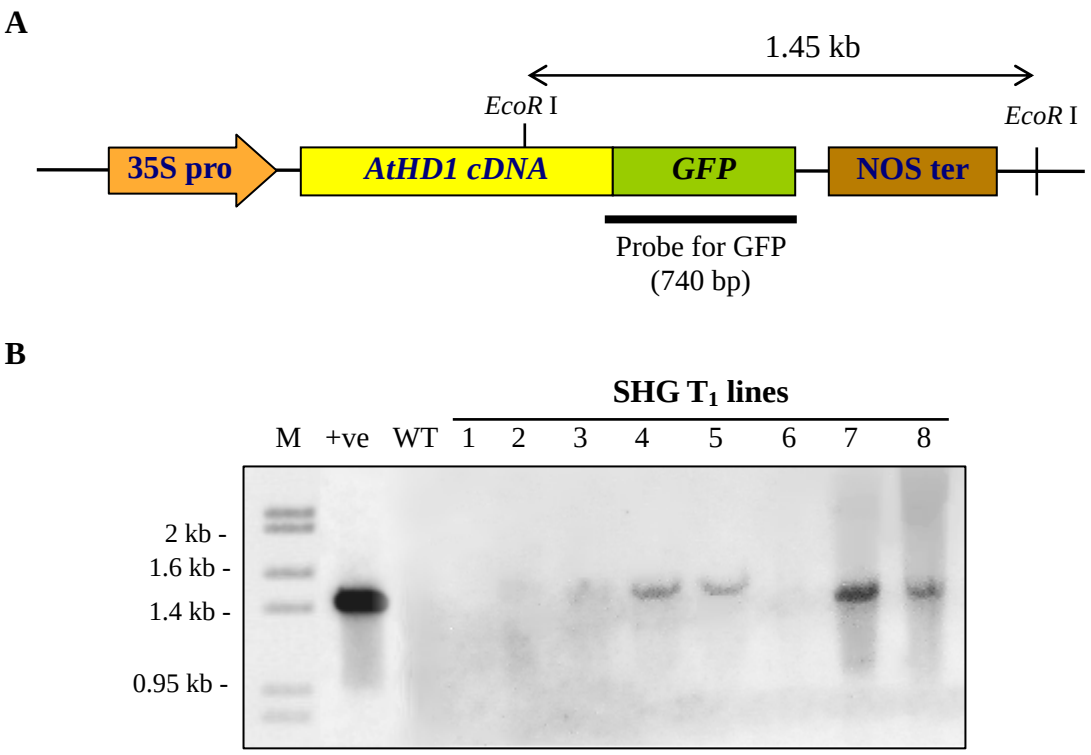

Figure 2.3. Southern blot analysis of SHG transgenic plants.

(A) A 1.45 kb fragment containing the GFP coding sequence was excised from the *35S::AtHD1-GFP* transgene by digestion with *EcoR* I. The excised fragment can be hybridized to a radiolabeled probe prepared by random priming method (Amersham Biosciences).
(B) The presence of *35S::AtHD1-GFP* transgene in eight T_1 plants was detected by Southern blot analysis. Genomic DNA (20µg) from wild type and SHG transgenic plants were digested with *EcoR* I, then separated by electrophoresis in a 1% agarose gel and transferred to Hybond-N+ membrane (Amersham Pharmacia). A radiolabeled probe specific for the GFP sequence was used in hybridization (indicated in Part A). The transgene was detected in four of the SHG T_1 lines. The plasmid pUC18/35S::AtHD1-GFP digested with *EcoR* I was used as a positive control (labeled as +ve). The marker (M) used was Lamda DNA/*EcoR* I + *Hind* III (Promega).

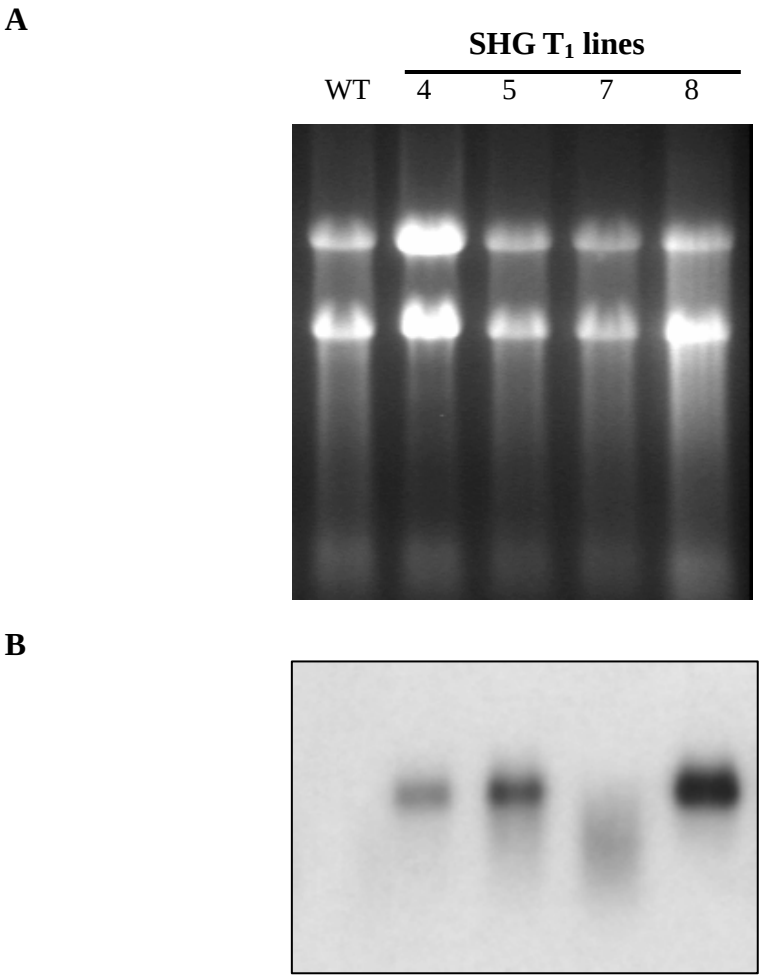

Figure 2.4. Northern blot analysis of SHG transgenic plants.

(A) Total RNA (20 μg) from wild type and SHG transgenic plants (with the presence of transgene verified by Southern blot) was separated by electrophoresis in a 1.5% agarose gel containing 2% formaldehyde and then transferred to a Hybond-N+ membrane (Amersham Pharmacia). The ethidium bromide stained RNA gel depicting the rRNAs is shown.
(B) Northern blot analysis using the radiolabeled probe specific for the GFP sequence showed that the *AtHD1-GFP* transcript was present in three of the SHG T_1 transgenic lines. Transgenic line 7 probably contains the transcript but the RNA was degraded during the experimental processes.

plants was assayed by conventional fluorescence microscopy. Non-green tissues including the roots and flower petals were examined under a dissecting microscope. The expression patterns of the AtHD1-GFP fusion protein in root and flower tissues are shown in Figures 2.5 and 2.6, respectively. Non-green tissues were used because they are free of chlorophyll autofluorescence (red) that will mask the GFP signal (green). When illuminated by blue light and viewed under the microscope, the root and flower tissues of transgenic *Arabidopsis*, but not wild type, gave green light signals which indicate the presence of GFP fusion proteins. The intensity of the GFP signals is highest at the central region of the root and at the veins in the petals. These findings suggest that *AtHD1-GFP* expression is higher in the vascular tissues.

To study the expression and *in vivo* distribution of AtHD1-GFP fusion protein at subcellular level, different tissues of the SHG plants were examined by confocal fluorescence microscopy. Plant tissues, including the roots, leaves, flowers and seeds, from SHG transgenic plants and wild type (WT) plants were viewed under white light using differential interference contrast (DIC) to reveal subcellular structure, then under blue light to reveal GFP fluorescence signals, and finally stained with DAPI to reveal the nuclei under UV illumination. The red autofluorescence of chlorophyll in green tissues were partially eliminated by a band-pass filter for GFP signals. Figures 2.7 to 2.13 show the expression of AtHD1-GFP fusion protein in the epidermal cells of developing seed coat, the guard cells and mesophyll cells of leaves, the epidermal cells (including a hair cell) of roots, and the epidermal cells of style in SHG transgenic and wild type *Arabidopsis*. The results not only confirm the findings of particle bombardment experiments that AtHD1 is localized in the nucleus, but also give insight into the possible function and regulation of AtHD1.

A. SHG roots under white light

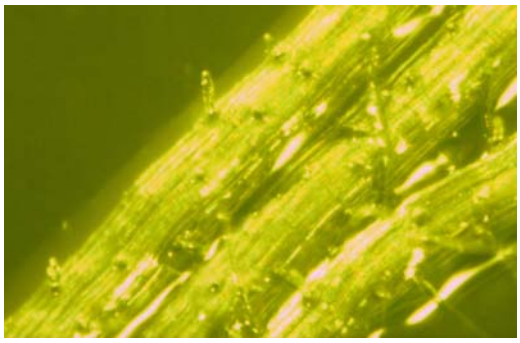

B. SHG roots under blue light

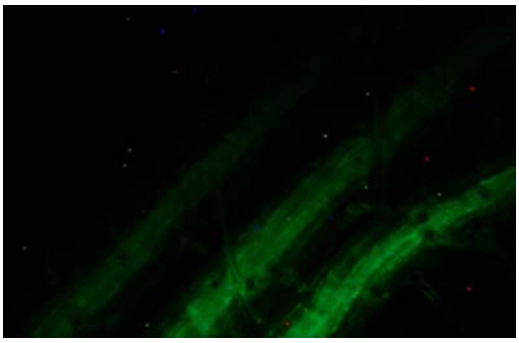

C. WT roots under white light

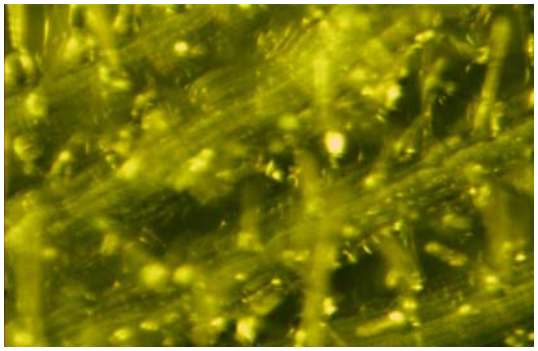

D. WT roots under blue light

Figure 2.5. Expression of AtHD1-GFP fusion protein in *Arabidopsis* root tissues.

Root tissues of transgenic (SHG) and wild type (WT) *Arabidopsis* seedlings were viewed under white light (**A and C**, respectively) and blue light (**B and D**, respectively). Fluorescent signal of GFP (green signal) is visible in the root tissues of transgenic *Arabidopsis* **(B)** but not in the wild type **(D)**. The green fluorescence signal in the roots of SHG plant appears to be confined to the central part that corresponds to the vascular tissues.

A. Petal of SHG plant under white light

B. Petal of SHG plant under blue light

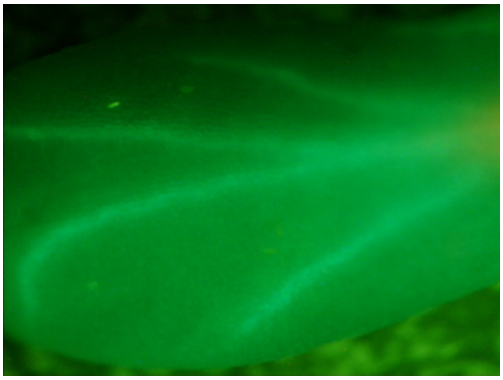

C. Petal of WT plant under white light

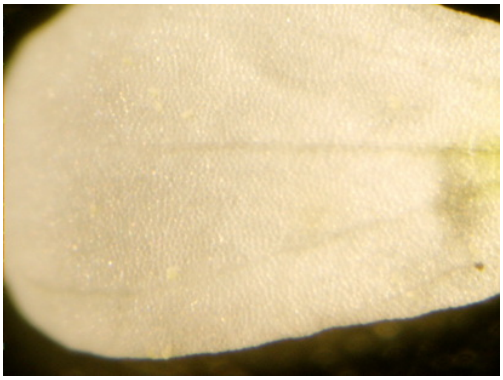

D. Petal of WT plant under blue light

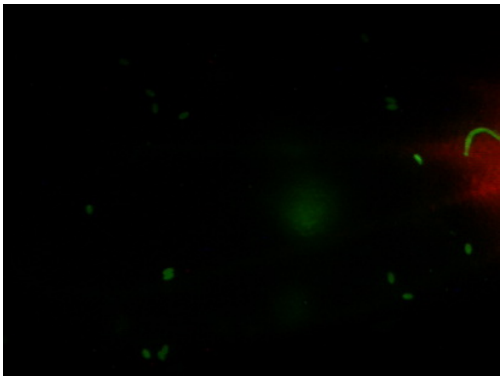

Figure 2.6. Expression of AtHD1-GFP fusion protein in *Arabidopsis* flower tissues. Petals of transgenic (SHG) and wild type (WT) *Arabidopsis* were viewed under white light (**A and C**, respectively) and blue light (**B and D**, respectively). Fluorescent signal of GFP (green signal) is visible in the petal of transgenic *Arabidopsis* **(B)** but not in the wild type **(D)**. The green fluorescence signals in the petal of the SHG plant are particularly strong in the vein consisting of vascular tissues.

A. SHG seed; DIC

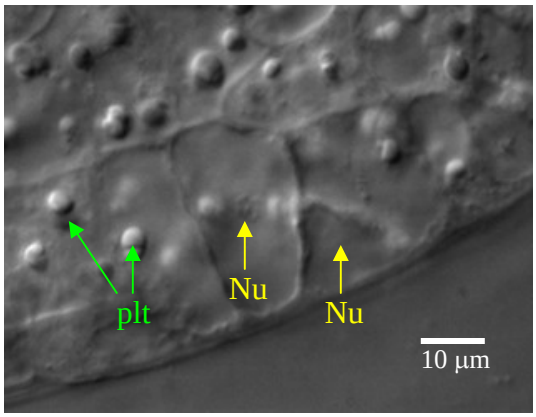

D. WT seed, DIC

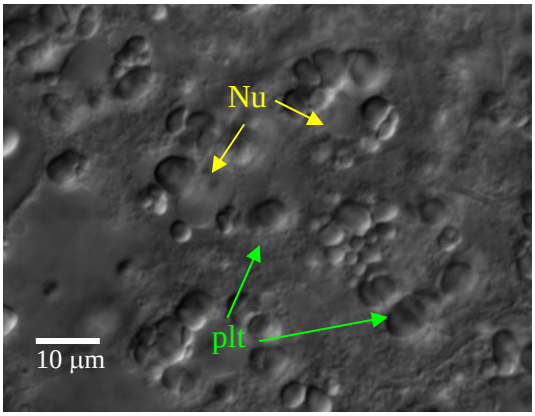

B. SHG seed stained with DAPI; UV

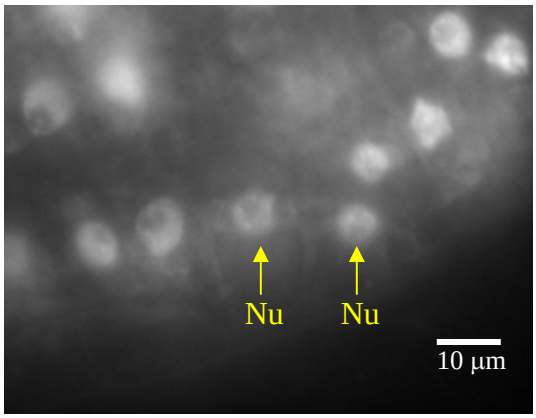

E. WT seed stained with DAPI; UV

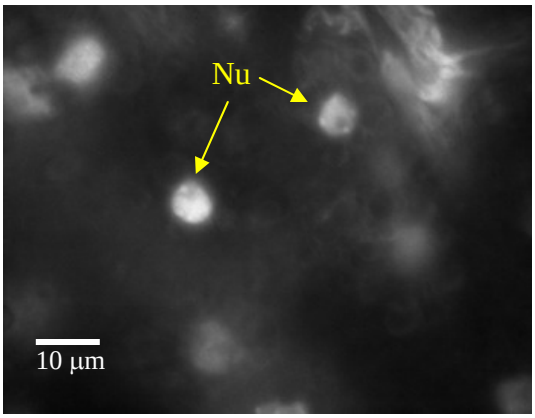

C. SHG seed; blue light with GFP filter

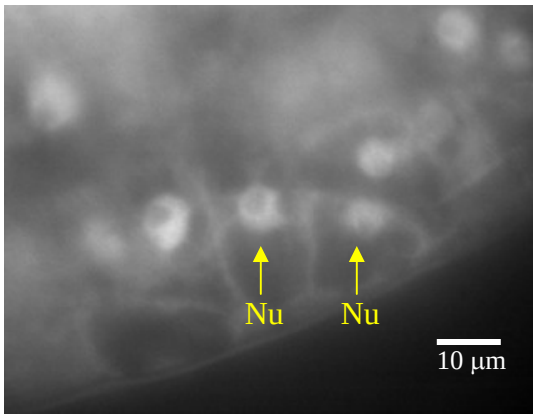

F. WT seed; blue light with GFP filter

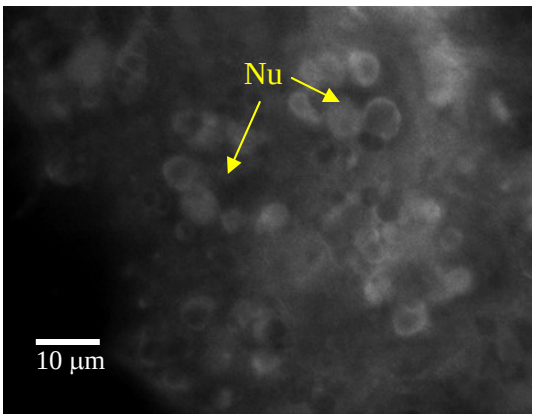

Figure 2.7. Expression of AtHD1-GFP fusion protein in developing seed coat.

The cells in the seed coat of immature seeds were examined by confocal microscopy. **(A) and (D)** show the differential interference contrast (DIC) images of the transgenic (SHG) and wild type (WT) plants, respectively. The plastids (plt) and nuclei (Nu) are labeled. To visualize the nuclei, the cells were stained with DAPI and viewed under UV light. The fluorescence nuclei are clearly visible in the SHG **(B)** and WT **(E)** plants. When viewed under blue light with a GFP filter, green fluorescence signals are detected in the nuclei of SHG plant cells **(C)**, but not in the WT **(F)**. The background fluorescence is caused by autofluorescence of the chlorophyll in the chloroplasts.

A. SHG guard cell; DIC

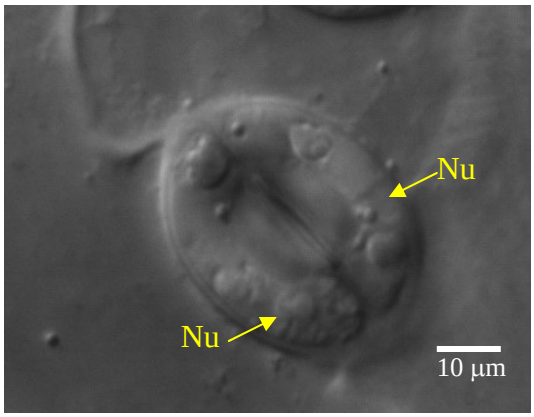

D. WT guard cell, DIC

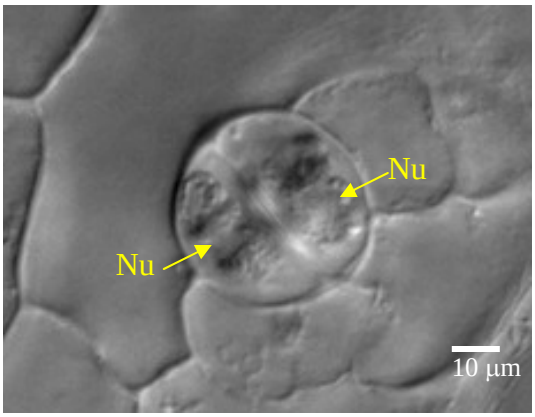

B. SHG guard cell stained with DAPI; UV

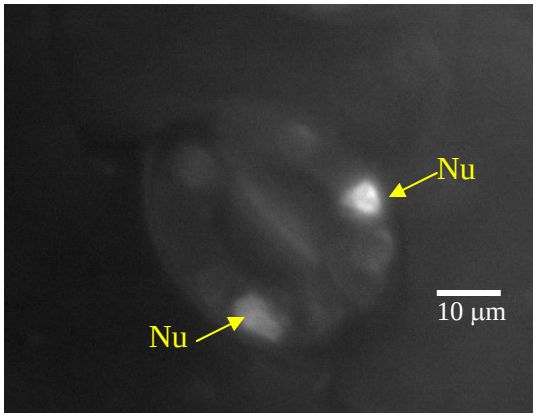

E. WT guard cell stained with DAPI; UV

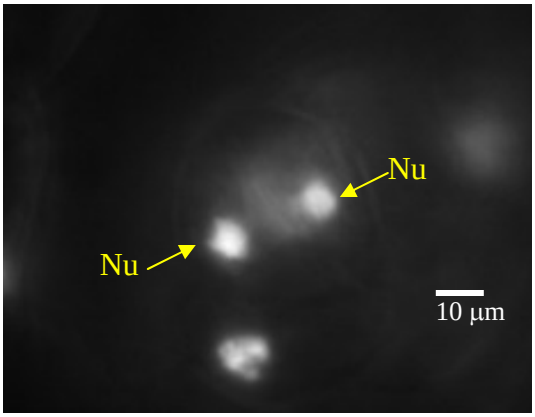

C. SHG guard cell; blue light with GFP filter

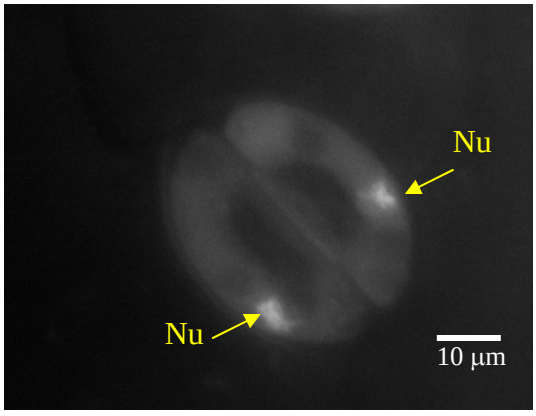

F. WT guard cell; blue light with GFP filter

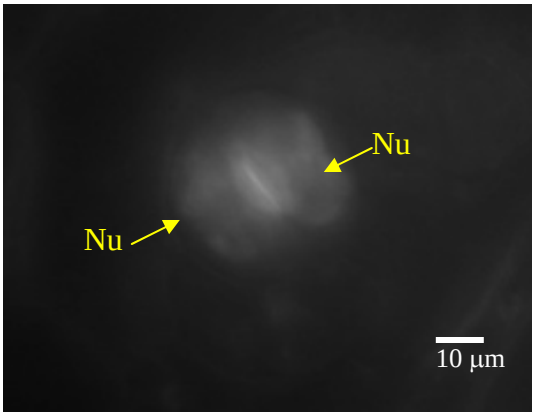

Figure 2.8. Expression of AtHD1-GFP fusion protein in leaf guard cells.

The guard cells in leaves were examined by confocal microscopy. The nuclei are not clearly visible in the DIC images (**A and D** for SHG and WT plants, respectively), but are very distinct under UV light when stained with DAPI (**B and E** for SHG and WT plants, respectively). The GFP signals are detected in the nuclei of SHG plant **(C)**, but not in the WT plant **(F)**.

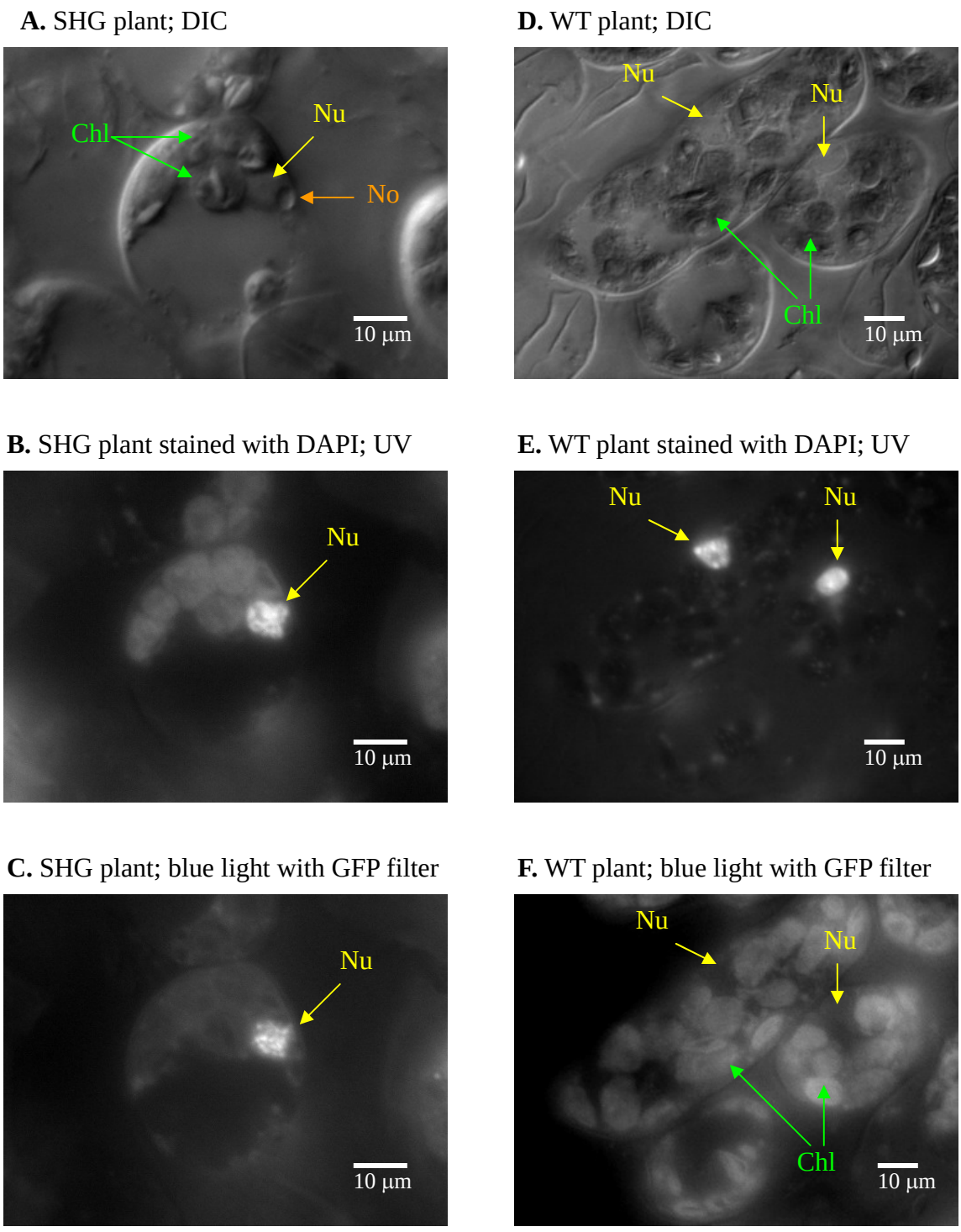

Figure 2.9. Expression of AtHD1-GFP fusion protein in leaf mesophyll cells.

The mesophyll cells in the leaves were examined by confocal microscopy. The nuclei (Nu) and chloroplasts (Chl) are distinct in the DIC images of SHG **(A and B)** and WT plants **(D and E)**. The nucleolus (No) is also visible in the DIC image of the SHG plant. Green fluorescence signal can be detected in the nucleus of the SHG plant **(C)**, while only autofluorescence of the chloroplasts can be seen in the WT plant **(F)**.

A. SHG root; DIC

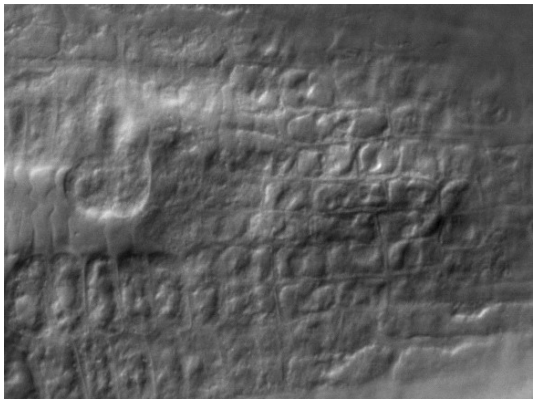

D. WT root; DIC

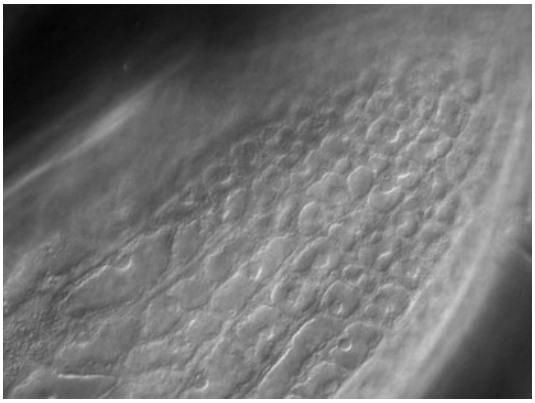

B. SHG root stained with DAPI; UV

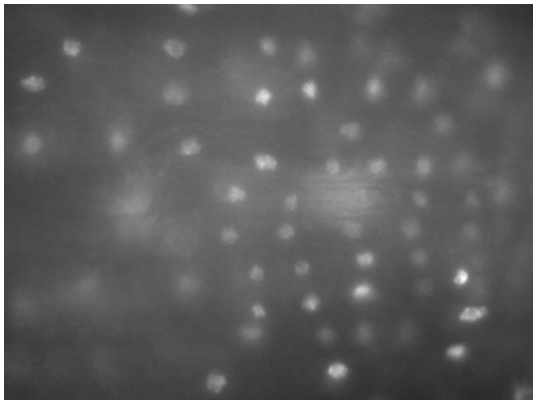

E. WT root stained with DAPI; UV

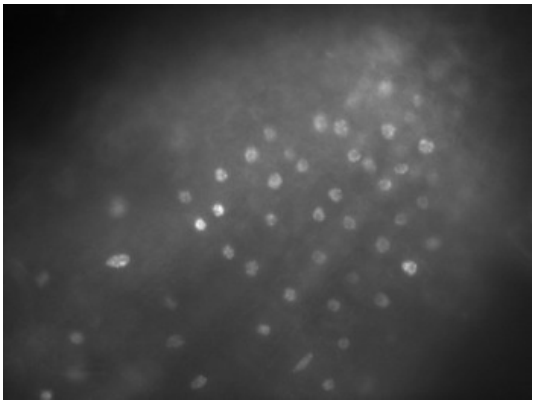

C. SHG root; blue light with GFP filter

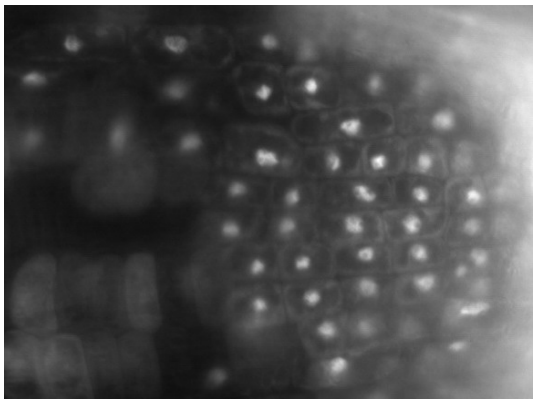

F. WT root; blue light with GFP filter

Figure 2.10. Expression of AtHD1-GFP fusion protein in root epidermal cells.

The epidermal cells in the roots were examined by confocal microscopy. The nuclei are visible in the DIC and DAPI-stained images. GFP signals are localized in the nuclei of the root epidermal cells in the SHG plant **(C)**, while no signals are detected in the WT plant **(F)**. Since there are no chloroplasts in the roots, autofluorescence interference is minimal.

A. SHG root; DIC

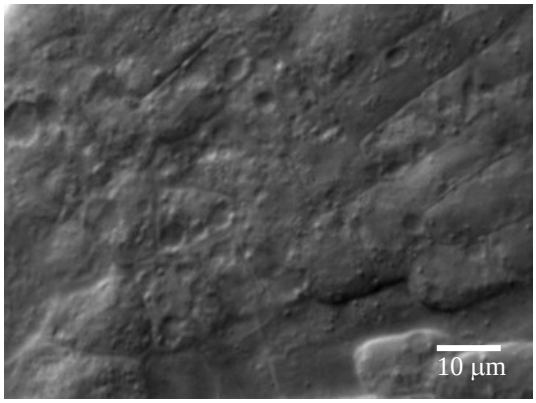

D. SHG root hair; DIC

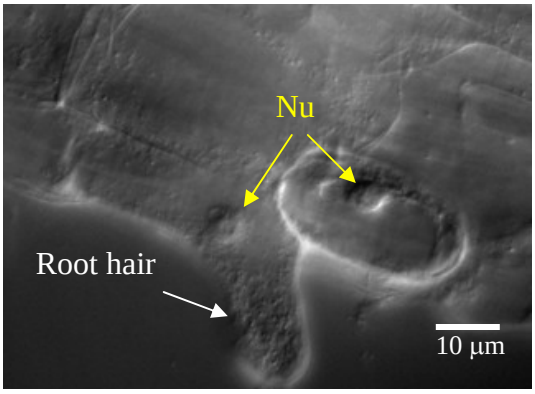

B. SHG root stained with DAPI; UV

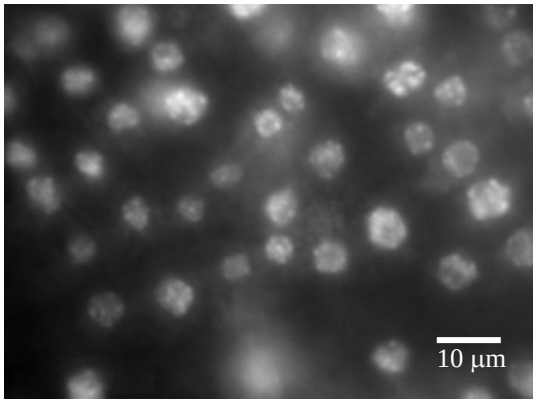

E. SHG root hair stained with DAPI; UV

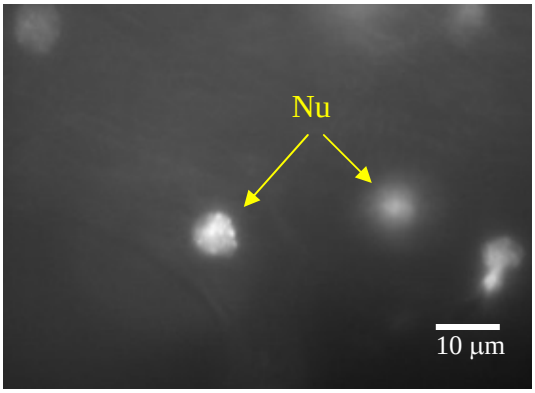

C. SHG root; blue light with GFP filter

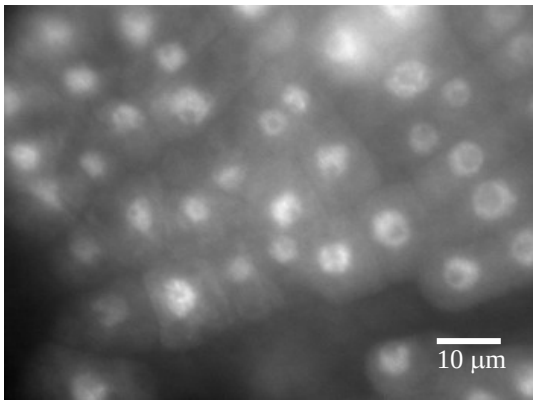

F. SHG root hair; blue light with GFP filter

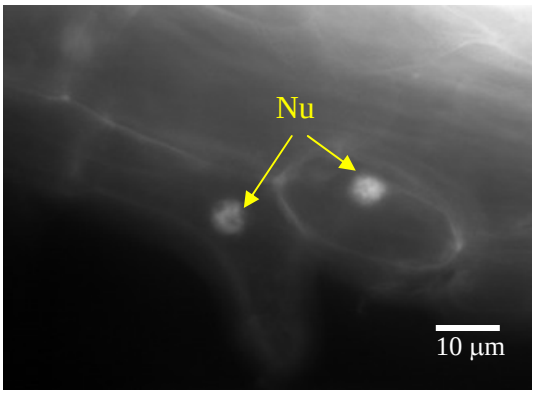

Figure 2.11. Expression of AtHD1-GFP fusion protein in root epidermal and hair cells.

The epidermal cells **(A, B and C)** and root hair cell **(D, E and F)** in the roots of SHG plants were examined by confocal microscopy. The nuclei are visible in the DIC and DAPI-stained images. GFP signals can be detected in the nuclei of epidermal and root hair cells of the SHG plants. Moreover, the AtHD1-GFP fusion protein appears to be excluded from the nucleolus as the central parts of the nuclei in root epidermal cells **(B and C)** appear dark.

A. SHG style; DIC

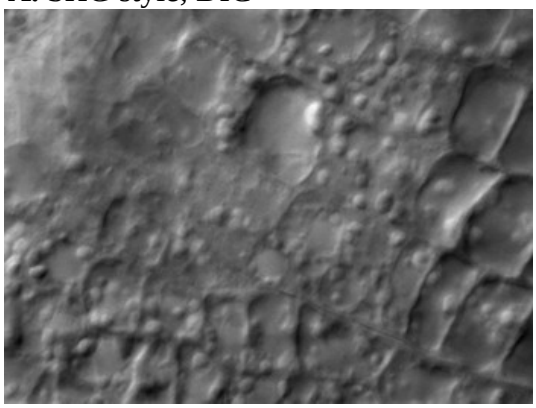

B. SHG style stained with DAPI; UV

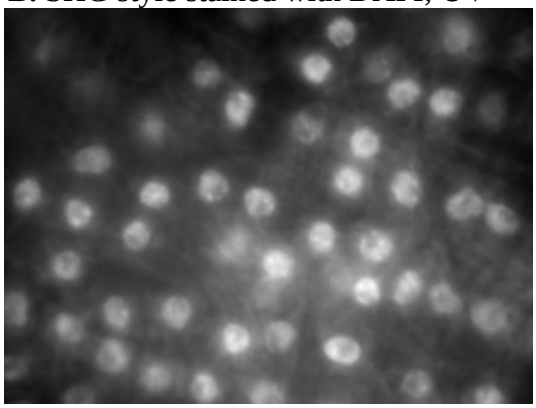

C. SHG style; blue light with GFP filter

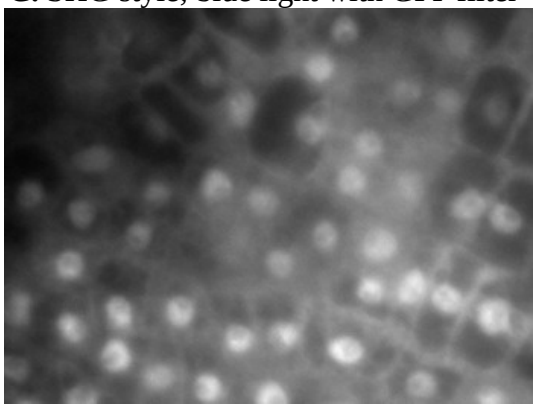

D. SHG leaf; DIC

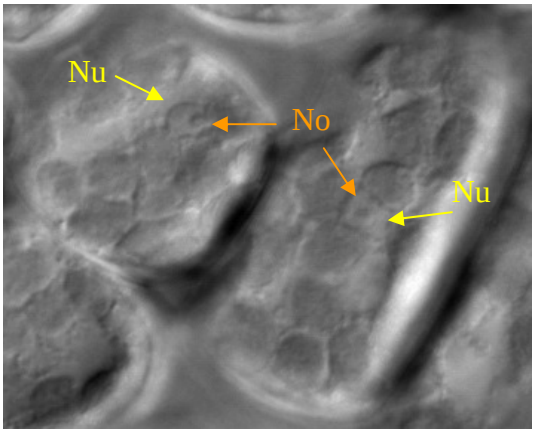

E. SHG leaf; blue light with GFP filter

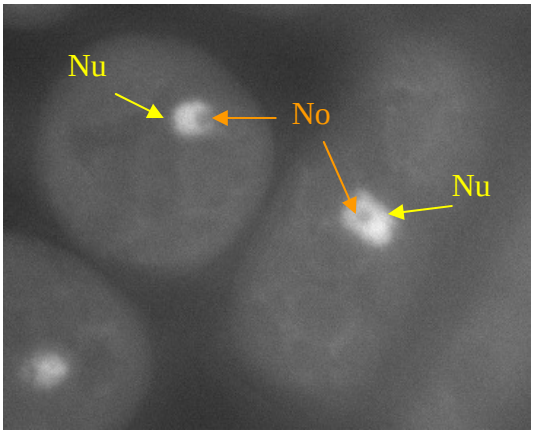

Figure 2.12. Expression of AtHD1-GFP fusion protein in style epidermal cells and leaf mesophyll cells.

The epidermal cells **(A, B and C)** in the style and mesophyll cells **(D and E)** in the leaf of SHG plants were examined by confocal microscopy. While the nuclei are barely visible in the DIC image of style epidermal cells **(A)**, the nuclei and nucleolus are visibly distinct in that of leaf mesophyll cells **(D)**. The DAPI and GFP fluorescence signals are localized in the nucleus and appear to be excluded from the nucleolus in the style epidermal cells **(B and C)**. In the leaf mesophyll cells, the GFP signals are also localized in the nucleus and appear to be excluded from the nucleolus.

A. SHG leaf; DIC

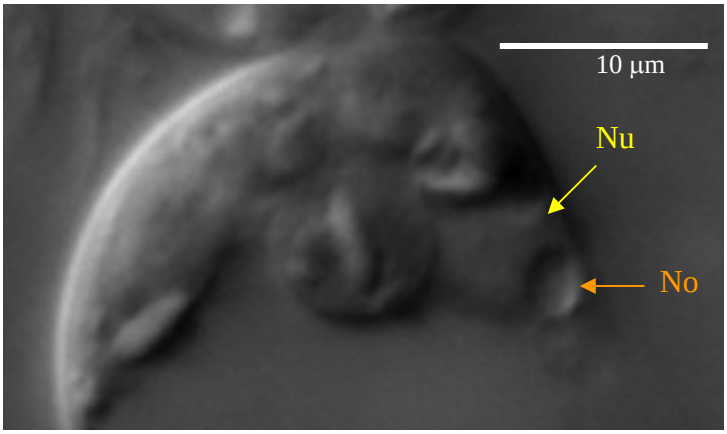

B. SHG leaf stained with DAPI; UV

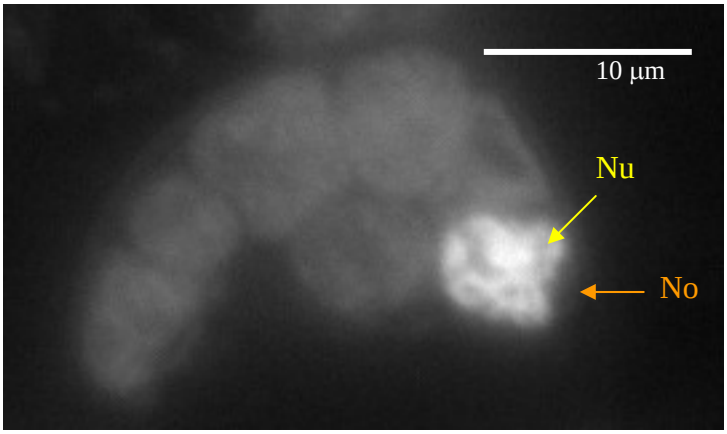

C. SHG plant; blue light with GFP filter

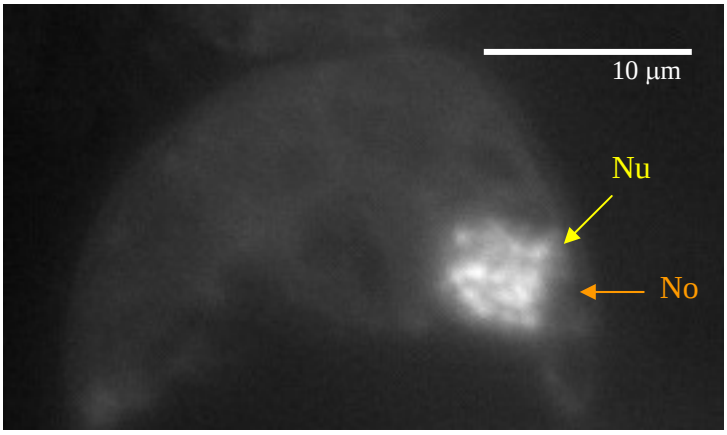

Figure 2.13. Distribution pattern of AtHD1-GFP fusion protein in the nucleus of a leaf mesophyll cell (SHG plant) in the prophase of cell division.

In **(A)**, the nucleus and nucleolus are distinct in the DIC image of a mesophyll cells in SHG plant. The DAPI-stained image in **(B)** shows that the cell was in the prophase of cell division and the organization of chromatin into chromatids is visible. In **(C)**, the GFP signals appear as speckles that are localized in the nucleus but excluded from the nucleolus.

In most, if not all, of the cells in SHG plant tissues, the AtHD1-GFP fusion protein is localized in the nucleus and almost absent from the cytoplasm. This suggests that AtHD1 is imported to the nucleus soon after it is synthesized, and is not likely to be regulated by nuclear-cytoplasmic shuttling. In addition, AtHD1-GFP protein appears to be excluded from the nucleolus as evident in Figures 2.7, 2.12 and 2.13 that reveal the absence of GFP and DAPI fluorescence signals in the nucleolus. This is in contrast to the HD2-type HDACs which have been found to be localized in the nucleolus in maize (Lusser, 1997) and Arabidopsis (Lawrence et al., 2004).

The image of a mesophyll cell at early prophase of the cell cycle was captured and is shown in Figure 2.13. From the DAPI fluorescence image (Figure 2.13B), it can be seen that the chromatin began to condense into chromatids, and the nucleolus was set aside in the nucleus. The corresponding GFP fluorescence image (Figure 2.13C) shows that the AtHD1-GFP protein aggregated into speckles. It appears that the AtHD1-GFP protein is associated with the condensing chromatids and this suggests a role for AtHD1 in mitosis.

DISCUSSION

Histone deacetylase 1 from *Arabidopsis* (AtHD1) is supposed to be a nuclear protein that modifies its substrate histone in the chromatins. However, there is no experimental evidence for its nuclear localization. Moreover, some histone deacetylases such as the human HDAC3, 4, 5, 7 and 9 are regulated by active transport out of the nucleus, while other HDACs like HD2 in maize are localized in the nucleolus. In order to study the subcellular localization and protein trafficking of AtHD1 *in vivo*, a *GFP* coding sequence was fused to the 3'-end of the *AtHD1* cDNA and the resulting chimeric gene was put under the control of CAMV 35S promoter for expression in plants.

To test the feasibility of using GFP fusion protein in the determination of AtHD1 subcellular localization before the stable expression in *Arabidopsis*, a transient expression assay using particle bombardment method was performed. Onion epidermal cells were used because they are large, transparent and free of autofluorescence interference from chlorophyll. Besides, a single epidermal layer of cells can be easily peeled off from the onion scale leaves for examination. The fluorescence microscopy images of the onion cells after particle bombardments show that AtHD1-GFP fusion protein can be expressed in plant cells, and appears to be localized in the nuclei.

To study the *in vivo* localization pattern of AtHD1 in *Arabidopsis*, the *35S::AtHD1-GFP* expression cassette was introduced into *Arabidopsis* plants by *Agrobacterium*-medium transformation. Successful transformants were selected and regenerated into intact transgenic plants. The intact living tissues of the mature SHG transgenic plants (four-week old) were dissected and examined by confocal scanning microscopy for the expression of AtHD1-GFP fusion protein. The results indicate that the AtHD1-GFP protein expressed in all the tissues examined, including roots, leaves, flowers and seeds. Being consistent with the result of particle bombardment experiments with onion cells, AtHD1-GFP protein was found to be localized in the nuclei of *Arabidopsis* cells. Further examination of the AtHD1-GFP localization patterns indicates that the protein is likely to be excluded from the nucleolus, and appear to be associated with the condensing chromatin during mitosis. This suggests that AtHD1 may play a role during mitosis in deacetylating histones for the compaction of chromatin.

The GFP protein used in this experiment is an engineered one called S65T GFP which contains a mutation in the chromophore with the serine 65 being replaced by

threonine, resulting in enhanced brightness, faster chromophore formation and slower photobelaching (Heim et al., 1995). The S65T and other types of GFP proteins without a targeting sequence have been shown to accumulate and distribute evenly in *Arabidopsis* and onion plant cells due to their small sizes (Chiu et al., 1996; Koroleva et al., 2004; Lawrence et al., 2004). The size exclusion limit of the nuclear pores has been estimated to be 40 to 60 kDa (Grebenok et al., 1997; Haasen et al., 1999). GFP protein having a molecular weight of 27 kDa can diffuse across the nuclear envelope while AtHD1-GFP protein that is 83 kDa in size should remain in the cytoplasm if AtHD1 lacks a nuclear localization signal. Therefore, although control experiments with the expression of only the GFP protein were not included in both of the transient and stable expression experiments, the conclusion for the nuclear localization of AtHD1 should still be valid.

MATERIALS AND METHODS

Construction of *AtHD1-GFP* chimeric gene

The *AtHD1* full-length cDNA was amplified from a clone in a pBlueScript plasmid by PCR using the following primers:

Forward primer: 5’-GC GTCGAC ATGGATACTGGGGGCAATTC-3’

Reverse primer: 5’-CATG CCATGG CTGTTTTAGGAGGAAACGCCTG-3’

The forward primer adds a *Sal* I site (underlined) to the 5’-end of the PCR product, while the reverse primer omits the stop codon of the *AtHD1* cDNA and adds a *Nco* I site (underlined) to the 3’-end of the amplified DNA. The resulting *AtHD1* cDNA fragment was cloned into the pUC18/CaMV35S-GFP(S65T) plasmid so that the 3’-end of *AtHD1* coding sequence was fused to the 5’-end of GFP in frame, and the whole chimeric gene lied downstream of and was under the control of the cauliflower mosaic virus (CaMV) 35S promoter.

The expression cassette of *35S::AtHD1-GFP* was excised from the pUC18 plasmid by *Xba* I and *EcoR* I double digestion and then subcloned into the binary vector pBI101. The sequence of the chimeric *AtHD1-GFP* gene in the pBI101 plasmid was checked by DNA sequencing and it was found to be correct and in-frame. The pBI101/35S::AtHD1-GFP plasmid was introduced into *Agrobacteria* by electroporation using the Gene Pulser apparatus (Biorad) at 25 μF, 2.5 kV and 600 ohms.

Transient expression in onion

For the transient expression assays of *AtHD1-GFP* chimeric gene, the pUC18/35S::AtHD1-GFP plasmid was introduced into onion cells by particle bombardment. Fresh onion bulbs purchased from local grocery store were cut into slices of 1 cm^2 and placed on the central area of a petri dish with 0.9% phytal agar as supporting medium. Tungsten particles of 1.1 μm in diameter were prepared and coated with plasmid DNA according to BioRad's protocol. Bombardments were performed using the Biolistic PDS-1000/He Particle Delivery System (BioRad) with the following parameters:

Holder level: 2

Sample level: 4

Gap distance: 0.63 cm

Target distance: 6 cm

Helium pressure: 1100 psi

Chamber vacuum: 27 inches Hg (~ 0.06 atm)

Amount of DNA/bombardment: 1μg

Amount of macrocarrier/bombardment: 500 μg of tungsten particle

Each sample received two times of bombardment, after which the samples were incubated in

a growth chamber at 25°C for 20-24 hours. The expression of GFP fusion protein was examined using the Olympus AX70 fluorescence microscope.

Transformation of *Arabidopsis*

Ten *Arabidopsis thaliana* (Columbia) plants were transformed with *Agrobacteria* harboring the binary vector pBI101/35S::AtHD1-GFP using the floral dip method (Clough and Bent, 1998). Seeds of T_0 plants were selected by germination on MS medium (Sigma) with 50 mg/L kanamycin. Successful transformants (T_1 plants) were regenerated and grown in soil. Transformation efficiency is about 1%. The presence of *AtHD1-GFP* transgene was detected in the T_1 plants by PCR using the following primers flanking the GFP coding sequence:

UP-GFP-1: ATGGTGAGCAAGGGCGAG

DN-GFP-720: TTACTTGTACAGCTCGTCCA

All plants were grown in a growth chamber with a cycle of 14 hr light at 22°C and 10 hr dark at 18°C.

Nuclei acid isolation and detection

Genomic DNA was isolated from *Arabidopsis* leaves using the Cetyltrimethylammonium bromide (CTAB) method described by Doyle *et al*. (1990). Briefly, 0.3 g of leaf tissues was ground in 600 μl of 2% CTAB buffer (2% CTAB, 0.1 M Tris-HCl, pH 8.0, 1.4 M NaCl, 20 mM EDTA and 0.2% β-mercaptoethanol) and the homogenate was incubated at 60°C for 1 hour with constant mixing. Chloroform/isoamyl alcohol mixture (24:1, v/v) (500 μl) was added to the homogenate followed by centrifugation at 14,000 rpm and 4°C for 15 minutes. The aqueous layer (500 μl) was

transferred to a new microfuge tube containing 500 μl of cold isopropanol and was kept at -20°C for 1 hour. The DNA pellet was precipitated by centrifugation and washed with 75% ethanol. After 5 minutes of vacuum drying, the pellet was resuspended in distilled water. Total RNA was extracted from *Arabidopsis* leaves by TRIZOL reagent (Invitrogen) according to the manufacturer's protocol.

In northern and Southern blot experiments, total RNA or genomic DNA digested with *EcoR* I was fractionated by electrophoresis in 1.5% agarose-formaldehyde or 1% agarose gels, respectively. The RNA or DNA was transferred to Hybond-N+ nylon membrane (Amersham Pharmacia) and then hybridized with DNA probe prepared by a random priming method (Amersham) with radioactive label (^{32}P-dCTP). Hybridization was performed according to the method described by Church and Gilbert (Church and Gilbert, 1984). The DNA and RNA blots were washed twice with 2× washing solution (2× SSC, 0.1% SDS) for 15 minutes at room temperature, and then washed twice with 0.5× washing solution (0.5× SSC, 0.1% SDS) for 15 minutes at 65°C. Detection of hybridization signals was carried out by the PhosphorImager BAS1800II (Fuji, Tokyo, Japan).

Detection of GFP signals by fluorescence microscopy

Transient expression of AtHD1-GFP fusion protein in onion epidermal cells was detected with the Olympus AX7 fluorescence microscope. After particle bombardments and incubation, a single epidermal layer of the onion scale leaf disc was peeled off and put on a slide for examination under 60× or 100× magnification. Nuclei were stained by adding one drop of DAPI staining solution (1μg/ml DAPI in PBS) to the onion epidermal cells and incubated for at least 5 minutes. DAPI fluorescence images were obtained by UV illumination of the specimen and a band-pass filter for DAPI. Green fluorescence signals

were obtained by blue light illumination and a band-pass filter for GFP.

Stable expression of AtHD1-GFP fusion protein in SHG transgenic plants was detected by confocal scanning microscopy. The images were acquired by Stanislav Vitha in the Microscopy and Imaging Center, Texas A & M University. Dissected intact tissues were stained with DAPI staining solution and examined by differential interference contrast (DIC) and fluorescence microscopy sequentially using the Zeiss Axiophot microscope with 40× or 100× magnification. Images of tissues at different confocal layers (Z-series) were taken with a 0.5 μm step size. GFP fluorescence images were acquired using a GFP filter set (Chroma Technologies, excitation HQ470/20, dichroic Q495LP, emission HQ525/50) and a Photometrics Coolsnap digital camera.

CHAPTER III

PRODUCTION OF RECOMBINANT AtHD1 AND HDAC ACTIVITY ASSAY

INTRODUCTION

The histone deacetylase activity of AtHD1 was first demonstrated in transgenic plants that had *AtHD1* knocked out by either antisense approach or T-DNA insertion in exon 2 of *AtHD1* gene. In these plants, the expression of *AtHD1* was blocked, resulting in a 10-fold increase in the histone acetylation levels and this feature was heritable in selfing progeny (Tian and Chen, 2001; Tian et al., 2003). To further characterize the enzyme, we attempted to produce recombinant AtHD1 to demonstrate its histone deacetylase activity *in vitro* and to determine its substrate specificity.

To obtain the target protein for characterization, the ideal source would be the native protein purified from the organism itself. The best-studied HDACs in plants including maize HD2, HD1A and HD1B were first purified from maize embryoes using a combination of different chromatography methods and they were all found to be active (Borsch et al., 1996a; Borsch et al., 1996b; Lusser et al., 1997). However, this method is expensive, time-consuming, labor intensive and requires a large amount of plant materials (usually in kilograms). Therefore, production of recombinant proteins in well-established expression systems is usually used. In the choice of protein expression system, the bacterial system is preferred unless the target protein is known to require post-translational processing for full activity. This is because bacteria are easily transformed, grow rapidly, express high levels of

recombinant proteins and are inexpensive to maintain. However, the recombinant proteins produced in bacteria may aggregate and become trapped in insoluble inclusion bodies, and will not have any eukaryotic post-translational modifications. An alternative to bacterial system is yeast expression system which is also fast and expresses high levels of recombinant proteins with most of the eukaryotic post-translational modifications. However, the transfection of and protein extraction from yeast cells can be difficult processes. A popular system for mass production of eukaryotic proteins is the baculovirus expression system, which involves the use of baculovirus to infect and multiply in cultured insect cells. The recombinant proteins can be expressed in high levels and contain most, if not all, of the post-translational modifications in higher eukaryotes. However, insect cells grow more slowly than bacterial and yeast cells and are more expensive to maintain.

In this study, recombinant AtHD1 was produced using a bacterial expression system for protein characterization. The histone deacetylase activity of the recombinant protein was determined by an assay using [^{3}H]-acetate-labeled histone peptides as substrates. The expression profiles of the RPD3-type *HDAC*s in *Arabidopsis*, including *HDA6*, *7*, *9* and *19* (*AtHD1*), were studied by RT-PCR analysis. Recombinant HDA6, 7, 9 and 19 proteins were produced by the baculoviral expression system for study of HDAC activity.

RESULTS

Production of recombinant AtHD1 in bacterial system

Escherichia coli (strain BL21) containing a pET21b expression vector that harbors a chimeric *AtHD1* gene was provided by my colleague Lu Tian. As shown in Figure 3.1A, the construct consists of a hexahistidine tag (6xHis) for protein purification, a maltose binding protein (MBP) for increasing the solubility of the recombinant protein so as to prevent the

formation of inclusion bodies in bacterial cells, a tobacco etch virus (TEV) cleavage site for removing the 6xHis tag and MBP fragment, and the *AtHD1* cDNA sequence. The chimeric gene was put under the control of the inducible T7 promoter.

Bacterial cells harboring the expression vector were cultured in NZCYM broth and expression of the *AtHD1* chimeric gene was induced by the addition of IPTG. Total proteins at different post-induction time points were extracted by sonication and then separated on a 15% SDS polyacrylamide gel. The recombinant protein of 100 kDa can be seen as a prominent band as early as 2 hours post-induction and reached the maximum accumulation level at 10 hours post-induction (Figure 3.1B). The recombinant protein was then purified by affinity column with Ni-NTA resins specific for 6xHis tag followed by further purification by amylose-conjugated agarose resins specific for the MBP fragment in the rAtHD1 protein. The 6xHis tag and MBP segment was removed from the recombinant protein by TEV protease (Figure 3.1C).

Expression profiles of RPD3-like HDACs in *Arabidopsis*

One-step RT-PCR was used to detect the expression of the four RDP3-like HDAC genes, including *HDA6, 7, 9* and *19*, in seedlings, roots, stems, leaves, flowers and siliques of two *Arabidopsis thaliana* ecotypes, Columbia (col) and Wassilewskija (ws). The result is shown in Figure 3.2.The total RNA from different tissues was treated with DNase to remove contaminating genomic DNA. PCR using the total RNA as templates and specific primers for actin did not yield any DNA products, indicating that the total RNA is free of genomic DNA contamination. The expression of actin was used as an internal control for RT-PCR analysis.

The result of RT-PCR analysis shows that the four RPD3-like HDAC genes show

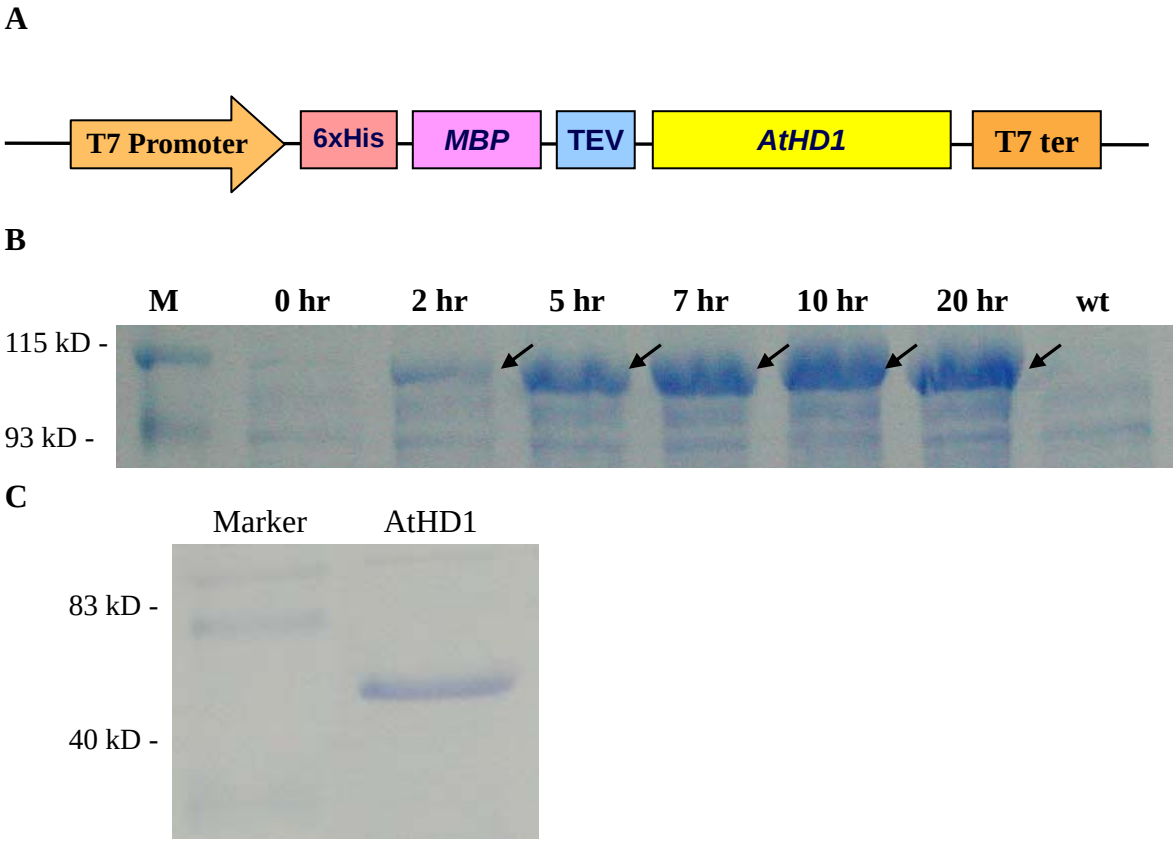

Figure 3.1. Expression of recombinant AtHD1 in *E. coli*.

(A) Expression cassette of chimeric *AtHD1* gene driven by the inducible viral T7 promoter. Upstream of *AtHD1* coding sequence there is a hexa-histidine (6×his) tag for purification by affinity column, a maltose-binding protein (MBP) segment for increasing the solubility of the recombinant protein, and a tobacco etch virus (TEV) protease cleavage site for removal of the 6×His-MBP segment.
(B) Expression profile of recombinant AtHD1 protein (indicated with arrows) at different time points after the addition of IPTG to the bacterial culture. Recombinant AtHD1 protein (~100 kD) accumulated to highest level after 10 hours of induction.
(C) Recombinant AtHD1 protein was purified from bacterial crude protein extract by Ni-NTA affinity column followed by amylose affinity column. The rAtHD1 protein was subsequently cleaved by TEV protease to remove the 6xHis-MBP tag. The AtHD1 protein of 57 kDa was visible as a single prominent band in the SDS-PAGE gel stained with Coomassie blue.

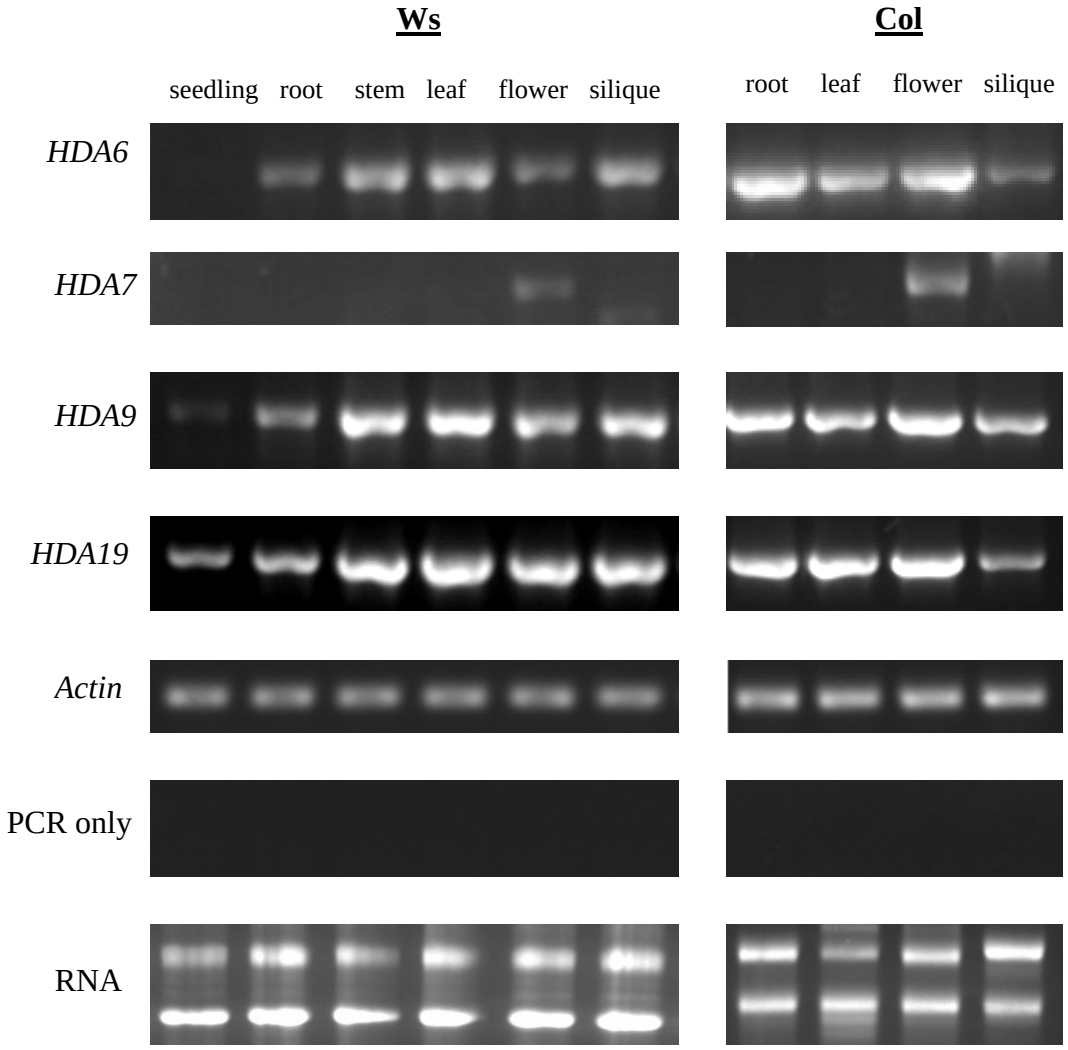

Figure 3.2. Expression profiles of RPD3-like *HDAC*s in *Arabidopsis thaliana.*

Total RNA from different tissues of two *Arabidopsis thaliana* ecotypes, Wassilewskija (Ws) and Columbia (Col), was treated with DNase I and then used for RT-PCR analysis of expression of RDP3-like HDAC genes. Actin was used as an internal control. PCR using total RNA as a template was used to show the absence of contaminating genomic DNA.

differential expression in different tissues and ecotypes of *Arabidopsis*. In general, *HDA19* (*AtHD1*) has the highest expression levels among the four RPD3-like HDACs genes, followed by *HDA9* and *HDA6*. *HDA7* has very low expression levels in flowers only. When examined in detail, *HDA6* in *Arabidopsis* ecotype Wassilewskija (ws) has a higher expression level in leaves, stems and siliques than in roots and flowers. But in Columbia (col), *HDA6* has a higher expression level in root, leaf and flower than in siliques. The expression of *HDA7* is very low and is flower-specific in ws and col. For *HDA9* in ws, it has a higher expression levels in leaves, stems, flowers and siliques, lower in roots, and very low in seedlings. In col, *HDA9* has similar expression levels in roots, leaves, flowers and siliques. For *HDA19* (*AtHD1*) in ws, it has higher expression levels in leaves, stems, flowers and siliques, and lower levels in roots in seedlings. In col, *HDA19* has higher expression levels in roots, leaves and flowers, and a bit lower in siliques.

Production of RPD3-like HDACs by baculovirus expression system

Cloning of HDAC cDNA and integration into baculoviral expression vector

The cDNAs of the four RPD3-like *HDACs* in *Arabidopsis thaliana* (Columbia), including *HDA6 (AtRPD3b)*, *HDA7*, *HDA9* and *HDA19 (AtHD1*, *AtRPD3a)*, were amplified by one-step RT-PCR (Invitrogen) using specific primers flanking the 5'- and 3'-ends of the *HDAC* genes (Figure 3.3A and B). The cDNAs obtained were inserted into a Gateway Entry Vector (Invitrogen) by T/A cloning. Restriction digestions and DNA sequencing were performed and the results confirmed that the inserted cDNAs were correct in sequence (100% match with the sequences in GenBank) and orientation, and were in-frame. The *HDAC* genes in the Entry vectors were then integrated into the baculoviral expression vector by site-specific LR recombination that occurs between specific attachment (*att*) sites: *attL*

A

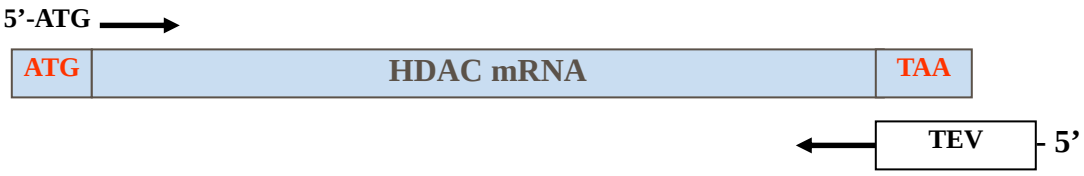

B

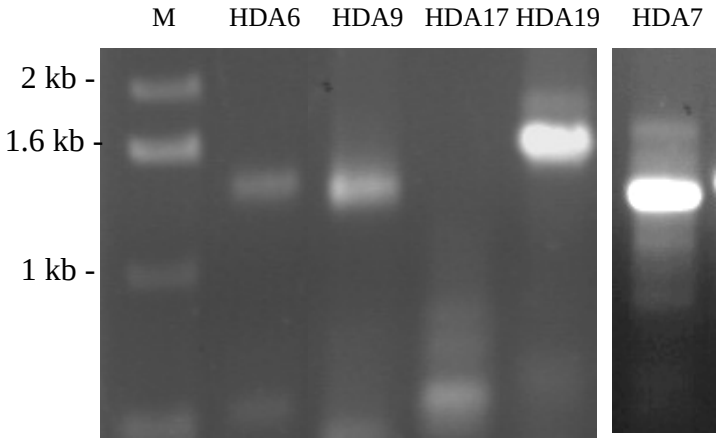

C

HDACs	Size of cDNA (bp)
HDA6	1416
HDA7	1230
HDA9	1281
HDA19	1506
HDA17	477

Figure 3.3. Cloning of RPD3-like *HDAC*s in *Arabidopsis thaliana.*

(A) Specific primers were used for amplification of *HDAC* cDNAs by reverse transcriptase (RT)-PCR. The forward primer contains an ATG start codon while the reverse primer omits the stop codon and adds a TEV protease cleavage site to the 3'-end of the amplified *HDAC* cDNA.
(B) Agarose gel showing the amplified HDAC cDNAs. The first lane is marker (M) followed by amplified *HDAC* cDNAs.
(C) A table showing the sizes (bp) of HDAC cDNAs.

on Entry vectors and *attR* on baculoviral expression vectors.

Transfection of insect cells and protein expression analyses

Baculoviral DNA with *HDAC* chimeric genes were introduced into SF9 insect cells by liposome-mediated transfection. Transfected cells with non-recombinant baculoviral DNA (i.e. those lacking *HDAC* chimeric genes) were eliminated by the addition of ganciclovir in the medium. Ganciclovir is a nucleoside analog that is converted into a toxic compound by the intact thymidine kinase gene in the non-recombinant baculoviral DNA. At 72-96 hours post-transfection, infected SF9 cells were lysed to release the recombinant baculovirus into the medium. The cell-free supernatant of this medium was collected as the P1 viral stock which had a low titer (i.e. low virus concentration). Two additional infection cycles were performed to obtain the P2 and P3 viral stocks with higher titers that would be used for recombinant protein expression. To confirm the presence of HDAC transgenes in the baculoviral DNA, baculoviral particles were precipitated from the P2 viral stocks and baculoviral DNAs were extracted for PCR. A universal primer pair flanking the recombination region of the baculoviral DNA was used to detect the presence of HDAC transgenes (Figure 3.4). The result of the PCR shows that all of the RPD3-like HDAC transgenes are present in the baculoviral DNA.

To assay the protein expression and to determine the optimum time post-infection that yields the highest levels of HDAC recombinant proteins, a time-course experiment was carried out. Insect cells seeded in each of the wells of four six-well plates were infected with P2 viral stock containing the chimeric genes for HDA6, 9, 17 and 19 at a multiplicity of infection (MOI) of five plaque-forming units (pfu) per cell. Infected insect cells from one of the four six-well plates were collected at 24, 48, 72 and 96 hours post-infection, and total

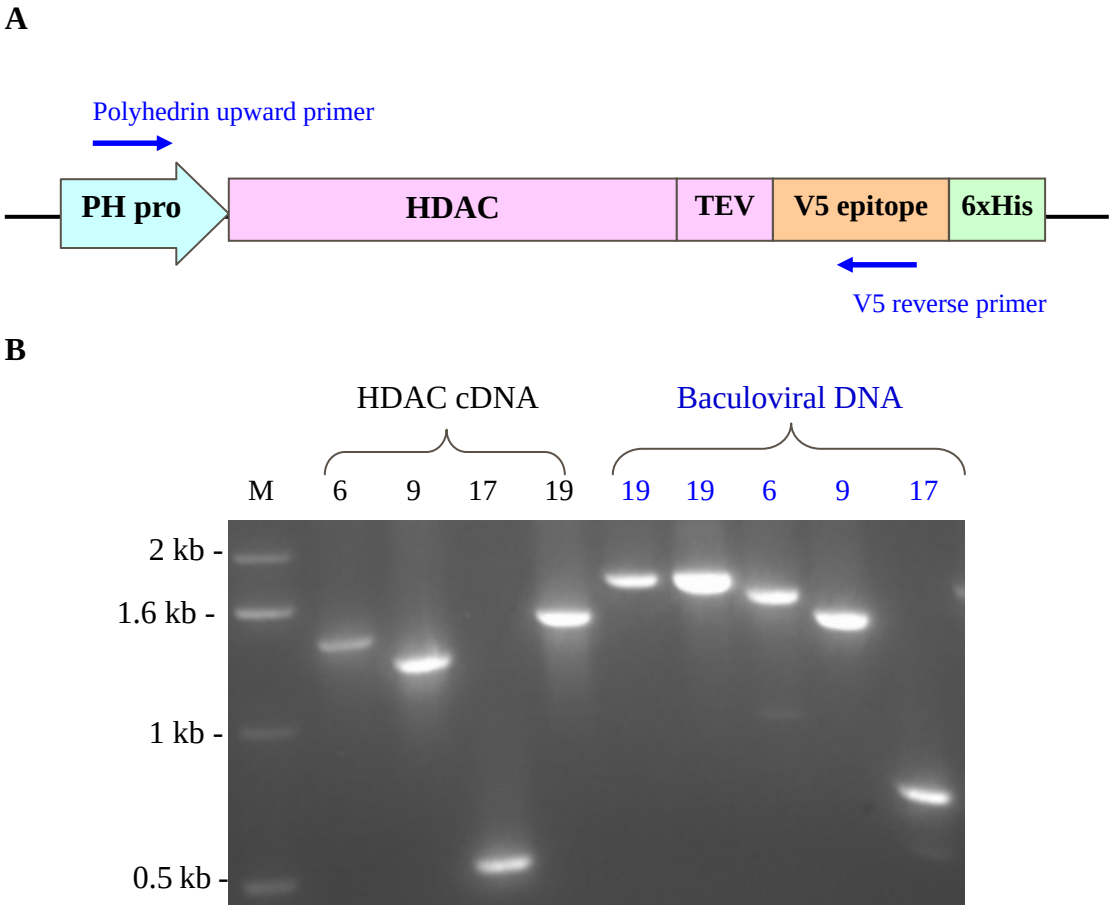

Figure 3.4. Expression cassette of HDAC chimeric genes in baculoviral expression vector.

(A) The baculoviral polyhedrin promoter (PH pro) drives the expression of the HDAC gene fused with a TEV cleavage site, a V5 epitope and a hexa-histidine (6×His) tag at the 3'-end. The V5 epitope and 6×His tag are used for detection and purification of the recombinant proteins, respectively. The two primers used to detect the presence of HDAC chimeric genes in the baculoviral DNA are the polyhedrin upward primer that is complementary to the polyhedrin promoter region, and the V5 reverse primer that is complementary to the V5 epitope region..
(B) Agarose gel showing the PCR-amplified fragments from HDAC cDNAs using the primer pairs for cloning **(Figure 3.3A)** and from baculoviral DNA using the polyhedrin upward and V5 reverse primers. Note that the DNA fragments amplified from the baculoviral DNA are 280 bp longer than the corresponding HDAC cDNA.

proteins were extracted. Total proteins were extracted from non-infected SF9 cells (wt) as a control. From the Coomassie blue stain of SDS-PAGE gel shown in Figure 3.5, distinct bands corresponding to the HDAC proteins can be seen in the 48-hour post-infection protein extracts, but not in the samples at other time points. The protein profile at 72- and 96-hour time points indicates that the proteins in the insect cells were degrading, suggesting extensive cell death.

To confirm the identities of the recombinant HDAC proteins, western blots were performed using anti-V5 antibody which is specific for the V5 epitope tag at the C-termini of the recombinant HDAC proteins. The results are shown in Figure 3.6. At the 24-hour time point, specific bands with sizes that correspond to the expected sizes of four HDAC recombinant proteins were detected. The non-specific bands that appeared at 48 and 72 hours post-infection might come from degraded HDAC recombinant proteins released from prematurely lysed cells. Thus, the optimal time for harvesting HDAC recombinant proteins from insect cells is 48 hours post-infection.

Production and purification of recombinant HDACs from insect cells

For large scale production of recombinant HDAC proteins, one liter of insect cell culture containing a total of 4×10^9 cells was used. About 1-2 mg of purified recombinant protein was obtained for each HDAC. HDA17 was not produced as it appears to be a partial duplication of HDA9 and is unlikely to have significant functions. The insect cells for HDA9 production were killed in an incident of high temperature due to the malfunction of the incubator. Therefore, only HDA6, 7 and 19 were produced.

Insect cells grown in spinner flasks at 27°C were infected with P3 baculoviral solution when they reached a density of 4×10^6 cells/ml. The cells were harvested after 48

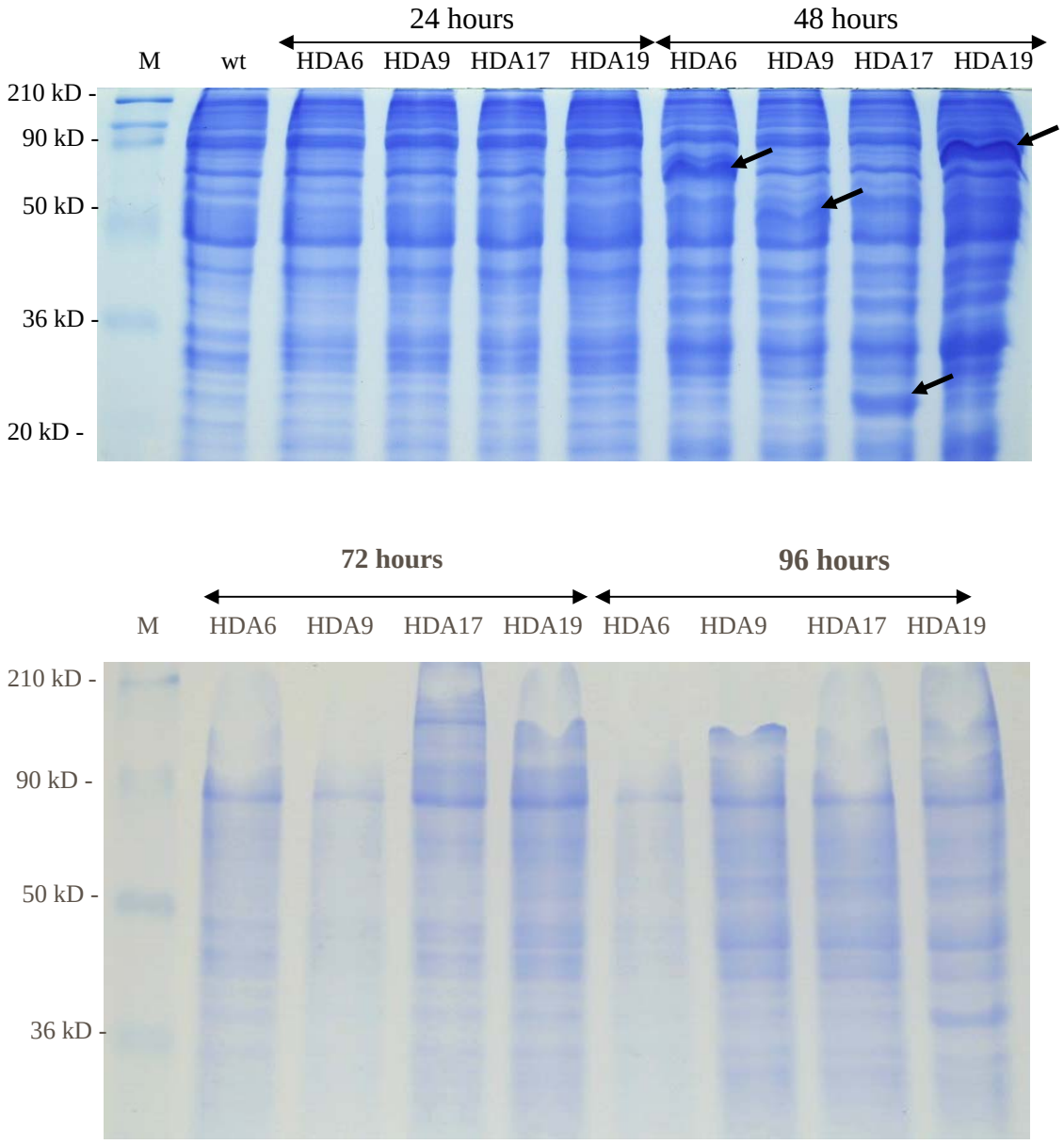

Figure 3.5. Protein profile of SF9 cells at different time points after infection.

Total proteins from infected and non-infected (wt) SF9 insect cells were extracted using TRI reagent. Approximately 100 μg of protein was loaded in each lane of an SDS-PAGE protein gel, and then separated by electrophoresis at 70V for 6 hours. The gel was stained with Coomassie blue. Bands corresponding to HDAC recombinant proteins (indicated by arrows) were visible in the 48-hour time point samples. Proteins extracted from 72- and 96-hour time points show signs of severe degradation, which may indicate extensive cell death.

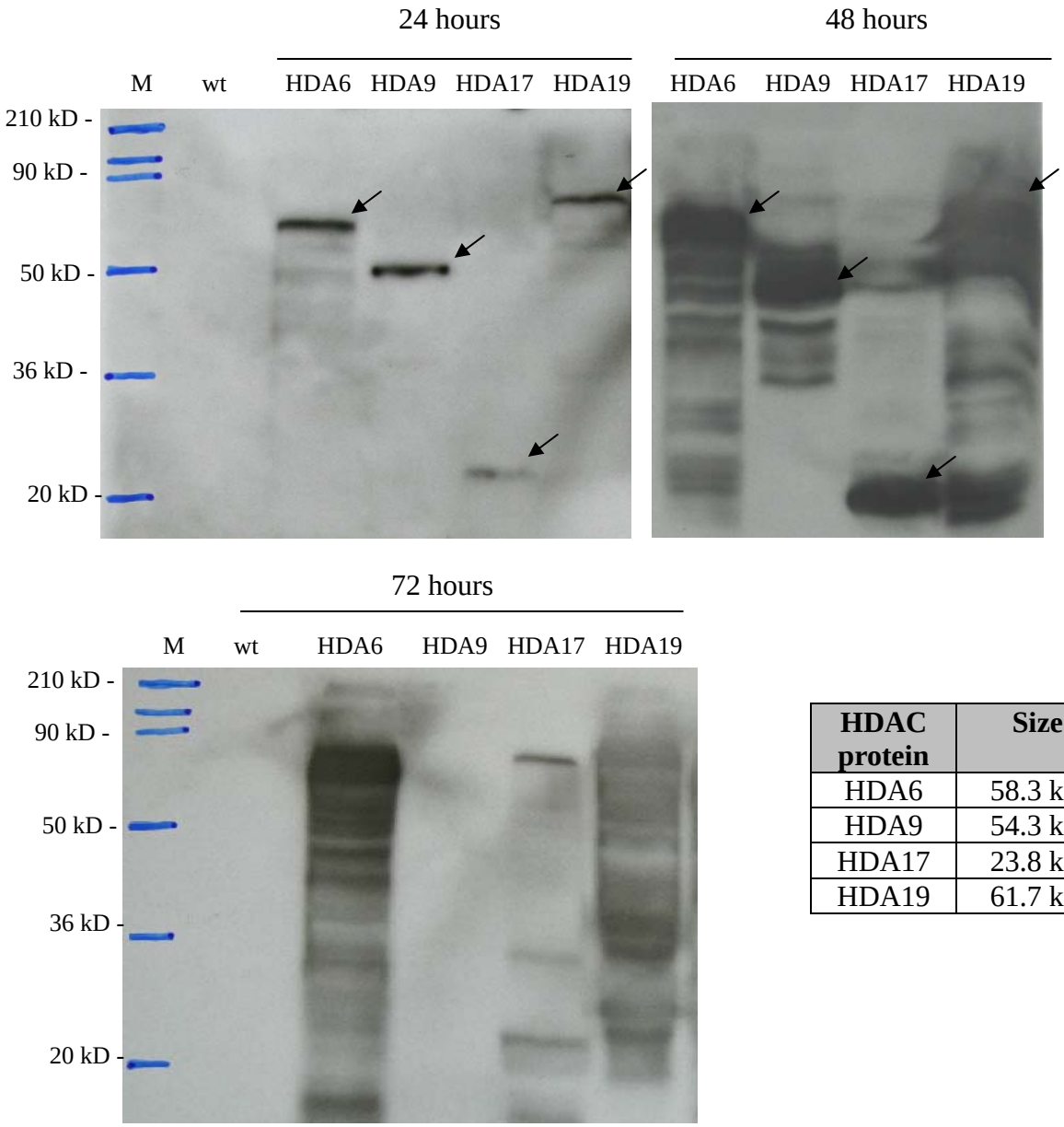

HDAC protein	Size
HDA6	58.3 kD
HDA9	54.3 kD
HDA17	23.8 kD
HDA19	61.7 kD

Figure 3.6. Western blots of SF9 total proteins at different time points.

Anti-V5 antibody specific for the V5 epitope was used to detect the HDAC recombinant proteins in total proteins extracted from SF9 insect cells at 24, 48 and 72 hours post-infection. The signals for the recombinant HDAC proteins are marked with arrows. The sizes of each of the recombinant HDAC proteins are shown in the table. Molecular weight markers (M) are indicated on the left sides of the 24- and 72-hour western blots.

hours and total proteins were extracted by sonication (see Materials and Methods section of this chapter). Recombinant HDAC proteins were purified using Ni-NTA column specific for the 6×His tag at the C-terminus of the proteins. SDS-PAGE analysis shows that the eluate from one-step affinity purification contains a number of non-specific proteins (Figure 3.7B). The purified protein solutions were subjected to second affinity purification on Ni-NTA column and the purity of the sample was greatly increased (Figure 3.7). Western blot analyses were performed using anti-V5 antibodies that are specific for the V5 epitope at the C-terminus of the recombinant HDAC proteins. The western blot results (Figure 3.7) confirm the identity of the recombinant proteins.

Histone deacetylase assay

A histone deacetylase assay kit (from Upstate) using a radioactive approach for detection was used to test the histone deacetylase activity of the purified recombinant HDACs from bacteria and insect cells. The recombinant HDACs were incubated with synthetic histone H3 or H4 peptides labeled with ^{3}H-acetyl groups on specific lysine residues. The radiolabeled histone peptides were immobilized on agarose beads and then incubated with a source of HDAC. The histone deacetylase activity of the recombinant protein, if any, would be proportional to the amount of ^{3}H-acetyl groups released from the acetylated histone peptides to the supernatant. The HeLa nuclear extract that contains a blend of HDACs was served as the positive control, while sodium butyrate that is a specific inhibitor of HDACs was added to the duplicates of each of the HDAC samples. After 16-20 hours of incubation at room temperature, the reaction mixtures were centrifuged and the amount of ^{3}H-acetate in the supernatant was measured by scintillation counting. While the HeLa nuclear extract gave an average of 3.5-fold increase in radioactive count per minute

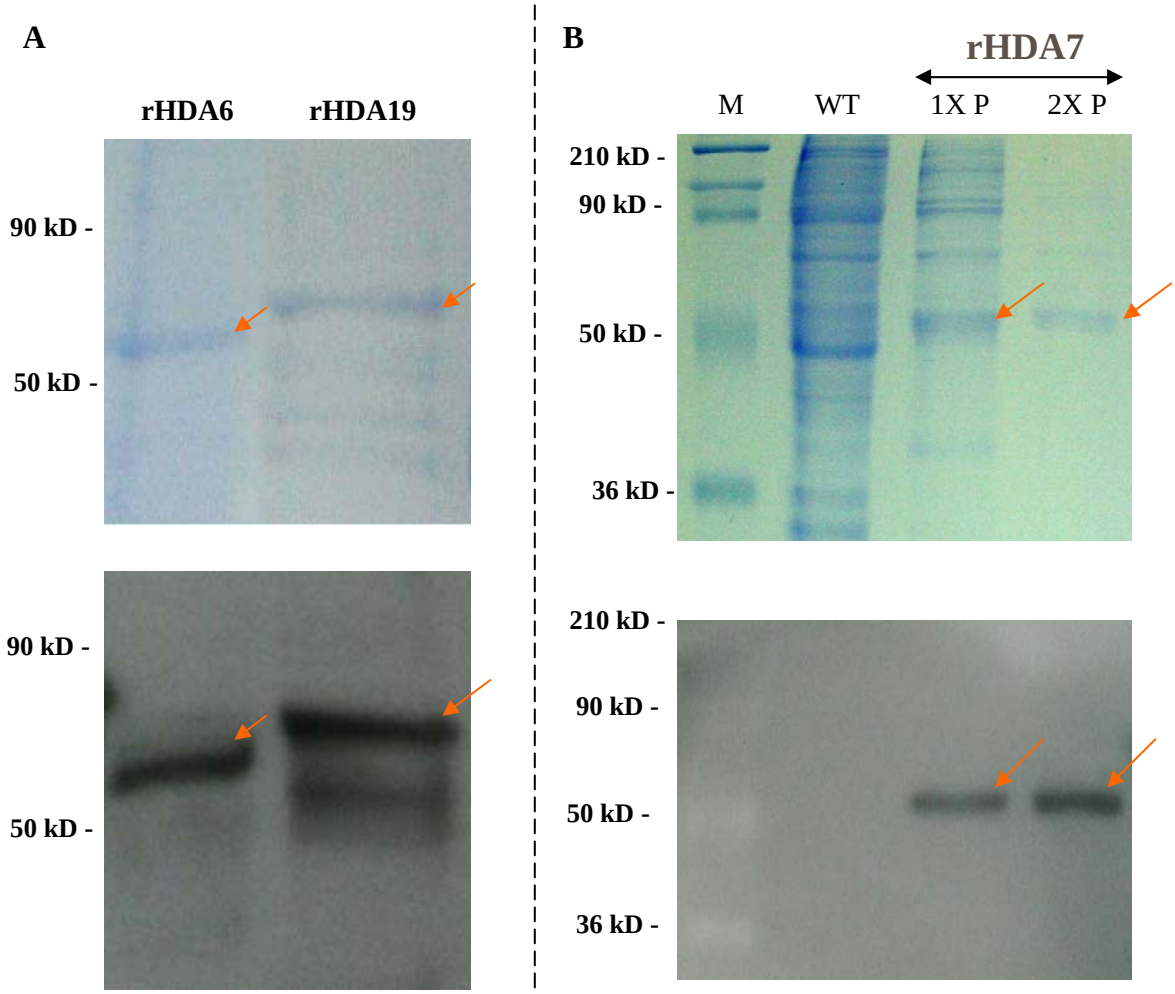

Figure 3.7. SDS-PAGE and western blots of purified HDACs.

(A) and (B) Recombinant proteins of HDA6, 7 and 19 were purified by Ni-NTA affinity column and then separated by 15% SDS-PAGE and the gel was stained with Coomassie blue or analyzed by western blot using anti-V5 antibody that is specific for the V5 epitope tag at the C-terminus of the recombinant proteins. The bands corresponding to the recombinant HDAC proteins are marked by arrows. The result of recombinant HDA7 purification **(B)** shows that the purity of the protein can be greatly increased by repeating the Ni-NTA column purification (2XP) when compared to a single-step purification (1XP).

(cpm) when compared with the negative(water) or specificity(sodium butyrate) controls, there is only an average of 30% increase in cpm for recombinant AtHD1 protein synthesized in bacteria (Figure 3.8). Recombinant HDACs produced in insect cells did not show any histone deacetylase activity, even when 20 μg of protein was used in the reactions.

DISCUSSION

Previous studies showed that the three RPD3-like HDAC genes in *Arabidopsis thaliana*, including HDA6, 9 and 19, are differentially expressed in leaves (Zhou et al., 2005) and other tissues (Plant Chromatin Database, http://chromdb.org). However, the expression of the other RPD3-like HDAC, HDA7, was not detected in previous studies. The results of RT-PCR in this study show that HDA6, 9 and 19 are differentially expressed in seedlings, roots, stems, leaves, flowers and siliques. In addition, the expression profiles of the four RPD3-like genes are different in the two *Arabidopsis thaliana* ecotypes, Columbia (col) and Wassilewskija (ws). Our study also indicates that *AtHD1* (*HDA19*) is expressed in all of the tissues examined. This result is consistent with previous data on *AtHD1* expression analyzed by RNA gel blot experiments (Wu et al., 2000b; Plant Chromatin Database, http://chromdb.org), suggesting that *AtHD1* is constitutively expressed in *Arabidopsis*. In contrast, the expression of HDA7 is detected in the flower tissues of ws and col ecotypes, and is absent in other tissues. This flower-specific expression pattern suggests that HDA7 may play a role in flowering. Interestingly, recent studies show that histone deacetylation and histone H3 dimethylation at lysines 9 and 27 are involved in *FLC* (*Flowering Locus C*) repression, whereas histone acetylation and histone H3 trimethylation at lysine 4 are associated with active *FLC* expression (reviewed by He and Amasino, 2005). Therefore, it would be interesting to investigate the effects of HDA7 on flower specific genes.

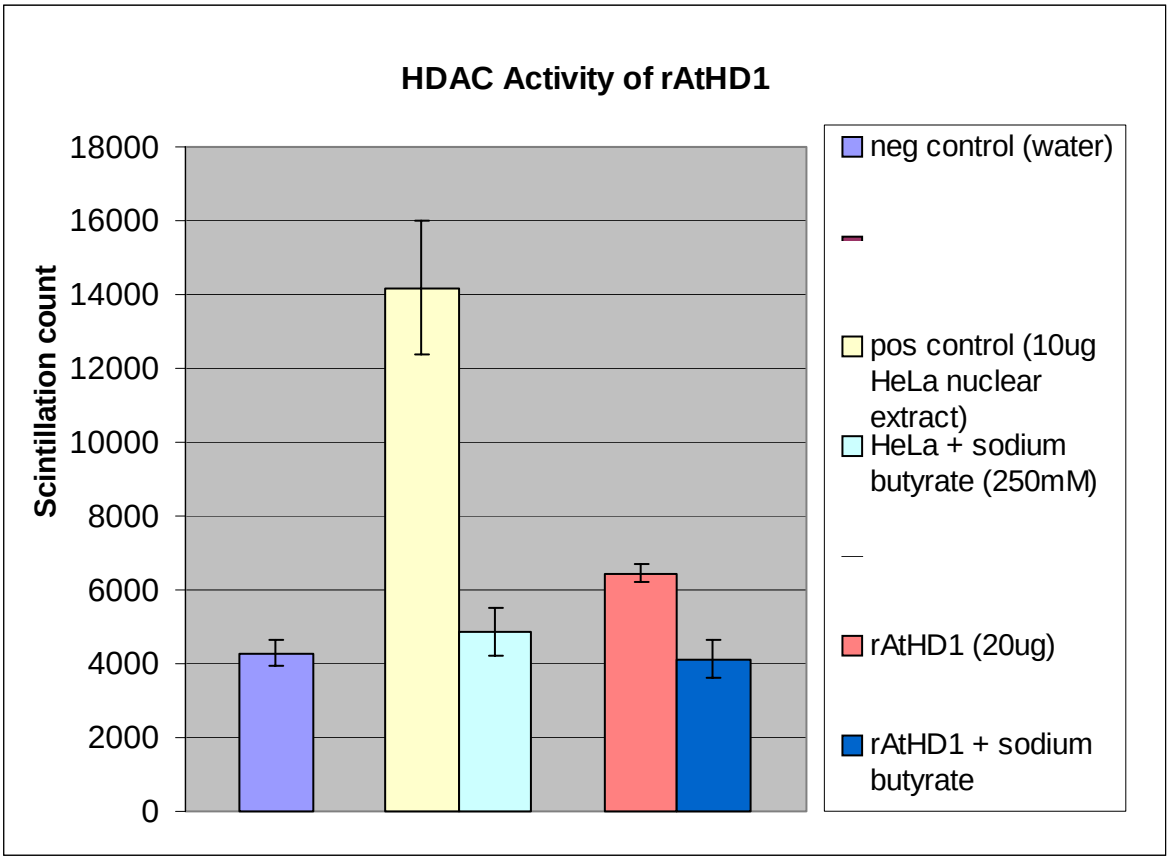

Figure 3.8. Histone deacetylase assay of purified AtHD1 from bacteria.

Compared with the negative control, the addition of purified AtHD1 (to a final concentration of 5 μg/ml) shows a 30% increase in cpm, indicative of histone deacetylase activity. The positive control with HeLa nuclear extract shows a three-fold increase in cpm. The addition of sodium butyrate, a specific inhibitor of histone deacetylases, inhibits the reactions containing HeLa nuclear extract and AtHD1.

Expression of recombinant AtHD1 (rAtHD1) in a bacterial system is quite high after 10 hours of induction. Analysis of the eluate from the Ni-NTA affinity column showed that there is a significant amount of contaminating proteins even though the column had been washed twice with 20 mM and then 70 mM imidazole. To increase the purity of recombinant AtHD1, the eluted proteins were purified further using amylose resin, and the N-terminal segment of the recombinant AtHD1 containing a 6×His tag and maltose binding protein (MBP) was removed by cleavage with TEV protease. After this double purification, the eluted rAtHD1 was free of major contaminating proteins (Figure 3.1C), and was tested immediately for any histone deacetylase activity.

The HDAC assay used is a radioactive approach that depends on the incubation of the enzyme with radiolabeled acetylated histone peptides, followed by extraction and quantification by scintillation counting of the radiolabeled acetate released from the immobilized histone peptide substrates. Although this method is time-consuming, expensive and not suitable for high-throughput screening, it is quite reliable as the results are quite consistent. HeLa nuclear extract that contains a blend of HDACs was used as the positive control, while sodium butyrate that is a specific HDAC inhibitor was used to demonstrate the specificity of the histone deacetylase activity.

The HDAC assay did not give conclusive results on the histone deacetylase activity of rAtHD1 synthesized in *E. coli*. While the negative control (water) provided a level of non-specific and non-enzymatic release of radiolabeled acetate in the reaction assay, the rAtHD1 showed some histone deacetylase activity (a 30% increase in released ^{3}H-acetatewhen compared with the negative control), but is not comparable to the 3.5-fold increase measured for the HeLa nuclear extract. However, the complete inhibition of

rAtHD1 by sodium butyrate suggests that rAtHD1 may indeed have histone deacetylase activity.

There are some possible reasons that can account for the low activity of rAtHD1 in the HDAC assay. First, the histone acetyltransferases (HAT) provided by the HDAC assay kit (Upstate) is PCAF (p300/CBP-associated factor), which has a narrow substrate specificity on histone acetylation. PCAF has a C-terminal half that bears a high degree of sequence homology to the yeast GCN5 nuclear HAT (Yang et al., 1996). It primarily acetylates Lysine 14 of histone H3 and acetylates Lysine 8 of histoneH4 less efficiently. PCAF does not acetylate other potential acetylation sites including Lysines 9, 18, 23 and 27 of histone H3, and Lysines 5, 12 and 16 of histone H4 (Schiltz et al., 1999). Therefore, if AtHD1 does not preferentially deacetylate the lysine residues acetylated by PCAF, it will show a low activity. To solve this problem, another HAT called p300 was used to acetylate histone peptides. P300 has been shown to have a wider specificity of HAT activity and can acetylate Lysines 14, 18 and 23 of H3, and Lysines 5, 8 and 12 of H4 (Ogryzko et al., 1996; Schiltz et al., 1999). However, histone peptides acetylated by P300 were not better substrates for recombinant AtHD1 in the HDAC assay, even though the acetylation efficiency of p300 was checked and found to be comparable to PCAF.

A second possible reason for the low activity of rAtHD1 is the lack of co-factors or requirement of complex formation with other proteins. It is remarkable that many purified recombinant HDACs are enzymatically inactive (Sengupta and Seto, 2004), with only the exception of yeast HOS3 and mammalian HDAC8 (Carmen et al., 1999; Hu et al., 2000; Lee et al., 2004).

Finally, AtHD1 may require post-translational modifications or specific chaperons

for proper folding, both of which are absent in the bacterial expression system. Phosphorylation is a major post-translation modification in HDACs. In the maize embryoes, phosphorylation of HD1A causes a change in substrate specificity of the enzyme (Borsch et al., 1992). Other HDACs, such as the maize HD2 (Lusser et al., 1997), human HDAC1, 2, 4 and 5 (Lu et al., 2000; Cai et al., 2001; Pflum et al., 2001; Tsai and Seto, 2002) are subjected to phosphorylation, which can modify or regulate their activities. Another post-translational modification that has been shown to regulate HDAC activity and function is called sumoylation, which involves the conjugation of small ubiquitin-related modifier (Colombo et al., 2002; David et al., 2002; Kirsh et al., 2002; Sengupta and Seto, 2003). However, sumoylation has been identified only in mammalian HDACs so far. Some HDACs are regulated by proteolytic processing. In maize, HDA1 is synthesized as an inactive precursor protein that is converted to the enzymatically active form by proteolytic removal of the C-terminal part of the protein (Pipal et al., 2003).

In an attempt to solve the problem caused by the lack of post-translational modifications, AtHD1 (also called HDA19) together with other RPD3-type HDACs in *Arabidopsis* including HDA6, 7 and 9, were produced by baculoviral expression system. The cDNA of HDA6, 7, 9 and 19 were amplified by RT-PCR and then cloned into the Gateway entry vector (Invitrogen) for fast and efficient integration of the HDAC genes into the baculoviral expression vector through LR recombination. The HDAC genes in the Gateway entry vector were sequenced to ensure that their sequences were correct and in-frame. Recombinant HDACs expressed in insect cells were extracted by sonication and purified by passage over a Ni-NTA affinity column. As in the case of purification of bacterial rAtHD1, the purity of the recombinant proteins was greatly increased by a second

round of purification. The purity and identity of the rHDACs was verified by SDS-PAGE and western blot analyses.

The HDAC activity of recombinant HDA6, 7 and 19 was tested by HDAC assay, described previously. However, all the rHDACs tested did not show any HDAC activity. Compared with bacterial rAtHD1 whose additional N-terminal segment has been cleaved, insect rAtHD1 (HDA19) has a C-terminal segment (38 amino acid residues) containing the V5 epitope and 6×His tag. Whether this additional segment interfered with the protein activity remains to be determined.

MATERIALS AND METHODS

RT-PCR of *HDAC* genes

Total RNA was extracted according to the protocol of TRIZOL reagent (Invitrogen). Total RNA (7 μg) was treated with RQ1 DNase (Promega) for removal of contaminating genomic DNA. One-step RT-PCR was performed according to the manufacturer's protocol (Invitrogen). In each RT-PCR reaction, 0.75 μg of total RNA was used as templates. Gene specific primers for *HDA6*, *HDA7*, *HDA9*, *HDA19* (*AtHD1*) and actin were used for PCR amplification. The RT-PCR products were separated in 1% agarose gels and stained with ethidium bromide.

Bacterial expression system

Induced expression of recombinant AtHD1 in bacterial host cells

Escherichia coli (strain BL21) harboring a pET21b expression vector (Novagen) that contains the chimeric *AtHD1* gene was provided by my colleague Lu Tian. The bacteria were grown in 0.5 L of NZCYM medium (Sigma) at 37°C, and IPTG

(isopropyl-β-D-thiogalactoside) was added to a final concentration of 1mM after 8 hours of incubation. The bacterial culture was further incubated at 20°C for an additional 12-15 hours before protein extraction.

Extraction and purification of recombinant AtHD1 from bacteria

Bacterial cells were collected from 0.5 L of bacterial culture by centrifugation and resuspended in 160 ml of PBS (pH 8.0) with 1 mg/ml of lysozyme, 1 mM PMSF and 2 mM β-mercaptoethanol. While keeping on ice, the cell suspension was sonicated four times at max power for 30s each with an interval of 5 minutes for cooling. After centrifugation, the supernatant was loaded to a Ni-NTA column pre-equilibrated with PBS and contained 4 ml bed volume of Ni-NTA resin (Invitrogen) to which the His-tag of the recombinant protein binds. After washing 2 times with 20 mM imidazole and then 70 mM imidazole in PBS, the target protein was eluted with 200 mM imidazole in PBS. To further purify the recombinant AtHD1 protein (rAtHD1), the eluent was loaded to a column containing 2 ml bed volume of amylose resin (New England Biolabs) to which the maltose-binding protein at the N-terminal of the rAtHD1 binds. After washing with 200 ml of TBS (pH 8.0), 50 units of TEV protease (Invitrogen) that cleaves specifically at the TEV site of rAtHD1 was added to the resin for in-column digestion. After 12 hours of incubation at 4°C, the rAtHD1 protein without the 6×His-MBP tag was eluted with TBS. The eluent was concentrated with Centricon filter (Millipore) with a nominal molecular weight limit of 50 kDa. The purified protein was resuspended in 500 μl of PBS with 2 mM β-mercaptoethanol and 15% glycerol.

Detection of recombinant AtHD1 by western blots

Recombinant AtHD1 protein was separated by 15% SDS-PAGE and transferred to PVDF membrane (Invitrogen) using a Trans-Blot SD Semi-dry Transfer Cell (Bio-Rad) in

the presence of a transfer buffer (48 mM Tris-HCl, 39 mM glycine, 0.0375% SDS, 20% methanol). Western blot analysis was performed according to the protocol of Western Breeze kit (Invitrogen). The primary antibody (anti-HD1) used is a polyclonal antibody produced in rabbit using the N-terminal fragment (1-199 amino acid residues) of AtHD1. The secondary antibody used was an anti-rabbit antibody conjugated with alkaline phosphatase. Detection was carried out by adding a chemiluminescent substrate (CPD-star) to the PVDF membrane and the signals were detected with Kodak X-ray film.

Baculoviral expression system

Construction of baculoviral expression vector with HDAC genes

The four RPD3-like HDACs cDNA in *Arabidopsis* were cloned by RT-PCR using the following primers:

For HDA6: 5'-ATGGAGGCAGACGAAAGCGGC-3' (forward primer) and 5'-GCCCTGAAAATACAGGTTTTCAGACGATGGAGGATTCACGTCTGG-3' (reverse primer); For HDA7: 5'-ATGGCGAGCTTAGCCGACGGA-3' (forward primer) and 5'-GCCCTGAAAATACAGGTTTTCAATGCGTGGATCATTTCTCTTCTC-3' (reverse primer); For HDA9: 5'-ATGCGTTCCAAGGACAAAATC-3' (forward primer) and 5'-GCCCTGAAAATACAGGTTTTCTGACGCATCGTTATCGTTGTCTCC-3' (reverse primer); For *HDA19* (*AtHD1*): 5'-GCGTCGACATGGATACTGGGGGCAATTC-3' (forward primer) and 5'-GCCCTGAAAATACAGGTTTTCTGTTTTAGGAGGAAACGCCTGCTC-3' (reverse primer).

Each forward primer contains an ATG start codon and each reverse primer omits the stop codon and adds the sequence for a TEV protease cleavage site (underlined) to the 3'-end of

the HDAC coding sequence. The cloning and expression of HDAC chimeric genes was performed according to the protocol of BaculoDirect Kit (Invitrogen). The PCR products were purified and inserted into Invitrogen's Gateway vector pCR8/GW/TOPO by TOPO T/A cloning. HDAC cDNA in the successfully transformed bacterial colonies were screened for correct orientation by restriction digestions. The HDAC constructs with the correct orientation in the pCR8/GW/TOPO cloning vector were sequenced to ensure that the sequence was correct and in-frame. Finally, the HDAC cDNAs were integrated into the baculoviral expression vector (Invitrogen) by site-specific recombination (LR recombination) so that a V5 epitope and a 6×His tag coding sequences were added to the 3'-end of the HDAC cDNA.

Insect cell culture and medium

The ovarian cell line SF9 from the moth *Spodoptera frugiperda* was used as the host cells for propagation of Baculovirus and production of recombinant HDACs. Grace's insect medium, supplemented (Gibco), or more commonly referred as TNM-FH (Trichoplusia ni Medium-Formulation Hink), together with 10% fetal bovine serum (FBS, Gibco) was used for culturing insect cells. Grace's insect medium, unsupplemented (Gibco), was used for transfection of insect cells. All insect cell cultures were grown in a non-CO_2 incubator at 27°C.

Transfection of insect cells

Baculoviral DNA harboring the HDAC chimeric genes were introduced into insect cells by lipid-mediated Transfection described in the BaculoDirect kit protocol (Invitrogen). Briefly, the baculoviral DNA was incubated with Cellfectin Reagent which contains a formulation of cationic lipids to enclose the DNA in liposome. This transfection mixture was

added to a monolayer of Sf9 insect cells adhered to the bottom of a six-well culture plate. The liposomes fuse with the cell and the baculoviral DNA is delivered into the cells. The transfected cells are grown in medium containing a nucleotide analog called ganciclovir at 100 μM for negative selection of insect cells transfected by non-recombinant baculoviral DNA.

Production of baculoviral stocks

Successfully transfected insect cells will lyse and release the virus 96 hours after transfection. The medium of transfected cells was collected and the supernatant was collected after centrifugation. This virus-containing solution is referred to as the P1 viral stock, which was used to infect more insect cells to generate a P2 viral stock with a higher titer (~1×10^5 to 1×10^6 pfu/ml). Baculoviral DNA was extracted according to the protocol described in the BaculoDirect kit (Invitrogen). The presence of the HDAC chimeric genes in the baculoviral DNA was verified by PCR using the following two primers provided by the BaculoDirect kit:

1. Polyhedrin upward primer in the polyherin promoter region:
   5'-AAATGATAACCATCTCGC-3'; and
2. V5 reverse primer at the 3'-end of the V5 epitope:
   5'-ACCGAGGAGAGGGTTAGGGAT-3'.

The P2 viral stocks for each RPD3-type HDAC were amplified further to produce large scale P3 viral stocks for infection of insect cells to produce the recombinant HDAC proteins.

Production of recombinant HDAC

In the time course experiment for determining the optimum time post-infection for obtaining highest yield of recombinant HDACs, a monolayer of 8×10^5 insect cells seeded in

each of the wells of four six-well plates was infected with 50 μl of P2 viral stock (titer = $8x10^7$ pfu/ml) with HDA6, 9, 17 and 19 at a multiplicity of infection (MOI) of 5 pfu/cell. Infected insect cells from one of the four six-well plates were collected at 24, 48, 72 and 96 hours post-infection, and total proteins were extracted using TRI reagent (Molecular Research Center).

In the large scale production of recombinant HDACs, suspension cultures with 0.5 L of TNM-FH complete medium containing insect cells at a density of 4×10^6 cells/ml in 1L spinner flasks were used. P3 viral stocks were added to the suspension cultures so that the MOI equaled 10 pfu/cell. Infected insect cell cultures were incubated at 27°C for 48 hours.

Extraction and purification of recombinant HDAC from insect cells

Total proteins from insect cells in suspension cultures were extracted using sonication and purified using Ni-NTA column as previously described.

Detection of recombinant HDAC proteins by western blot

Crude or purified proteins from insect cells were fractionated in 15% SDS-PAGE. Western blots were performed using Western Breeze kit (Invitrogen) as previously described. The primary antibody used was anti-V5 that was specific for the V5 epitope at the C-terminus of recombinant HDACs.

Histone deacetylase assay

Labeling of synthetic histone H3 and H4 peptides

The acetylation of synthetic histone H3 and H4 peptides was performed according to the protocol described in the HDAC Activity Assay kit (Upstate). Briefly, synthetic H4 peptides corresponding to amino acids 2-24 of Histone H4, and synthetic H3 peptides

corresponding to amino acids 1-21 of histone H3, both followed by a GSGS linker and biotinylated lysine, were enzymatically acetylated using ^{3}H-acetyl coenzyme A (Amersham) as a substrate in a reaction catalyzed by the histone acetyltransferases PCAF or p300. Labeled acetylated histone H3 or H4 peptides were harvested by agarose resin conjugated with streptavidin and the labeling efficiency was determined by the protocol described in the manual.

Detection of HDAC activity

Recombinant proteins purified from bacteria or insect cells were added to same amount of tritium-labeled acetylated histone H3 or H4 peptides to test for HDAC activity. For each test sample, a duplicate assay with 50 mM sodium butyrate, a specific inhibitor of HDAC, was included to demonstrate the specificity of deacetylation. HeLa nuclear extract that contains a blend of histone deacetylases was used as the positive control. Since the histone peptides were immobilized on agarose beads, the histone deacetylase activity, if any, would be proportional to the amount of ^{3}H-acetyl groups released from the acetylated histone peptides to the mobile phase. After 16-20 hours of incubation at room temperature, the reaction mixtures were centrifuged and the radioactivity of the supernatant was measured by scintillation counting using the Beckman LS 6500 Scintillation counter.

CHAPTER IV

TRANSGENIC EXPRESSION OF RECOMBINANT HISTONE DEACETYLASE 1 IN *Arabidopsis*

INTRODUCTION

Several HDACs have been characterized as one of the components in stable large multi-subunit complexes and most, if not all, HDACs interact with other cellular proteins for functional activity or modulation (Sengupta and Seto, 2004). Through interactions with other proteins, HDACs are sequestered into cellular compartments, recruited to the target chromatin regions, and are activated or inhibited. The interactions of HDACs with other proteins have been studied extensively in mammals but poorly studied in plants. The mammalian class I HDACs that are closely related to yeast Rpd3 are the best characterized. It has been shown that human HDAC1 and HDAC2 coexist in three distinct multi-protein complexes called the Sin3, the NuRD/NRD/Mi2, and the CoREST complexes (Hassig et al., 1997; Laherty et al., 1997; Zhang et al., 1997, 1998; Tong et al., 1998; Ayer, 1999; Ng and Bird, 2000; Humphrey et al., 2001; You et al., 2001). These complexes are recruited by a variety of transcription repressors to specific genes or to the entire chromosomal domains (Xu et al., 1999). For example, human HDAC1 has been shown to exist in a complex containing Methyl-CpG-binding protein 2 (MeCP2) which recruits HDAC1 to methylated DNA to repress transcription (Jones et al., 1998; Nan et al., 1998; Wade et al., 1999).

The commonly used methods to study protein-protein interactions include yeast two-hybrid system and co-immunoprecipitation. In the yeast two-hybrid system, the target

protein is fused to a DNA-binding domain and transfected in a yeast host cell bearing a reporter gene whose transcription is controlled partly by the DNA-binding domain. The fusion protein can then be used as a bait to screen a library of cDNA clones that are fused to an activation domain. The cDNA clones within the library that encode proteins capable of interacting with the target protein are identified by activation of the reporter gene. The main advantage of this method over expression in bacteria is that yeast cells perform post-translational modifications of proteins, and that the protein-protein interactions are identified *in vivo* so that experimental artifacts are reduced (Criekinge and Beyaert, 1999). However, the yeast two-hybrid approach is time-consuming and labor-intensive because it involves the construction and screening of a cDNA library and the culturing and transfection of yeast cells. Moreover, false positive clones are common in the screening process.

On the other hand, co-immunoprecipitation (Co-IP) or pull-down assay is a biochemical method which has been extensively used in the identification and isolation of interacting proteins. In this approach, the target protein is fused with a tag which can be recognized by and bound to an antibody or other types of ligand that are immobilized on a matrix. Any interacting proteins that can form a complex with the tagged target protein will be co-immunoprecipitated or pulled down with the target protein. This method is relatively fast and simple compared with the yeast two-hybrid system, but it requires a large quantity of high quality antibodies and that the recombinant target protein is correctly folded. In a study that used a recombinant Methyl-CpG-binding protein 2 (MeCP2) fused to a glutathione S-transferase (GST) tag, a number of interacting proteins including the mammalian Sin3 complex and a histone deacetylase (HDAC1) were identified and the result suggests a link between DNA methylation and histone deacetylation in the transcriptional

repression of methylated DNA (Nan et al., 1998; Jones et al., 1998).

In an attempt to isolate proteins interacting with AtHD1, an epitope-tagged AtHD1 was overexpressed in transgenic *Arabidopsis* and an immunoaffinity column was used to isolate the protein complexes. The human c-myc epitope, which has a high specificity and affinity for the monoclonal antibody 9E10, was fused to the C-terminus of AtHD1 for detection and immunoprecipitation of the recombinant protein.

RESULTS

Expression of epitope-tagged AtHD1 in *Arabidopsis*

The *AtHD1-cmyc* chimeric gene in the binary vector pBI101 (Figure 4.1) was introduced into the *Arabidopsis* genome by *Agrobacterium*-mediated transformation using the floral dipping method. Six independent lines of successful transformants were selected and the T_1 transgenic plants were regenerated. These transgenic plants, called SHC for the transgene (*35**S**::At**H**D1-**c**myc*) they contained, were propagated until all the progeny of a single plant gave a 3:1 ratio of green seedlings versus white seedlings when germinated in a selection medium containing 50 mg/L kanamycin. Three homozygous transgenic lines carrying the *35S::AtHD1-cmyc* transgene were generated.

The presence of SHC transgene in four of the transgenic lines was detected by Southern blot analysis. The restriction digestion with *Xba* I and *Not* I released a 2.1 kb fragment from the transgene and a radiolabeled probe specific for the 2×cmyc epitope and part of the 3'-end of *AtHD1* coding sequence was used for hybridization (Figure 4.1A). The result of Southern blot analysis shows that the SHC transgene was present in three of the four transgenic lines (Figure 4.1B). Northern blot analysis was performed to detect the presence of the SHC transcript in the three transgenic lines containing the transgene. The result shows

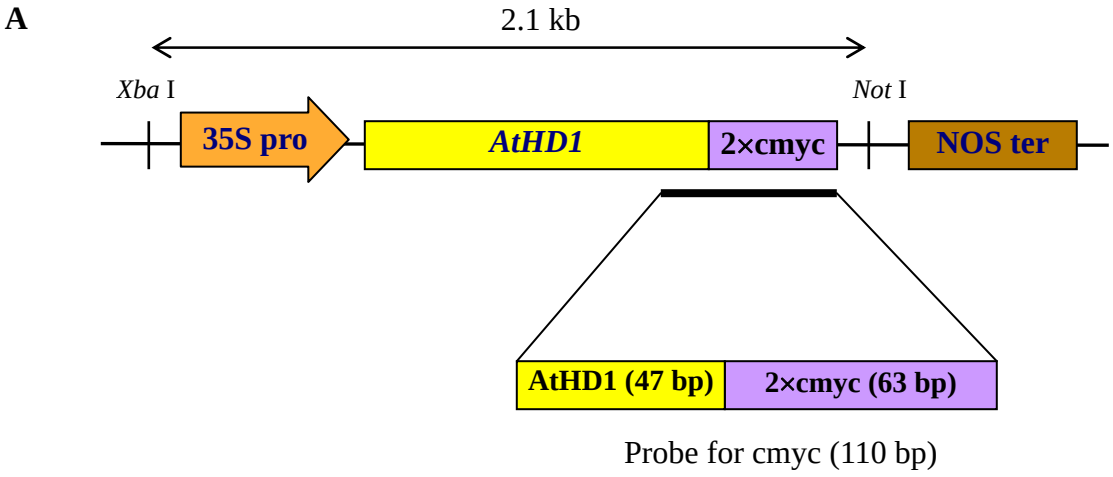

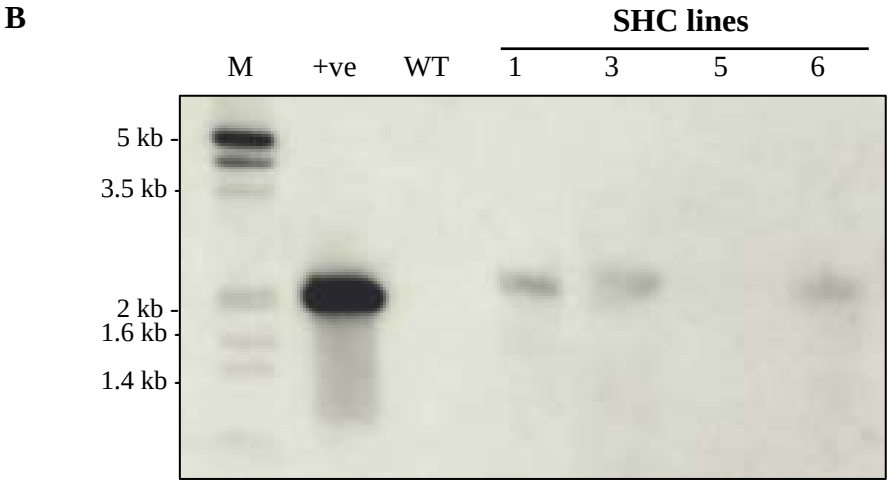

Figure 4.1. Southern blot analysis of SHC transgenic plants.

(A) The *35S::AtHD1T-cmyc* (SHC) chimeric gene consists of a double c-myc epitope fused to the 3'-end of the *AtHD1* cDNA and the resulting chimeric gene is put under the control of the CaMV 35S promoter. When the SHC transgene is digested with *Xba* I and *Not* I, a 2.1 kb fragment will be excised and it can be hybridized to a radiolabeled probe specific for the 2×cmyc epitope and part of the 3'-end of *AtHD1* sequences.
(B) In Southern blot analysis, genomic DNA (20 µg) from wild type and SHC transgenic plants were digested with *Xba* I and *Not* I, then separated by electrophoresis in 1% agarose gel and transferred to Hybond-N+ membrane (Amersham Pharmacia). A radiolabeled probe described in **(A)** was used in hybridization. The transgene was detected in 3 of the 4 SHC T_2 transgenic lines. The plasmid pUC18/35S::AtHD1-cmyc digested with the same restriction enzymes was used as the positive control (+ve). The marker used was Lamda DNA/EcoR I + Hind III (Promega).

that the transcription levels of the transgene were high in transgenic lines 1 and 3, but very low in line 6 (Figure 4.2). The expression of AtHD1-cmyc protein in SHC transgenic plants was studied by western blots using two antibodies, anti-myc and anti-HD. Anti-myc is a monoclonal (clone 9E10) antibody specific for the c-myc epitope, while anti-HD are polyclonal antibodies specific for the N-terminus of native AtHD1 protein. Western blots using anti-myc detected the presence of AtHD1-cmyc protein in SHC transgenic line 3 but not in line 5 (Figure 4.3A), as expected base on Southern analysis result. The size of the recombinant AtHD1-cmyc protein band (65-70 kDa) is larger than the expected size (58.6 kDa). When anti-HD was used (Figure 4.3B), the native AtHD1 protein bands were detected in the wild type and all SHC transgenic plants, and at very low levels in the CASH transgenic plants in which the expression of *AtHD1* is blocked by an antisense approach (Tian and Chen, 2001).

In an attempt to isolate proteins having interaction or association with AtHD1, the total protein extract of SHC transgenic plants (line 3) was passed through an immunoaffinity column with agarose resin conjugated with polyclonal anti-myc antibodies (Sigma). In the first few trials of purification, the column was washed six times with PBS and eluted with 0.1 M ammonium hydroxide at pH 11 according to Sigma's protocol. However, no proteins (not even the cmyc-tagged AtHD1 protein) were detected in western blot analysis using anti-myc antibody (Figure 4.4). In later trials, a proprietary elution buffer (Pierce) containing primary amines at pH 2.8 was used for elution. Two protein bands were detected in the western blot analysis using anti-myc antibody, although many non-specific contaminating proteins were also detected upon silver stain analysis of the SDS-PAGE duplicate (Figures 4.4 and 4.5). The size of the purified AtHD1-cymc detected in the western blots is 75 kDa,

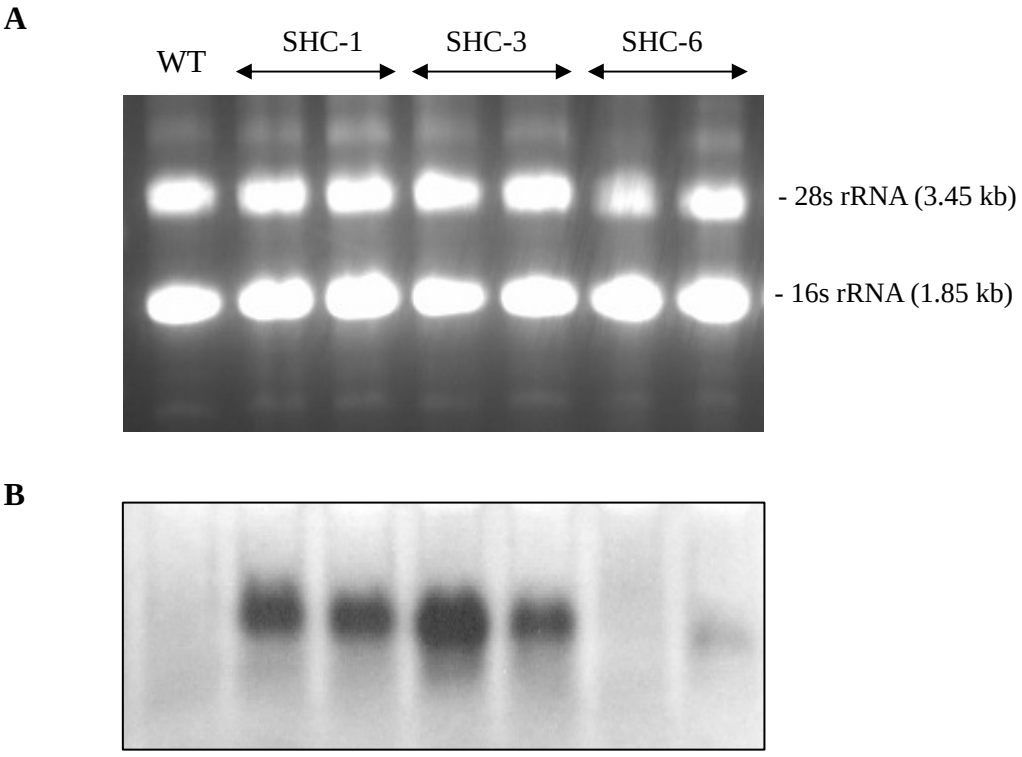

Figure 4.2. Northern blot analysis of SHC transgenic plants.

(A) Total RNA (30 μg) from wild type and SHG transgenic plants (with the presence of transgene verified by Southern blot) was separated by electrophoresis in a 1.5% agarose gel containing 2% formaldehyde and then transferred to Hybond-N+ membrane (Amersham Pharmacia).
(B) Northern blot analysis using the same radiolabeled probe described in Figure 4.1A showed that *AtHD1-cmyc* transcript was present in the SHC transgenic lines 1 and 3. The size of the *AtHD1-cmyc* transcript is about 1.6 kb.

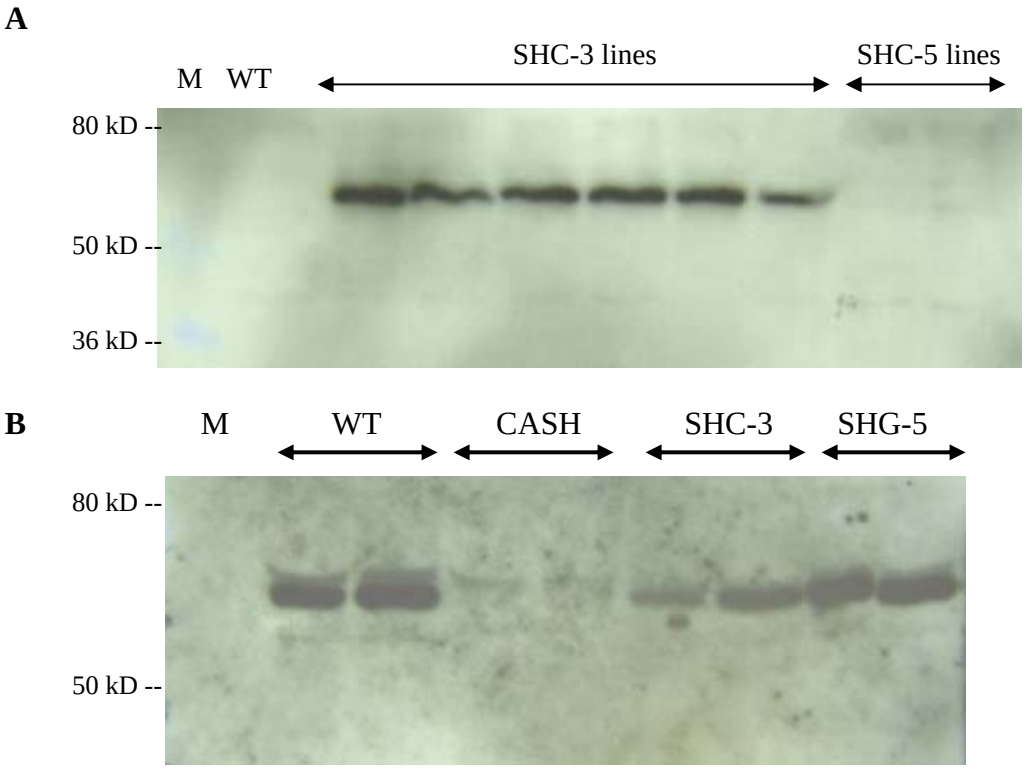

Figure 4.3. Western blot analyses of SHC, wild type and CASH plants.

Total proteins extracted from wild type, CASH (constitutive antisense histone deacetylase 1) and SHC transgenic plants were run on 15% SDS-PAGE and then transferred to PVDF membrane by electroblotting.
(A) Anti-myc monoclonal antibody was used to detect the presence of AtHD1-cmyc recombinant protein. Strong signals were detected in each of the SHC-3 lines, while no signal detected in the wild type and the SHC-5 lines.
(B) Anti-HD polyclonal antibodies were used to detect the native AtHD1 protein in wild type, CASH and SHC transgenic plants. Strong signals were detected in wild type and SHC plant proteins but not in CASH plant proteins.

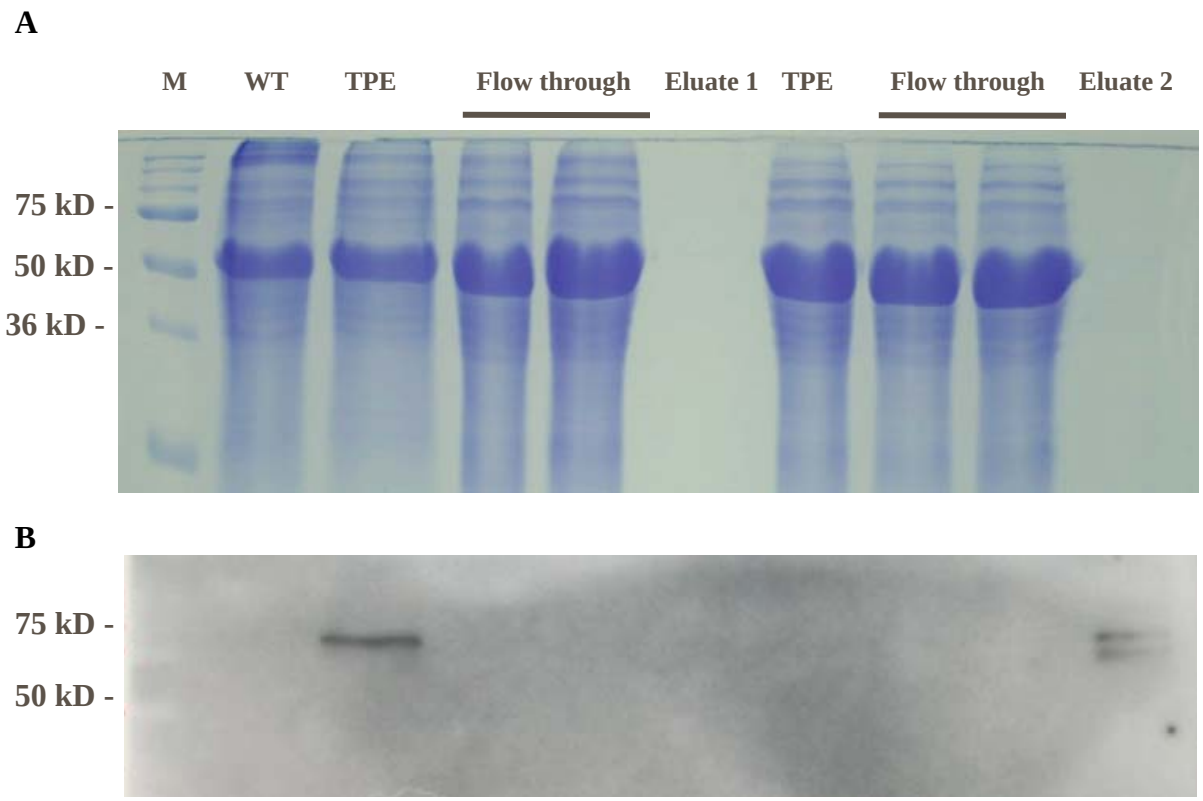

Figure 4.4. SDS-PAGE and western blot analyses of SHC proteins after anti-myc affinity column purification.

The crude total protein extracts (TPE) of SHC transgenic plants were allowed to run through an affinity column with agarose resin conjugated with polyclonal anti-myc antibodies. The columns were washed six times with PBS. Two elution buffers were used. The first one (Eluent 1) contained 0.1 M ammonium hydroxide at pH 11 (Sigma), while the second one is a proprietary formula containing primary amines at pH 2.8 (Pierce).
(A) Proteins from the wild type (WT), SHC total protein extracts (TPE) and those after running through the immunoaffinity column (flow through), and the eluates were run on a 15% SDS-PAGE and stained with Coomassie blue. No apparent bands can be found in the two eluates.
(B) A duplicate of the SDS-PAGE in **(A)** was used for western blot analysis. Anti-myc monoclonal antibody was used for detection of the AtHD1-cmyc protein. A single band was detected in SHC TPE while there were two bands in the eluate with low pH buffer.

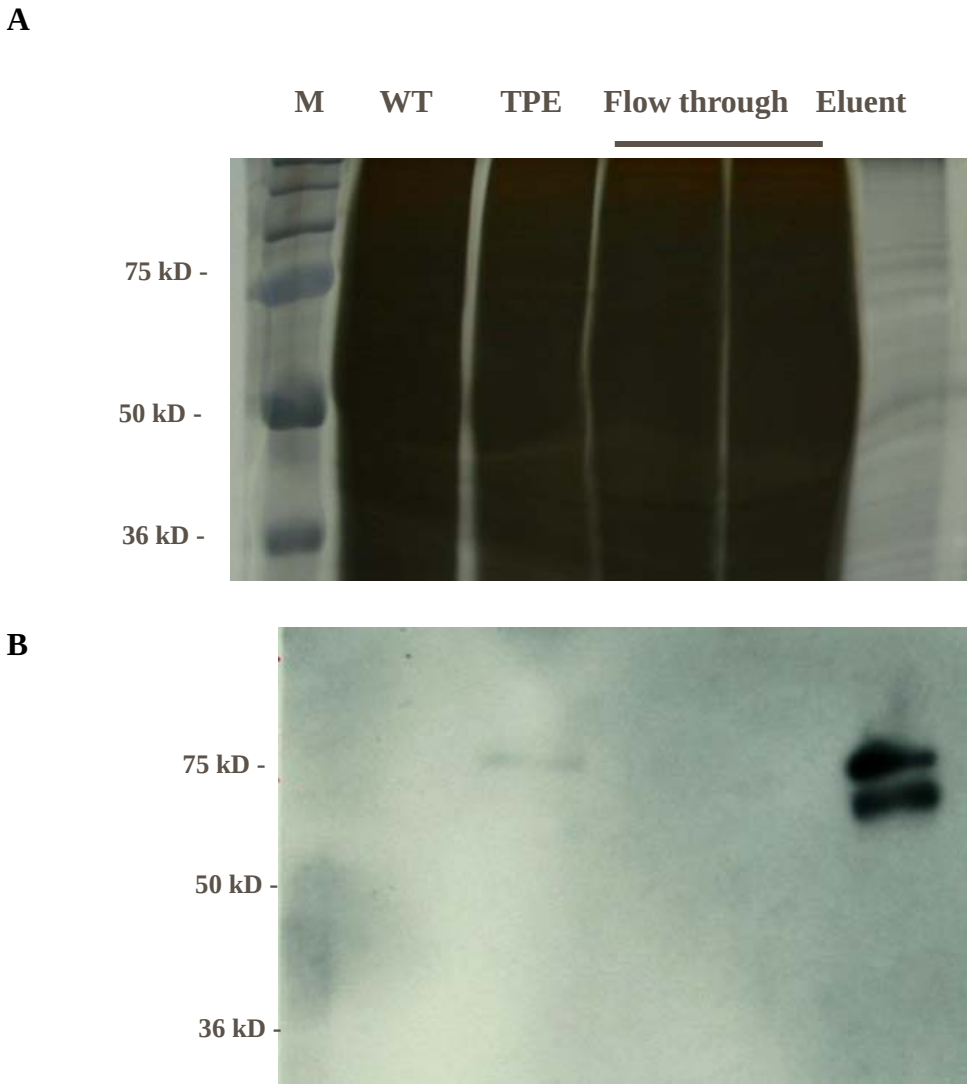

Figure 4.5. SDS-PAGE and western blot analyses of AtHD1-cmyc protein purified by anti-myc affinity column.

(A) Proteins from the wild type (WT), SHC total protein extract (TPE) and its flow through, and the proteins eluted by low pH elution buffer were run on a 15% SDS-PAGE and visualized by silver stain. The gel was over-stained to reveal the weak signals in the eluate. Many bands were found in the eluate.
(B) A duplicate of the SDS-PAGE in **(A)** was used for western blot analysis with anti-myc monoclonal antibody as the primary antibody. The result is similar to Figure 4.4B, but the signals for the purified proteins in the eluate were much stronger. One of the bands in the eluate has the same size (apparently 75 kDa) as the native AtHD1-cmyc recombinant protein found also in SHC TPE, while the other one has a slightly smaller size (~65 kDa).

which is larger than the expected size (58.6 kDa) of the recombinant protein. The second band detected in the eluent has a slightly smaller size (~65 kDa) but equally strong signal intensity when compared with the AtHD1-cmyc protein. Overall, the results show that some form of the AtHD1-cmyc protein can be purified by immunoprecipitation, but improvements need to be made to increase the purity. Further, the identity of the additional band needs to be ascertained.

DISCUSSION

A recombinant AtHD1 protein with a double c-myc epitope tag fused to its C-terminus was expressed in *Arabidopsis* plants and was used for the isolation of interacting proteins by co-immunoprecipitation. The integration of the SHC transgene in the transgenic *Arabidopsis* genome and the transcription of the transgene has been verified in Southern and northern blot analyses, respectively. The expression of the recombinant AtHD1-cmyc protein in the transgenic plants was also detected as strong and specific signals in western blot analyses, but the size of the recombinant AtHD1-myc and the native AtHD1 protein band signals (~70 kDa, Figure 4.3) is larger than the expected sizes (58.6 and 56 kDa, respectively). However, a previous study using anti-HD to detect the native AtHD1 protein in wild type plants also yield a protein band signal with an apparent size of 65-70 kDa (Tian and Chen, 2001). Therefore, the size discrepancy may be due to artifacts of the protein markers. However, the possibility of post-translational modifications of recombinant AtHD1-cmyc protein cannot be ruled out.

The immunoprecipitation of recombinant AtHD1-cmyc was not very successful in terms of quantity and purity. This is partly due to the low expression level of AtHD1-cmyc in the transgenic plant and this problem may be solved by increasing the amount of plant

materials used. The elution of the immunoprecipitation contains many contaminating proteins, partly because the anti-myc antibodies in the immunoaffinity column are polyclonal. The monoclonal anti-myc antibody from the clone 9E10 used in the western blot analyses of AtHD1-cmyc protein has proven to be very specific. To increase the purity of the immunoprecipitated AtHD1-cmyc protein, the use of monoclonal anti-myc antibody and a more stringent wash may help.

Western blot analyses of the immunoprecipitated AtHD1-cmyc protein reveals two protein bands with equally strong signal intensity. One of the band has size (~70 kDa) equals to that in SHC total protein extract, while the other band has a slightly smaller size (~65 kDa). The smaller protein may be derived from the original AtHD1-cmyc protein after proteolytic cleavage, but it is intriguing that this smaller protein was not detected in the crude protein extracts from SHC plants.

MATERIALS AND METHODS

Construction of *AtHD1-cmyc* chimeric gene

The double c-myc (2×cmyc) DNA was constructed by the method descried by Nakajima and Yaoita (1997) using the two following primers:

Forward primer:

5'-CATG CCATGG AGCAAAAGCTCATCTCTGAAGAGGATTTGGAGCAA-3'

Reverse primer:

5’-ATAGTTTAGCGGCCGCTTACAAATCCTCTTCAGAGATGAGCTTTTGCTCCAAA TC-3’

The two restriction sites (underlined) in the forward and reverse primers are *Nco* I and *Not* I, respectively. The 2×cmyc DNA synthesized by PCR was purified and digested with *Nco* I

and *Not* I. The GFP coding sequence in the plasmid pUC18/35S::AtHD1-GFP was excised with *Nco* I and *Not* I double digest and the 2×cmyc DNA was ligated to the resulting pUC18/35S::AtHD1 plasmid. The expression cassette of *35S::AtHD1-cmyc* was excised by *Xba* I and *EcoR* I double digest and then ligated into the pBI101 binary vector. The sequence of the *AtHD1-cmyc* chimeric gene in the pBI101 plasmid was checked by DNA sequencing and it was found to be correct and in-frame. The pBI101/35S::AtHD1-cmyc plasmid was introduced into *Agrobacteria* by electroporation using the Gene Pulser apparatus (Biorad) at 25 μF, 2.5 kV and 600 ohms.

Transformation of A*rabidopsis*

The *AtHD1-cmyc* chimeric gene was introduced into *Arabidopsis* by *Agrobacterium*-mediated transformation as described in Chapter II. Initial selection of the T_0 seedlings yielded about 20 successful transformants and six of these were selected to propagate for the generation of homozygous transgenic plants.

Nuclei acid isolation and detection

The extraction of genomic DNA and total RNA from SHC transgenic plants and the detection of the SHC transgene and transcript were performed as described in Chapter II.

Protein extraction and detection

For SDS-PAGE and western blot analysis, total protein was extracted from *Arabidopsis* plants by grinding 10 g of fresh or frozen plant materials in 20 ml of protein extraction buffer (20 mM Tris-HCl, 1 mM EDTA, 150 mM NaCl, 2 mM β-mercaptoethanol, pH 7.5) with 1× protease inhibitor cocktail (Sigma). For immunoprecipitation, the presence of amino groups in Tris may interfere with the protein bindings. Therefore, phosphate buffer

saline (100 mM sodium phosphate, 10 mM KCl, 68 mM NaCl, 2 mM β-mercaptoethanol, pH 7.5) with 1× protease inhibitor cocktail (Sigma) was used. Plant debris and insoluble materials were removed by centrifugation and the supernatants were stored at -20°C with 15% glycerol.

In SDS-PAGE and western blot analyses, approximately 100 μg of protein for each sample was separated in a 15% polyacrylamide gel, which was either stained with Coomassie blue or silver stain (Pierce). For western blot analysis, proteins in the gel were transferred to PVDF membrane by electroblotting (Biorad) and detected by the Western Breeze kit (Invitrogen) using either Anti-myc or Anti-HD antibodies.

Immunoprecipitation

Total protein extract of SHC transgenic plants was allowed to incubate with 1 ml of agarose resin conjugated with polyclonal Anti-myc antibodies (Sigma) for one hour at 4°C in an immunoaffinity column. The column was washed six times with BupH^{TM} modified Dulbecco's PBS (140 mM NaCl, 8 mM sodium phosphate, 2 mM potassium phosphate and 10 mM KCl, pH 7.4) and eluted with ImmunoPure IgG elution buffer (Pierce) containing primary amine at pH 2.8.

CHAPTER V

SUMMARY AND DISCUSSION

In this study, we have taken biochemical and molecular biology approaches to investigate the expression profile, subcellular localization and protein activity of histone deacetylase 1 (AtHD1) in *Arabidopsis thaliana*. Expression analysis shows that the four RPD3-like histone deacetylases in *Arabidopsis*, including *AtHD1* (*HDA19*), *HDA6*, *HDA7* and *HDA9*, are differentially expressed in different tissues and ecotypes of *Arabidopsis thaliana*. *AtHD1* is expressed at high levels in the roots, leaves, flowers and siliques, suggesting that AtHD1 is a global regulator involved in various physiological and developmental processes. The other three RPD3-like *HDAC*s, including *HDA6*, *HDA7* and *HDA9*, show different expression profiles and this suggests that they play different roles in plants. In particular, *HDA7* is expressed at low levels in flower tissues only, suggesting a role in the regulation of flowering.

The expression of the AtHD1-GFP fusion protein transiently in onion cells and permanently in transgenic *Arabidopsis* plants reveals that AtHD1 is localized predominantly in nucleus and is excluded from the nucleolus. Moreover, AtHD1 appears to associate with condensing chromatins at early prophase of the cell cycle and this suggests a role of AtHD1 in mitosis. The recombinant AtHD1 protein synthesized in bacteria has been shown to have significant histone deacetylase activity in this study. Further experiments can be done to investigate the substrate specificity and enzyme kinetics of AtHD1.

Finally, an epitope-tagged AtHD1 was expressed in transgenic *Arabidopsis* in an attempt to isolate the interacting proteins by co-immunoprecipitation. However, the

expression levels of the recombinant AtHD1 were very low and only a small amount of protein could be purified by immunoaffinity column chromatography. Improvements could be made by increasing the amount of plant materials for protein extraction. An alternative approach may be synthesizing the epitope-tagged AtHD1 in bacteria, then immobilizing it on an immunoaffinity column, and allowing the total protein extract from *Arabidopsis* to run through the column. Proteins interacting with AtHD1 could be co-immunoprecipitated, eluted and analyzed.

REFERENCES

Alland, L., Muhle, R., Hou, H., Jr., Potes, J., Chin, L., Schreiber-Agus, N., and DePinho, R.A. (1997). Role for N-CoR and histone deacetylase in Sin3-mediated transcriptional repression. Nature **387**, 49-55.

Amedeo, P., Habu, Y., Afsar, K., Scheid, O.M., and Paszkowski, J. (2000). Disruption of the plant gene MOM releases transcriptional silencing of methylated genes. Nature **405,** 203-208.

Ayer, D.E. (1999). Histone deacetylases: transcriptional repression with SINers and NuRDs. Trends Cell Biol **9,** 193-198.

Baek, S.H., Ohgi, K.A., Rose, D.W., Koo, E.H., Glass, C.K., and Rosenfeld, M.G. (2002). Exchange of N-CoR corepressor and Tip60 coactivator complexes links gene expression by NF-kappaB and beta-amyloid precursor protein. Cell **110,** 55–67.

Bannister, A.J., Zegerman, P., Partridge, J.F., Miska, E.A., Thomas, J.O., Allshire, R.C., and Kouzarides, T. (2001). Selective recognition of methylated lysine 9 on histone H3 by the HP1 chromo domain. Nature **410,** 120-124.

Bastow, R., Mylne, J.S., Lister, C., Lippman, Z., Martienssen, R.A., and Dean, C. (2004). Vernalization requires epigenetic silencing of FLC by histone methylation. Nature **427,** 164-167.

Baumbusch, L.O., Thorstensen, T., Krauss, V., Fischer, A., Naumann, K., Assalkhou, R., Schulz, I., Reuter, G., and Aalen, R.B. (2001). The *Arabidopsis thaliana* genome contains at least 29 active genes encoding SET domain proteins that can be assigned to four evolutionarily conserved classes. Nucleic Acids Res **29,** 4319-4333.

Bird, A. (2002) DNA methylation patterns and epigenetic memory. Genes Dev **16,** 6-21

Blander, G., and Guarente, L. (2004). The Sir2 family of protein deacetylases. Annu Rev Biochemistry **73,** 417-435.

Bordoli, L., Husser, S., Luthi, U., Netsch, M., Osmani, H., and Eckner, R. (2001). Functional analysis of the p300 acetyltransferase domain: the PHD finger of p300 but not of CBP is dispensable for enzymatic activity. Nucleic Acids Res **29**, 4462-4471.

Cai, R., Kwon, P., Yan-Neale, Y., Sambuccetti, L., Fischer, D., and Cohen, D. (2001). Mammalian histone deacetylase 1 protein is posttranslationally modified by phosphorylation. Biochem Biophys Res Commun **283,** 445-453.

Cao, X., and Jacobsen, S.E. (2002a). Role of the *Arabidopsis* DRM methyltransferases in de novo DNA methylation and gene silencing. Curr Biol **12,** 1138-1144.

Cao, X., and Jacobsen, S.E. (2002b). Locus-specific control of asymmetric and CpNpG methylation by the DRM and CMT3 methyltransferase genes. Proc Natl Acad Sci USA **99,** 16491-16498.

Cao, R., Wang, L., Wang, H., Xia, L., Erdjument-Bromage, H., Tempst, P., Jones, R.S., and Zhang, Y. (2002). Role of histone H3 lysine 27 methylation in polycomb-group silencing. Science **298,** 1039-1043.

Carmen, A.A., Griffin, P.R., Calaycay, J.R., Rundlett, S.E., Suka Y., and Grunstein, M. (1999). Yeast HOS3 forms a novel trichostatin A-insensitive homodimer with intrinsic histone deacetylase activity. Proc Natl Acad Sci USA **96,** 12356-12361.

Carrozza, M.J., Utley, R.T., Workman, J.L., and Cote, J. (2003). The diverse functions of histone acetyltransferase complexes. Trends Genet **19,** 321-329.

Chiu, W., Niwa, Y., Zeng, W., Hirano, T., Kobayashi, H., and Sheen, J. (1996). Engineered GFP as a vital reporter in plants. Curr Biol **6,** 325-30.

Church, G.M., and Gilbert, W. (1984). Genomic sequencing. Proc Natl Acad Sci USA **81,** 1991-1995.

Clough, S.J., and Bent, A.F. (1998). Floral dip: a simplified method for *Agrobacterium*-mediated transformation of *Arabidopsis thaliana.* Plant J **16,** 735-43.

Colombo, R., Boggio, R., Seiser, C., Draetta, G.F., and Chiocca, S. (2002). The adenovirus protein Gam1 interferes with sumoylation of histone deacetylase 1. EMBO Rep **3,** 1062-1068.

Conaway, R.C., Brower, C.S., and Conaway, J.W. (2002). Emerging roles of ubiquitin in transcription regulation. Science **296,** 1254-1258.

Corona, D.F., Langst, G., Clapier, C.R., Bonte, E.J., Ferrari, S., Tamkun, J.W., and Becker, P.B. (1999). ISWI is an ATP-dependent nucleosome remodeling factor. Mol Cell **3,** 239-245.

Criekinge, W.V., and Beyaert, R. (1999). Yeast two-hybrid: state of the art. Biological Procedure Online **2,** 1-38.

Czermin, B., Schotta, G., Hulsmann, B.B., Brehm, A., Becker, P.B., Reuter, G., and Imhof, A. (2001). Physical and functional association of SU(VAR)3-9 and HDAC1 in *Drosophila*. EMBO Rep **2,** 915-919.

Czermin, B., Melfi, R., McCabe, D., Seitz, V., Imhof, A., and Pirrotta, V. (2002). *Drosophila* enhancer of Zeste/ESC complexes have a histone H3 methyltransferase activity that marks chromosomal Polycomb sites. Cell **111,** 185-196.

David, G., Neptune, M.A., and DePinho, R.A. (2002). SUMO-1 modification of histone deacetylase 1 (HDAC1) modulates its biological activities. J Biol Chem **277,** 23658-23663.

Davie, J.R., and Murphy, L.C. (1990). Level of ubiquitinated histone H2B in chromatin is coupled to ongoing transcription. Biochemistry **29,** 4752-4757.

Dennis, K., Fan, T., Geiman, T., Yan, Q., and Muegge, K. (2001). Lsh, a member of the SNF2 family, is required for genome-wide methylation. Genes Dev **15,** 2940-2944.

Doyle, J.D., Doyle, J.L., and Bailey, L.H. (1990). Isolation of plant DNA from fresh tissue. Focus **12,** 13-15

Eden, S., and Cedar, H. (1994). Role of DNA methylation in the regulation of transcription. Curr Opin Genet Dev **4,** 255-259.

Eisen, J.A., Sweder, K.S., and Hanawalt, P.C. (1995). Evolution of the SNF2 family of proteins: subfamilies with distinct sequences and functions. Nucleic Acids Res **23,** 2715-2723.

Freitag, M., Hickey, P.C., Khlafallah, T.K., Read, N.D., and Selker, E.U. (2004). HP1 is essential for DNA methylation in *Neurospora*. Mol Cell **13,** 427-434.

Finnegan, E.J., and Kovac, K.A. (2000). Plant DNA methyltransferases. Plant Mol Biol **43,** 189-201.

Gaudin, V., Libault, M., Pouteau, S., Juul, T., Zhao, G., Lefebvre, D., and Grandjean, O. (2001). Mutations in LIKE HETEROCHROMATIN PROTEIN 1 affect flowering time and plant architecture in *Arabidopsis*. Development **128,** 4847-4858.

Gavin, I., Horn, P.J., and Peterson, C.L. (2001). SWI/SNF chromatin remodeling requires changes in DNA topology. Mol Cell **7,** 97-104

Gendrel, A.V., Lippman, Z., Yordan, C., Colot, V., and Martienssen, R.A. (2002). Dependence of heterochromatic histone H3 methylation patterns on the *Arabidopsis* gene *DDM1*. Science **297,** 1871-1873.

Grebenok, R.J., Galbraith, D.W., and Penna, D.D. (1997). Characterization of *Zea mays* endosperm C-24 sterol methyltransferase, one of two types of sterol methyltransferase in higher plants. Plant Mol Biol **34,** 891-896.

Grozinger, C.M., and Schreiber, S.L. (2000). Regulation of histone deacetylase 4 and 5 and transcriptional activity by 14-3-3-dependent cellular localization. Proc Natl Acad Sci USA **97,** 7835-7840.

Guarente, L. (2000). Sir2 links chromatin silencing, metabolism, and aging. Genes Dev **14**,

1021-1026.

Hassig, C.A., Fleischer, T.C., Billin, A.N., Schreiber, S.L., and Ayer, D.E. (1997). Histone deacetylase activity is required for full transcriptional repression by mSin3A. Cell **89,** 341-347.

Havas, K., Flaus, A., Phelan, M., Kingston, R., Wade, P.A., Lilley, D.M., and Owen-Hughes, T. (2000). Generation of superhelical torsion by ATP-dependent chromatin remodeling activities. Cell **103,** 1133-1142.

He, Y., and Amasino, R.M. (2005) Role of chromatin modification in flowering-time control. Trends Plant Sci **10,**30-35.

Heim, R, Cubitt, A.B., and Tsien, R.Y. (1995) Improved green fluorescence. Nature **373,** 663-664.

Horn, P.J., and Peterson, C.L. (2002). Molecular biology. Chromatin higher order folding--wrapping up transcription. Science **297,** 1824-1827.

Hu, E., Chen, Z., Fredrickson, T., Zhu, Y., Kirkpatrick, R., Zhang, G.F., Johanson, K., Sung, C.M., Liu, R., and Winkler, J. (2000). Cloning and characterization of a novel human class I histone deacetylase that functions as a transcription repressor. J Biol Chem **275,** 15254-15264.

Humphrey, G.W., Wang, Y., Russanova, V.R., Hirai, T., Qin, J., Nakatani, Y., and Howard, B.H. (2001). Stable histone deacetylase complexes distinguished by the presence of SANT domain proteins CoREST/kiaa0071 and Mta-L1. J Biol Chem **276,** 6817-6824.

Imai, S., Armstrong, C.M., Kaeberlein, M., and Guarente, L. (2000). Transcriptional silencing and longevity protein Sir2 is an NAD-dependent histone deacetylase. Nature **403,** 795-800.

Imhof, A., and Wolffe, A.P. (1999). Purification and properties of the *Xenopus* Hat1 acetyltransferase: association with the 14-3-3 proteins in the oocyte nucleus. Biochemistry **38,** 13085-13093.

Jackson, J.C., and Lopes, J.M. (1996). The yeast UME6 gene is required for both negative and positive transcriptional regulation of phospholipid biosynthetic gene expression. Nucleic Acids Res **24,** 1322-1329.

Jackson, J.P., Lindroth, A.M., Cao, X., and Jacobsen, S.E. (2002). Control of CpNpG DNA methylation by the KRYPTONITE histone H3 methyltransferase. Nature **416,** 556-560.

Jasencakova, Z., Soppe, W.J., Meister, A., Gernand, D., Turner, B.M., and Schubert, I.

(2003). Histone modifications in *Arabidopsis*- high methylation of H3 lysine 9 is dispensable for constitutive heterochromatin. Plant J **33,** 471-480.

Jeddeloh, J.A., Stokes, T.L., and Richards, E.J. (1999). Maintenance of genomic methylation requires a SWI2/SNF2-like protein. Nat Genet **22,** 94-97.

Jenuwein, T., and Allis, C.D. (2001). Translating the histone code. Science **293,** 1074-1080.

Johnson, L., Cao X., and Jacobsen, S. (2002). Interplay between two epigenetic marks: DNA methylation and histone H3 lysine 9 methylation. Curr Biol **12,** 1360-1367.

Jones, P.L., Veenstra, G.J., Wade, P.A., Vermaak, D., Kass, S.U., Landsberger, N., Strouboulis, J., and Wolffe, A.P. (1998). Methylated DNA and MeCP2 recruit histone deacetylase to repress transcription. Nat Genet **19,** 187-191.

Joyce, J.A., Lam, W.K., Catchpoole, D.J., Jenks, P., Reik, W., Maher, E.R., and Schofield, P.N. (1997). Imprinting of IGF2 and H19: lack of reciprocity in sporadic Beckwith-Wiedemann syndrome. Hum Mol Genet **6,** 1543-1548.

Kadosh, D., and Struhl, K. (1997). Repression by Ume6 involves recruitment of a complex containing Sin3 corepressor and Rpd3 histone deacetylase to target promoters. Cell **89,** 365-371.

Kadosh, D., and Struhl, K. (1998). Histone deacetylase activity of Rpd3 is important for transcriptional repression in vivo. Genes Dev **12,** 797-805.

Kankel, M.W., Ramsey, D.E., Stokes, T.L., Flowers, S.K., Haag, J.R., Jeddeloh, J.A., Riddle, N.C., Verbsky, M.L., and Richards, E.J. (2003). *Arabidopsis* MET1 cytosine methyltransferase mutants. Genetics **163,** 1109-1122.

Kao, H.Y., Verdel, A., Tsai, C.C., Simon, C., Juguilon, H., and Khochbin, S. (2001). Mechanism for nucleocytoplasmic shuttling of histone deacetylase 7. J Biol Chem **276,** 47496–47507.

Khochbin, S., and Wolffe, A.P. (1997). The origin and utility of histone deacetylases. FEBS Lett **419,** 157-160.

Kingston, R.E., and Narlikar, G.J. (1999). ATP-dependent remodeling and acetylation as regulators of chromatin fluidity. Genes Dev **13,** 2339-2352.

Kirsh, O., Seeler, J.S., Pichler, A., Gast, A., Muller, S., Miska, E., Mathieu, M., Harel-Bellan, A., Kouzarides, T., Melchior, F., and Dejean, A. (2002). The SUMO E3 ligase RanBP2 promotes modification of the HDAC4 deacetylase. EMBO J **21,** 2682-2691.

Kolle, D., Brosch, G., Lechner, T., Pipal, A., Helliger, W., Taplick, J., and Loidl, P. (1999). Different types of maize histone deacetylases are distinguished by a highly complex substrate and site specificity. Biochemistry **38,** 6769-6773.

Koroleva, O.A., Tomlinson, M.L., Leader, D., Shaw, P., and Doonan, J.H. (2004). High-throughput protein localization in *Arabidopsis* using *Agrobacterium*-mediated transient expression of GFP-ORF fusions. Plant J **41,** 162-174.

Kotake, T., Takada, S., Nakahigashi, K., Ohto, M., and Goto, K. (2003). *Arabidopsis TERMINAL FLOWER 2* gene encodes a heterochromatin protein 1 homolog and represses both *FLOWERING LOCUS T* to regulate flowering time and several floral homeotic genes. Plant Cell Physiol **44,** 555-564.

Krogan, N.J., Dover, J., Wood, A., Schneider, J., Heidt, J., Boateng, M.A., Dean, K., Ryan, O.W., Golshani, A., Johnston, M., Greenblatt, J.F., and Shilatifard, A. (2003). The Paf1 complex is required for histone H3 methylation by COMPASS and Dot1p: linking transcriptional elongation to histone methylation. Mol Cell **11,** 721-729.

Kuo, M.H., and Allis, C.D. (1998). Roles of histone acetyltransferases and deacetylases in gene regulation. Bioessays **20,** 615-626.

Kuzmichev, A., Nishioka, K., Erdjument-Bromage, H., Tempst, P., and Reinberg, D. (2002). Histone methyltransferase activity associated with a human multiprotein complex containing the enhancer of Zeste protein. Genes Dev **16,** 2893-2905.

Lachner, M., O'Carroll, D., Rea, S., Mechtler, K., and Jenuwein, T. (2001). Methylation of histone H3 lysine 9 creates a binding site for HP1 proteins. Nature **410,** 116-120.

Laherty, C.D., Yang, W.M., Sun, J.M., Davie, J.R., Seto, E., and Eisenman, R.N. (1997). Histone deacetylases associated with the mSin3 corepressor mediate mad transcriptional repression. Cell **89,** 349-356.

Lawrence, R.J., Earley, K., Pontes, O., Silva, M., Chen, Z.J., Neves, N., Viegas, W., and Pikaard, C.S. (2004). A concerted DNA methylation/histone methylation switch regulates rRNA gene dosage control and nucleolar dominance. Mol Cell **13,** 599-609.

Lee, H., Rezai-Zadeh, N., and Seto, E. (2004). Negative regulation of histone deacetylase 8 activity by cyclic AMP-dependent protein kinase A. Mol Cell Biol **24,** 765-773.

Li, G., Chandrasekharan, M.B., Wolffe, A.P., and Hall, T.C. (2001). Chromatin structure and phaseolin gene regulation. Plant Mol Biol **46,** 121-129.

Lindroth, A.M., Cao, X., Jackson, J.P., Zilberman, D., McCallum, C.M., Henikoff, S., and Jacobsen, S.E. (2001). Requirement of CHROMOMETHYLASE3 for maintenance of CpXpG methylation. Science **292,** 2077-2080.

Luger, K., Mader, A.W., Richmond, R.K., Sargent, D.F., and Richmond, T.J. (1997). Crystal structure of the nucleosome core particle at 2.8 A resolution. Nature **389,** 251-260.

Lusser, A., Brosch, G., Loidl, A., Haas, H., and Loidl, P. (1997). Identification of maize histone deacetylase HD2 as an acidic nucleolar phosphoprotein. Science **277,** 88-91.

Lusser, A. (2002). Acetylated, methylated, remodeled: chromatin states for gene regulation. Curr Opin Plant Biol **5,** 437-443.

Lyon, M.F. (1993). Epigenetic inheritance in mammals. Trends Genet **9,** 123-128.

Malagnac, F., Bartee, L., and Bender, J. (2002). An *Arabidopsis* SET domain protein required for maintenance but not establishment of DNA methylation. EMBO J **21,** 6842-6852.

Marmorstein, R. (2001). Structure and function of histone acetyltransferases. Cell Mol Life Sci **58,** 693-703.

Martienssen, R.A., and Colot, V. (2001). DNA methylation and epigenetic inheritance in plants and filamentous fungi. Science **293,** 1070-1074.

McKenzie, E.A., Kent, N.A., Dowell, S.J., Moreno, F., Bird, L.E., and Mellor, J. (1993). The centromere and promoter factor, 1, CPF1, of *Saccharomyces cerevisiae* modulates gene activity through a family of factors including SPT21, RPD1 (SIN3), RPD3 and CCR4. Mol Gen Genet **240,** 374-386.

McKinsey, T.A., Zhang, C.L., Lu, J., and Olson, E.N. (2000). Signal dependent nuclear export of a histone deacetylase regulates muscle differentiation. Nature **408,** 106-111.

Miska, E.A., Karlsson, C., Langley, E., Nielsen, S.J., Pines, J., and Kouzarides, T. (1999). HDAC4 deacetylase associates with and represses the MEF2 transcription factor. EMBO J **18,** 5099-5107.

Muller, J., Hart, C.M., Francis, N.J., Vargas, M.L., Sengupta, A., Wild, B., Miller, E.L., O'Connor, M.B., Kingston, R.E., and Simon, J.A. (2002). Histone methyltransferase activity of a *Drosophila* Polycomb group repressor complex. Cell **111,** 197-208.

Nakajima, K., and Yaoita, Y. (1997). Construction of multiple-epitope tag sequence by PCR for sensitive Western blot analysis. Nucleic Acids Research **25,** 2231-2232

Nan, X., Ng, H.H., Johnson, C.A., Laherty, C.D., Turner, B.M., Eisenman, R.N., and Bird, A. (1998). Transcriptional repression by the methyl-CpG-binding protein MeCP2 involves a histone deacetylase complex. Nature **393,** 386-389.

Narlikar, G.J., Fan, H.Y., and Kingston, R.E. (2002). Cooperation between complexes that regulate chromatin structure and transcription. Cell **108**, 475-487.

Ng, H.H., and Bird, A. (2000). Histone deacetylases: silencers for hire. Trends Biochem Sci **25,** 121-126.

Ogas, J., Kaufmann, S., Henderson, J., and Somerville, C. (1999). PICKLE is a CHD3 chromatin-remodeling factor that regulates the transition from embryonic to vegetative development in *Arabidopsis*. Proc Natl Acad Sci USA **96,** 13839-13844.

Ogryzko, V.V., Schiltz, R.L., Russanova, V., Howard, B.H., and Nakatani, Y. (1996). The transcriptional coactivators p300 and CBP are histone acetyltransferases. Cell **87,** 953-959.

Pal-Bhadra, M., Leibovitch, B.A., Gandhi, S.G., Rao, M., Bhadra, U., Birchler, J.A., and Elgin S.C. (2004). Heterochromatic silencing and HP1 localization in *Drosophila* are dependent on the RNAi machinery. Science **303,** 669-672.

Pandey, R., Muller, A., Napoli, C.A., Selinger, D.A., Pikaard, C.S., Richards, E.J., Bender, J., Mount, D.W., and Jorgensen, R.A. (2002). Analysis of histone acetyltransferase and histone deacetylase families of Arabidopsis thaliana suggests functional diversification of chromatin modification among multicellular eukaryotes. Nucleic Acids Res **30,** 5036-5055.

Papa, C.M., Springer, N.M., Muszynski, M.G., Meeley, R., and Kaeppler, S.M. (2001). Maize chromomethylase Zea methyltransferase2 is required for CpNpG methylation. Plant Cell **13,** 1919-1928.

Paul, A.L., and Ferl, R.J. (1998). Permeabilized *Arabidopsis* protoplasts provide new insight into the chromatin structure of plant alcohol dehydrogenase genes. Dev Genet **22,** 7-16.

Pennisi, E. (2001) Behind the scenes of gene expression. Science **293,** 1064-1067

Pflum, M.K., Tong, J.K., Lane, W.S., and Schreiber, S.L. (2001). Histone deacetylase 1 phosphorylation promotes enzymatic activity and complex formation. J Biol Chem **276,** 47733-47741.

Phelan, M.L., Schnitzler, G.R., and Kingston, R.E. (2000). Octamer transfer and creation of stably remodeled nucleosomes by human SWI-SNF and its isolated ATPases. Mol Cell Biol **20,** 6380-6389.

Pipal, A., Goralik-Schramel, M., Lusser, A., Lanzanova, C., Sarg, B., Loidl, A., Lindner, H., Rossi, V., and Loidl, P. (2003). Regulation and processing of maize histone deacetylase Hda1 by limited proteolysis. Plant Cell **15,** 1904-1917.

Probst, A.V., Fransz, P.F., Paszkowski, J., and Scheid, O.M. (2003). Two means of transcriptional reactivation within heterochromatin. Plant J **33,** 743-749.

Rea, S., Eisenhaber, F., O'Carroll, D., Strahl, B.D., Sun, Z.W., Schmid, M., Opravil, S., Mechtler, K., Ponting, C.P., Allis, C.D., and Jenuwein, T. (2000). Regulation of chromatin structure by site-specific histone H3 methyltransferases. Nature **406,** 593-599.

Reik, W., and Murrell, A. (2000). Genomic imprinting: silence across the border. Nature **405,** 408-409.

Rogina, B., and Helfand, S.L. (2004). Sir2 mediates longevity in the fly through a pathway related to calorie restriction. Proc Natl Acad Sci USA **101,** 15998-16003.

Rossi, V., Hartings, H., and Motto, M. (1998). Identification and characterisation of an RPD3 homologue from maize (*Zea mays* L.) that is able to complement an *rpd3* null mutant of *Saccharomyces cerevisiae*. Mol Gen Genet **258,** 288-296.

Saitoh, H., and Hinchey, J. (2000). Functional heterogeneity of small ubiquitin-related protein modifiers SUMO-1 *versus* SUMO-2/3. J Biol Chem **275,** 6252-6258.

Schiltz, R.L., Mizzen, C.A., Vassilev, A., Cook, R.G., Allis, C.D., and Nakatani, Y. (1999). Overlapping but distinct patterns of histone acetylation by the human coactivators p300 and PCAF within nucleosomal substrates. J Biol Chem **274,** 1189-1192.

Schotta, G., Ebert, A., Krauss, V., Fischer, A., Hoffmann, J., Rea, S., Jenuwein, T., Dorn, R., and Reuter, G. (2002). Central role of *Drosophila* SU(VAR)3-9 in histone H3-K9 methylation and heterochromatic gene silencing. EMBO J **21,** 1121-1131.

Sengupta, N., and Seto, E. (2004). Regulation of histone deacetylase activities. *J Cell* Biochemistry **93,** 57-67.

Shiio, Y., and Eisenman, R.N. (2003). Histone sumoylation is associated with transcriptional repression. Proc Natl Acad Sci USA **100,** 13225-13230.

Singer, T., Yordan, C., and Martienssen, R.A. (2001). Robertson's mutator transposons in *A. thaliana* are regulated by the chromatin-remodeling gene Decrease in DNA Methylation (DDM1). Genes Dev **15,** 591-602.

Smith, J.S., Brachmann, C.B., Celic, I., Kenna, M.A., Muhammad, S., Starai, V.J., Avalos, J.L., Escalante-Semerena, J.C., Grubmeyer, C., Wolberger, C., and Boeke, J.D. (2000). A phylogenetically conserved NAD^+-dependent protein deacetylase activity in the Sir2 protein family. Proc Natl Acad Sci USA **97,** 6658-6663.

Stam, M., Belele, C., Dorweiler, J.E., and Chandler, V.L. (2002). Differential chromatin structure within a tandem array 100 kb upstream of the maize b1 locus is associated with paramutation. Genes Dev **16,** 1906-1918.

Stillman, D.J., Dorland, S., and Yu Y. (1994). Epistasis analysis of suppressor mutations

that allow HO expression in the absence of the yeast SW15 transcriptional activator. Genetics **136,** 781-788.

Stockinger, E.J., Mao, Y., Regier, M.K., Triezenberg, S.J., and Thomashow, M.F. (2001). Transcriptional adaptor and histone acetyltransferase proteins in *Arabidopsis* and their interactions with CBF1, a transcriptional activator involved in cold-regulated gene expression. Nucleic Acids Res **29,** 1524-1533.

Strich, R., Surosky, R.T., Steber, C., Dubois, E., Messenguy, F., and Esposito, R.E. (1994). UME6 is a key regulator of nitrogen repression and meiotic development. Genes Dev **8,** 796-810.

Sung, S., and Amasino, R.M. (2004). Vernalization in *Arabidopsis thaliana* is mediated by the PHD finger protein VIN3. Nature **427,** 159-164.

Tariq, M., Saze, H., Probst, A.V., Lichota, J., Habu, Y., and Paszkowski, J. (2003). Erasure of CpG methylation in *Arabidopsis* alters patterns of histone H3 methylation in heterochromatin. Proc Natl Acad Sci USA. **100,** 8823-8827.

Tariq, M., and Paszkowski, J. (2004). DNA and histone methylation in plants. Trends Genet **20,** 244-251.

Tatham, M.H., Jaffray, E., Vaughan, O.A., Desterro, J.M., Botting, C.H., Naismith, J.H., and Hay, R.T. (2001). Polymeric chains of SUMO-2 and SUMO-3 are conjugated to protein substrates by SAE1/SAE2 and Ubc9. J Biol Chem **276,** 35368-35374.

Taunton, J., Hassig, C.A., and Schreiber, S.L. (1996). A mammalian histone deacetylase related to the yeast transcriptional regulator Rpd3p. Science **272,** 408-411.

Tian, L., and Chen, Z.J. (2001). Blocking histone deacetylation in *Arabidopsis* induces pleiotropic effects on plant gene regulation and development. Proc Natl Acad.Sci USA **98,** 200-205.

Tian, L., Wang, J., Fong, M.P., Chen, M., Cao, H., Gelvin, S.B., and Chen, Z.J. (2003). Genetic control of developmental changes induced by disruption of *Arabidopsis* histone deacetylase 1 (AtHD1) expression. Genetics **165,** 399-409.

Tong, J.K., Hassig, C.A., Schnitzler, G.R., Kingston, R.E., and Schreiber, S.L. (1998). Chromatin deacetylation by an ATP-dependent nucleosome remodelling complex. Nature **395,** 917-921

Tsai, S.C., and Seto, E. (2002). Regulation of histone deacetylase 2 by protein kinase CK2. J Biol Chem **277,** 31826-31833.

Varotto, S., Locatelli, S., Canova, S., Pipal, A., Motto, M., and Rossi, V. (2003). Expression profile and cellular localization of maize Rpd3-type histone deacetylases

during plant development. Plant Physiol **133,** 606-617.

Varshavsky, A., Levinger, L., Sundin, O., Barsoum, J., Ozkaynak, E., Serdlow, P., and Finley, D. (1982). Cellular and SV40 chromatin: replication, segregation, ubiquitination, nuclease hypersensitive sites, HMG-containing nucleosomes and heterochromatin-specific protein. Cold Spring Harb Symp Quant Biol **47,** 511-528.

Vidal, M., and Gaber, R.F. (1991). RPD3 encodes a second factor required to achieve maximum positive and negative transcriptional states in *Saccharomyces cerevisiae.* Mol Cell Biol **11,** 6317-6327.

Wade, P.A., Jones, P.L., Vermaak, D., and Wolffe, A.P. (1998). A multiple subunit Mi-2 histone deacetylase from *Xenopus laevis* cofractionates with an associated Snf2 superfamily ATPase. Curr Biol **8,** 843-846

Wade, P.A., Gegonne, A., Jones, P.L., Ballestar, E., Aubry, F., and Wolffe, A.P. (1999). Mi-2 complex couples DNA methylation to chromatin remodelling and histone deacetylation. Nat Genet **23,** 62-66.

Wade, P.A. (2001). Transcriptional control at regulatory checkpoints by histone deacetylases: molecular connections between cancer and chromatin. Hum Mol Genet **10,** 693-698.

Wagner, D., and Meyerowitz, E.M. (2002). SPLAYED, a novel SWI/SNF ATPase homolog, controls reproductive development in *Arabidopsis*. Curr Biol **12,** 85-94.

Wagner, D. (2003). Chromatin regulation of plant development. Curr Opin Plant Biol **6,** 20-28.

Wang, A.H., Kruhlak, M.J., Wu, J., Bertos, N.R., Vezmar, M., Posner, B.I., Bazett-Jones, D.P., and Yang, X.J. (2000). Regulation of histone deacetylase 4 by binding of 14-3-3 proteins. Mol Cell Biol **20**, 6904-6912.

Wood, J.G., Rogina, B., Lavu, S., Howitz, K., Helfand, S.L., Tatar, M., and Sinclair, D. (2004). Sirtuin activators mimic caloric restriction and delay ageing in metazoans. Nature **430,** 686-689.

Wu, K., Tian, L., Malik, K., Brown, D., and Miki, B. (2000a). Functional analysis of HD2 histone deacetylase homologues in *Arabidopsis thaliana*. Plant J **22,** 19-27.

Wu, K., Malik, K., Tian, L., Brown, D., and Miki, B. (2000b) Functional analysis of a RPD3 histone deacetylase homologue in *Arabidopsis thaliana*. Plant Mol Biol **44**,167-76.

Wu, K., Tian, L., Zhou, C., Brown, D., and Miki, B. (2003). Repression of gene expression by *Arabidopsis* HD2 histone deacetylases. Plant J **34,** 241-247.

Xu, L., Glass, C.K., and Rosenfeld, M.G. (1999). Coactivator and corepressor complexes in nuclear receptor function. Curr Opin Genet Dev **9,** 140-147.

Yang, X.J., Ogryzko, V.V., Nishikawa, J., Howard, B.H., and Nakatani, Y. (1996). A p300/CBP-associated factor that competes with the adenoviral oncoprotein E1A. Nature **382,** 319-324

You, A., Tong, J.K., Grozinger, C.M., and Schreiber, S.L. (2001). CoREST is an integral component of the CoREST-human histone deacetylase complex. Proc Natl Acad Sci USA **98,** 1454-1458.

Zhang, J., Kalkum, M., Chait, B.T., and Roeder, R.G. (2002). The N-CoR-HDAC3 nuclear receptor corepressor complex inhibits the JNK pathway through the integral subunit GPS2. Mol Cell **9,** 611-623.

Zhang, Y., Iratni, R., Erdjument-Bromage, H., Tempst, P., and Reinberg, D. (1997). Histone deacetylases and SAP18, a novel polypeptide, are components of a human sin3 complex. Cell **89,** 357-364.

Zhang, Y., LeRoy, G., Seelig, H.P., Lane, W.S., and Reinberg, D. (1998). The dermatomyositis-specific autoantigen Mi2 is a component of a complex containing histone deacetylase and nucleosome remodeling activities. Cell **95,** 279-289.

Zhang, Y., and Reinberg, D. (2001). Transcription regulation by histone methylation: interplay between different covalent modifications of the core histone tails. Genes Dev **15,** 2343-2360.

Zhou, C., Labbe, H., Sridha, S., Wang, L., Tian, L., Latoszek-Green, M., Yang, Z., Brown, D., Miki, B., and Wu, K. (2004). Expression and function of HD2-type histone deacetylases in *Arabidopsis* development. Plant J **38,** 715-724.

Zhou, C., Zhang, L., Duan, J., Miki, B., and Wu, K. (2005). HISTONE DEACETYLASE19 is involved in jasmonic acid and ethylene signaling of pathogen response in *Arabidopsis*. Plant Cell **17**, 1196-1204.

VITA

Man Kim Fong

ADDRESS Room 2301, Block B, Hong Yat Court, Lam Tin, Kowloon, Hong Kong, China

EDUCATION B.S., 1998, Biochemistry, The Chinese University of Hong Kong, China
M.S., 2001, The Chinese University of Hong Kong, China

HONORS & AWARDS

Kong E Suen Memorial Scholarship, The Chinese University of Hong Kong, 1995-1996
Joyce M. Kuok Foundation Scholarship, The Chinese University of Hong Kong, 1996-1997
Cheung Chuk Shan Scholarship, The Chinese University of Hong Kong, 1996-1997
Ko Fook Son Prize in Biochemistry, The Chinese University of Hong Kong, 1996-1997
Joyce M. Kuok Foundation Scholarship, The Chinese University of Hong Kong, 1997-1998
Fong Yun Wah Scholarship, The Chinese University of Hong Kong, 1997-1998
Ko Fook Son Prize in Biochemistry, The Chinese University of Hong Kong, 1997-1998

PUBLICATION

Tian, L., J. Wang, M. K. Fong, M.K., Chen, H. Cao, S. B. Gelvin, and Z. J. Chen (2003) Genetic control of developmental changes induced by disruption of *Arabidopsis* histone deacetylase 1 (*AtHD1*) expression. Genetics **165**, 399-409.